MEDIZINISCHE UNIVERSITÄT WIEN

The role of SLC20A1 in physiological and stress erythropoiesis.

Doctoral thesis at the Medical University of Vienna

For obtaining the academic degree

Doctor of Philosophy

Submitted by
Federica Quattrone, MSc

Supervisor
Univ. Prof. Dr. Sylvia Knapp, PhD

Department of Internal Medicine I, Laboratory of Infection Biology, Medical University of Vienna

Research Center for Molecular Medicine (CeMM) of the Austrian Academy of Sciences Vienna

Vienna, 07/2021

Declaration

The doctoral candidate, Federica Quattrone, conducted her PhD studies under the supervision of Prof. Dr. Sylvia Knapp, PhD at the (I) Department of Medicine I, Laboratory of Infection Biology, Medical University of Vienna and (II) the Research Center for Molecular Medicine (CeMM) of the Austrian Academy of Sciences. Additionally, a research exchange was conducted abroad at Sanquin Research, Amsterdam, The Netherlands where the candidate spent 1 month as research fellow under the supervision of Dr. Marieke von Lindern. The work was granted with a Doctoral Fellowship from the Austrian Academy of Science.

For the publication “SLC20A1 facilitates heme transport and drives red pulp macrophage and erythroblast differentiation”, Federica Quattrone conceived the study, designed, performed and analyzed the majority of experiments and wrote the manuscript. Rui Martins, provided assistance with the CRISPR screen and heme biochemistry assays. Anna-Dorothea Gorki performed cell sorting and provided assistance with *in-vivo* experiments, transcriptome library preparation and analysis. Anastasiya Hladik and Karin Lakovits provided assistance with both *in-vitro* and *in-vivo* experiments. Manuele Rebsamen and Enrico Girardi provided assistance with CRISPR screen and its analysis. Andrea Alvarez-Hernandes performed histological staining. Florian Mayrhofer and Asma Farhat provided assistance with *in-vivo* experiments. Additionally, Asma Farhat prepared the transcriptome libraries. Martin Luther Watzenboeck provided assistance with bioinformatic analysis. Emile van den Akker and Marieke von Lindern, Giulio Superti-Furga and Ingrid Simonitsch-Klupp provided intellectual input. Sylvia Knapp conceived the study, founded, directed and supervised the work and wrote the manuscript. Riem Gawish supervised the work, designed and provided assistance with *in-vivo* experiments and wrote the manuscript.

Table of Contents

List of figures

Thesis figures

Published figures

List of tables

Published tables

Abstract

Heme is a key regulator of several biological processes. It acts both as a prosthetic group, for protein complexes requiring oxygen- and electron- binding capability, and as cell-differentiation regulator, in those cells handling large quantities of it. At the same time, labile heme is highly cytotoxic as it promotes inflammation, and it contributes to the activation of cell death programs. As such, organisms must tightly control the labile heme pool via its scavenging, degradation and compartmentalization.

Though heme metabolism has been extensively studied, the mechanisms regulating its transport and the underlying regulated processes are still largely unknown. To identify novel genes involved in heme transport, we performed a loss-of-function, CRISPR-based genetic screening using heme as cytotoxic selective pressure. Deletion of *SLC20A1* conferred the starkest resistance to heme-induced cell death, independently of its appointed phosphate transport function. *In-vivo,* conditional *Slc20a1* deletion caused a non-resolving anemia characterized by impaired erythroblast differentiation and failed expansion of the red pulp macrophages (RPM) pool. To dissect *Slc20a1'*s specific cellular contributions, we conditionally deleted the gene either in the erythroid or myeloid lineages. Erythroid-specific *Slc20a1* deletion caused a block in terminal erythropoiesis at pro-erythroblast stage and it led to embryonic lethality around E12.5. Thus, indicating that *Slc20a1* is essential for terminal erythroid differentiation. To clarify the processes altered by *Slc20a1* deletion, we analyzed the transcriptome of *Slc20a1*-deleted pro-erythroblasts and observed activation of heme-deficiency response programs. Myeloid-specific *Slc20a1* deletion did not affect the RPM pool at steady state. However, upon anemia challenge, *Slc20a1*-deletion hampered the expansion of the RPM pool by dysregulating the expression of *Spic*, the heme-inducible master regulator of RPM differentiation. Taken together, our data highlighted a link between *Slc20a1* heme import. Thus, to test our hypothesis, we challenged *SLC20A1*-deleted cells with heme and observed reduced uptake of the molecule and reduced induction of its degrading enzyme HMOX1. Altogether, our data demonstrate for the first time that SLC20A1 facilitates heme transport and that this function is essential to support erythroblasts and RPM differentiation.

Kurzfassung

Häm ist ein Schlüsselregulator für mehrere biologische Prozesse. Es fungiert sowohl als prosthetische Gruppe für Proteinkomplexe, die Sauerstoff- und Elektronenbindungsfähigkeit benötigen, als auch als Regulator der Zelldifferenzierung in den Zellen, die große Mengen davon aufnehmen. Gleichzeitig ist labiles Häm hochgradig zytotoxisch, da es Entzündungen fördert, und es trägt zur Aktivierung von Zelltodprogrammen bei. Aus diesem Grund müssen Organismen den Pool an labilem Häm durch dessen Abbau und Kompartimentierung genauestens kontrollieren. Obwohl der Häm-Stoffwechsel ausgiebig erforscht wurde, sind die Mechanismen, die seinen Transport regulieren, und die zugrunde liegenden regulierten Prozesse noch weitgehend unbekannt. Um neue Gene zu identifizieren, die am Häm-Transport beteiligt sind, haben wir ein CRISPR-basiertes genetisches Screening durchgeführt, das Häm als zytotoxischen Selektionsdruck nutzt. Die Deletion von SLC20A1 bewirkte die stärkste Resistenz gegen den Häm-induzierten Zelltod, unabhängig von seiner Funktion als Phosphattransporteur. In-vivo verursachte die konditionale Deletion von Slc20a1 eine sich nicht auflösende Anämie, die durch eine beeinträchtigte Erythroblasten-Differenzierung und eine fehlende Expansion des Pools der roten Pulpa-Makrophagen (RPM) gekennzeichnet war. Um die spezifischen zellulären Beiträge von Slc20a1 zu entschlüsseln, haben wir das Gen entweder in den erythroiden oder myeloischen Linien konditional deletiert. Erythroide-spezifische Slc20a1-Deletion verursachte eine Blockade der terminalen Erythropoese im Pro-Erythroblasten-Stadium und führte zu embryonaler Letalität um E12,5. Dies deutet darauf hin, dass Slc20a1 für die terminale erythroide Differenzierung essentiell ist. Um die durch Slc20a1-Deletion veränderten Prozesse zu klären, analysierten wir das Transkriptom von Slc20a1-deletierten Pro-Erythroblasten und beobachteten die Aktivierung von Häm-Mangel-Reaktionsprogrammen. Die myeloidspezifische Slc20a1-Deletion hatte keinen Einfluss auf den RPM-Pool im Steady-State. Bei einer Anämie-Herausforderung behinderte die Slc20a1-Deletion jedoch die Expansion des RPM-Pools durch Dysregulation der Expression von Spic, dem häm-induzierbaren Master-Regulator der RPM-Differenzierung. Zusammengenommen zeigten unsere Daten einen Zusammenhang zwischen Slc20a1 und dem Häm-Import. Um unsere Hypothese zu testen, haben wir SLC20A1-deletierte Zellen mit Häm herausgefordert und eine reduzierte Aufnahme des Moleküls und eine reduzierte Induktion seines abbauenden Enzyms HMOX1 beobachtet. Insgesamt zeigen unsere Daten zum ersten

Mal, dass SLC20A1 den Häm-Transport erleichtert und dass diese Funktion essentiell ist, um Erythroblasten und die RPM-Differenzierung zu unterstützen.

Publications arising from this thesis

Manuscript submitted on 07/05/2021:

“SLC20A1 facilitates heme transport and drives red pulp macrophage and erythroblast differentiation”

Federica Quattrone, Rui Martins*, Anna-Dorothea Gorki*, Anastasiya Hladik, Karin Lakovits, Manuele Rebsamen, Enrico Girardi, Andrea Alvarez-Hernandez, Florian Mayrhofer, Asma Farhat, Martin L. Watezenboeck, Emile van den Akker, Marieke von Lindern, Ingrid Simonitsch-Klupp, Riem Gawish** and Sylvia Knapp**.

* These authors contributed equally
** These authors contributed equally

Abbreviations

ABC	ATP-bindng cassette family
AGM	Aortic-Gonad Mesonephros
aka	also known as
ALA	5' Aminolevulinic acid
BFU-E	Burst-forming unit erythroid
BVR	Biliverdin Reductase A
Cas9	CRISPR associated protein 9
CD11b	Cluster of differentiation 11b, aka ITGAM
CD163	Cluster of differentiation 163
CD169	Cluster of differentiation 169, aka Siglec-1
CD71	Cluster of differentiation 71 ak Tfrc
CFU-E	Colony-forming unity erythroid
CMP	Common myeloid progenitor
CRISPR	Clustered Regularly Interspaced Short Palindromic Repeats
EBI	Erythroblastic island
eiF2α	Eukaryotic Translation Initiation Factor 2 Alpha
EIF2AK1	Eukaryotic Translation Initiation Factor 2 Alpha Kinase 1, aka HRI
Epo	Erythropoietin
EpoR	Erythropoietin receptor
ERFE	Erythroferrone
FACS	Fluorescence activated cell sorting
FeLV	Feline Leukemia Virus
FTH	Ferritin heavy chain
HAMP	Hepcidin
Hb	Hemoglobin
Hbe	Embryonic hemoglobin
Hbf	Fetal hemoglobin
HBM	Heme binding motifs
HCT	Hematocrit
HDL	High density lipoprotein
HMB	Hydroxymethylbilane
HMOX1	Heme oxygenase 1
HRG1	Heme regulated gene 1, aka SLC48A1
HRI	Heme regulated inhibitor, aka EIF2AK1
HRM	Heme regulatory motifs
HSC	Hematopoietic stem cell
ISR	Integrated stress response
LDH	Lactate dehydrogenase
LDL	Low density lipoprotein
LT HSC	Long term hematopoietic stem cell
MARE	MAF recognition elements
MEP	Megakaryocyte-Erythroid protenitor

MPP	Multipotent Progenitor
NES	Nuclear export signal
PBG	Porphobilinogen
PHZ	Phenylhydrazine
PIT1	Inorganic Phosphate Transporter 1, aka SLC20A1
PP	Protoporphyrin
PPG-III	Protoporhophyrogen III
RBCs	Red blood cells
ROS	Reactive oxygen species
RPM	Red Pulp Macrophages
scRNAseq	single-cell RNA sequencing
sgRNA	single guide RNA
SLC	Solute carrier transporter family
SLC20A1	Solute carrier family 20 member 1, aka Pit1
***Slc20a1*$^{\Delta CD169}$**	*CD169*$^{Cre/+}$*Rosa26*$^{Stop\text{-}eYFP/+}$*Slc20a1*$^{fl/f}$
***Slc20a1*$^{\Delta EpoR}$**	*EpoR*$^{GFP\text{-}Cre/+}$ *Slc20a1*$^{fl/fl}$
***Slc20a1*$^{\Delta LysM}$**	*CD169*$^{Cre/+}$*Rosa26*$^{Stop\text{-}eYFP/+}$*Slc20a1*$^{fl/f}$
***Slc20a1*^{iKo}**	*Rosa26*$^{ERCre/Stop\text{-}eYFP}$ *Slc20a1*$^{fl/fl}$
SLC48A1	Solute carrier family 48 member 1, aka HRG1
SLC49A1	Solute carrier family 49 member 1, aka FLVCR1
SLC49A2	Solute carrier family 49 member 1, aka FLVCR2
ST HSC	Short term hematopoietic stem cell
Tfrc	Transferrin receptor 1
TGF-β	Tumor growth factor beta
TLR4	Toll-like receptor 4
TNFa	Tumor necrosis factor α
TRAIL	TNF-related apoptosis-inducing ligand
URO	Uroporphobilinogen
VCAM1	Vascular Cell Adhesion Molecule 1
WBC	White blood cell

Acknowledgments

Each time a PhD student graduates and hands in the thesis, the section that I find myself always reading is this one: the acknowledgments. While the overall corpus of the thesis teaches something new about the world, this section teaches you something about the person behind that “Science”. I must confess, I highly procrastinated writing this part, in part because I highly value this section and I would like to present it at its best, and in part because I’m dreading the end of this journey. I have no fear for the challenges to come, rather, I’m taken by a nostalgia for the PhD adventures I shared with all of you, colleagues, friends and family.

The first thought goes to those who I shared with most of my time in the last years: the “Knappsies”. I’ll start with our *big potato* first, who first believed that the girl from Milan showing up at the interview in high heels and questionable fashion choices would have made a good PhD candidate. Thank you, Sylvia, for trusting me, for the teaching and the mentorship and for being a model of fierce woman in life as well as in science.

Thank you to all *present* and *past* “Knappsies” for being caring, smart, kind and playful colleagues and friends. Anastasiya and Karin, my lab-moms, providers of the craziest laughter during coffee breaks and the most amazing cakes, thank you for all the help, teaching and moral support you gave me from moment 0. Riem, Rui, Stefanie and Phil, the columns of the lab, thank you for all the moral support and the teaching. I’ve learnt a lot from you: to question everything critically (in science as well as in life), to stand-up for myself, to be (almost) consistent, and to value a good bottle of wine kept at -80°C for 1 hour and/or *outlaw* burgers during/after difficult days. Asma, Mariem, Sophie and Lisa, you are a great bunch of eye-rolling comic savages. Thank you for the moral support and the laughter, any other office feels empty without you. Nina and Thea, you are my columns, my advisors, my gossip gals, you are the good morning coffee breaks, the sewing, the game night, the friendship. Thank you for being with me.

Many thanks to CeMM, the Center for Molecular Medicine of the Austrian Academy of Sciences. Thank you for founding, putting together and allowing a community of awesome human beings to grow in a one-in-a-kind scientific playground.

A shout out and thank you to all collaborators, whose work and advice was essential to complete the work presented in this thesis.

A special thank you goes to you, Barbara. You helped me navigate through most of my PhD. It has been a blessing to have you by my side.

My dear *Super-duper cherry chums*, Lydia, Julia, Ruochen, Alex, Michi, Rob and Martin, thank you for being the best year-mates, travel buddies and party people I could have wished for.

A huge thank you to my (*no longer very*) local acquired family, Matthias and Ele, you danced with me across the rough, complicated, and joyous times. You provided comfort, food, solutions to *almost* all problems (including fridge meltdowns) and loads of hugs. Thank you.

Amore mio, Karolis, you are my lobster, my safe place. Thank you for your constant support and motivation, and for brightening my days.

E adesso voi, famiglia mia adorata. Grazie per tutto l'amore che mi avete dimostrato e dato. Grazie per essermi sempre stati vicini e aver creduto in me. Niente sfugge mai dal vostro sguardo protettivo e attento, nemmeno se mediato da uno schermo. Mi avete sempre dimostrato che nonostante ci siano migliaia di km, alpi e fiumi a dividerci, l'amore ci tiene sempre tutti uniti e che non c'è niente che un vostro *abbraccio di gruppo* non possa curare. Cari Gio, Franci, Willy, Ste, Cri, Giorgia, Nausicaa e Riccardo, grazie per non avermi mai lasciata sola, per tutte le volte che mi siete venuti a prendere in aeroporto nonostante significasse 3 ore di viaggio in macchina, per tutte le volte che siete venuti a trovarmi, per tutte le volte che vi siete fatti trovare a casa, per tutti i giochi, le risate e gli abbracci. Cari Mamma e Papà, con voi due il cerchio del dottorato si è aperto e concluso. E' con voi che sono arrivata a Vienna, dove vi siete assicurati che quel appartamento in affitto potesse ricordarmi un po' della nostra casa. Ed è da voi che son tornata quando è stato il momento di concludere questo capitolo della mia vita e scrivere la tesi. E' stato bello tornare a essere una studentessa che vive in casa dei genitori e regredisce un pochino. Se sono arrivata fino a questo punto è soprattutto merito vostro, questo lavoro lo dedico a voi. Infine, vi prometto che questa è davvero l'ultima tesi che scrivo. Sopportarmi nel periodo tesi per ben 3 volte è davvero troppo per chiunque.

1. Introduction

In this thesis the discovery of a novel gene involved in heme transport and its *in-vivo* functions will be presented. The work relates to several topics in the fields of cell biology, hematology and immunology. In this introductory chapter I will offer an overview about the current concepts of heme biology and erythropoiesis, with a focus on the contradicting roles of heme as cytotoxic yet functional molecule for the establishment of the erythropoietic niche. Further, an overview regarding the multiple, discrepant roles attributed to SLC20A1 will be provided. Together, this introductory chapter shall provide the background information required for understanding the rationale of the experiments and the observed results.

1.1 Heme is a double-edged sword

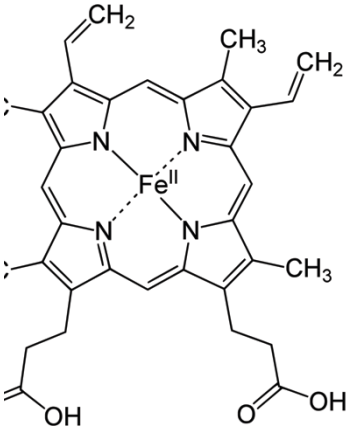

Heme is an amphiphilic molecule composed of an atom of ferrous (Fe^{2+}) or ferric (Fe^{3+}, i.e. hemin) iron surrounded by a protoporphyrin ring (Figure 1). The central iron can coordinate the binding to divalent gases and electrons[3], with different affinity depending on its oxidation state. Organisms use heme to execute numerous cellular processes such as mitochondrial respiration, oxygen storage, oxygen transport and transcriptional and translational control[4] (as described in "*1.1.1 The physiological roles of heme"*). Yet, heme can be highly deleterious for cells and organisms as it can sustain the generation of damage-prone reactive oxygen species (ROS) and it can dysregulate several signaling pathways[5] (as described in "*1.1.2 The pathological roles of heme"*). For these reasons, heme as such is considered a double-edged sword[6]. In this paragraph, these two opposing roles of heme will be introduced.

1.1.1 The physiological roles of heme

Heme can bind proteins via specific amino acids motifs interchangeably named heme binding motifs (HBMs)[7] or heme regulatory motifs (HRMs)[8] . Such motifs allow covalent- and non-covalent- interactions with heme and can ensure stable and long-

lasting interactions whenever heme serves a prosthetic group, or, short-lived interactions when heme serves as signaling molecule[4].

Heme as prosthetic group

Heme is an optimal prosthetic group for those protein complexes which require oxygen (e.g. hemoglobin, myoglobin, peroxidases) or electrons as reaction substrates (e.g. cytochromes) as it is capable to coordinate them[4]. When heme is employed as prosthetic group in protein complexes, it often binds to motifs located within deep pockets, characterized by low solvent accessibility[9]. In these interactions, heme's mobility is restricted[9] and its potential to act as a ROS catalyst is dampened, as the catalytically active iron ion is hindered[10].

Heme as signaling molecule

Heme's interaction with proteins can induce conformational changes, thereby leading to the activation of diverse downstream pathways[6]. When the interactors are transcriptional or translational factors, heme can regulate their activity and, consequently, it can influence cell differentiation[11,12]. Such heme-mediated regulation of cell-differentiation is particularly marked in those cell types handling large quantities of heme as erythrocytes[11,13] and the splenic iron-recycling macrophages (Red Pulp Macrophages, RPM)[12]. In these cells, numerous key master regulators of cell differentiation are modulated by heme. Between these BACH1[12], Spi-C[12], GATA1[11], and EIF2AK1[13] are of particular interest for the understanding of the presented work.

BACH1

The BTB and CNC homology (BACH) family consists of the transcriptional repressors BACH1 and BACH2. Both form heterodimeric complexes with the small MAF transcription factors and bind to specific DNA sequences named MAF Recognition Elements (MARE) (Figure 2)[14] (Figure 2A). Heme binding to BACH1's HBM, induces a conformational change to BACH1 inhibiting its binding to MAF, the exposure of its nuclear export signal (NES) and its consequent ubiquitination and degradation[14] (Figure 2B). Degradation of BACH1 de-represses the MARE sequences and allows binding of antagonist transcription factors, as the Nuclear Factor Erythroid Related 2

(NRF2) [14] (Figure 2B). NRF2 sustains the expression of several antioxidant response genes, among which heme oxygenase 1 (HMOX1)[14] (Figure 2B).

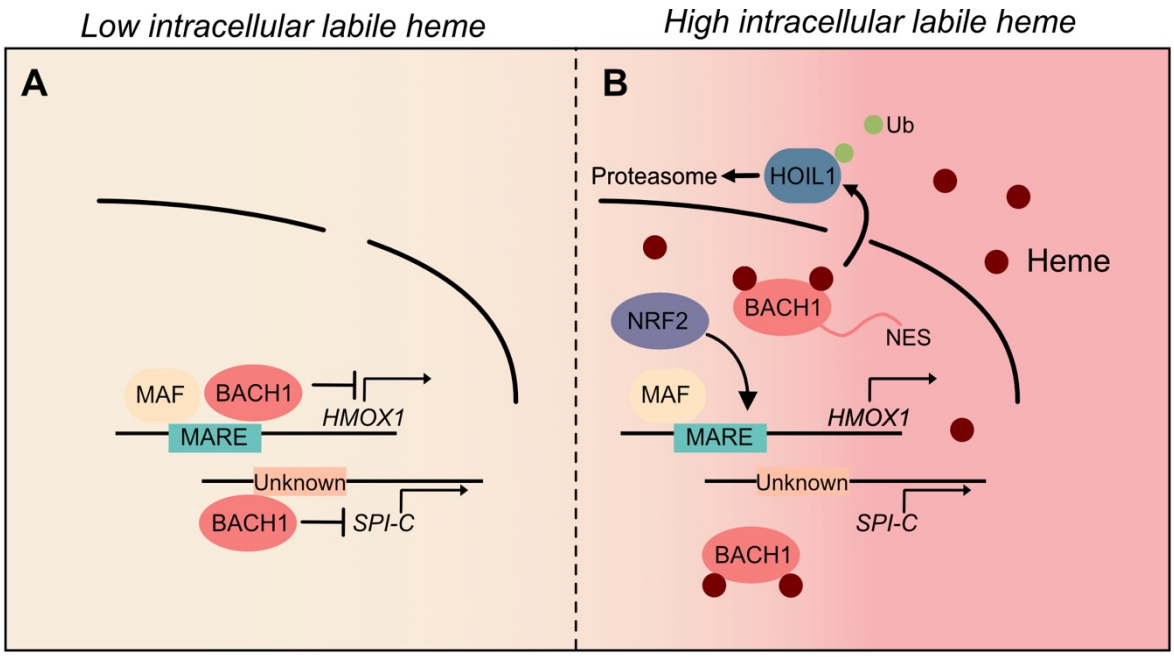

Figure 2 - Heme regulation of BACH1 activity and Spi-C transcription.
A) When intracellular labile heme concentration is low, BACH1 complexes with MAF. The complex binds to specific sequences (e.g. MARE in the promoter of HMOX1, unknown in the promoter of SPI-C) and represses gene expression (HMOX1, SPI-C). (B) When intracellular labile heme concentration is elevated, heme binding to BACH1 leads to its disassembly from the complex, its export from the nucleus (NES signal exposed), its ubiquitination (Ub) by HOIL and its proteasomal degradation

Spi-C

Spi-C is a transcription factor, member of the Ets family together with Ets-1, Elf-1, PU.1 (Spi-1) and Spi-B. Spi-C expression is regulated by heme-mediated BACH1 degradation (Figure 2B). As such, Spi-C is highly expressed in cells handling large quantities of intracellular labile heme, such as RPMs[15]. Here, Spi-C sustains the expression of several genes involved in iron and heme metabolism like the heme scavenger receptor CD163, HMOX1 and the iron exporter ferroportin (SLC40A1)[15]. In RPMs, Spi-C is essential to allow for their differentiation and erythrophagocytosis. Murine strains where Spi-C expression is depleted by gene knockout[15] or dysregulated heme import[16], exhibit a severely reduced RPM pool and suffer from splenic iron overload[15,16].

GATA1

GATA1 is a transcription factor regulating cell differentiation programs in numerous cell types such as: erythrocytes, megakaryocytes, dendritic cells (DCs), mast cells, eosinophils and basophils[17]. Within these different lineages, modulation of GATA1-driven transcription is multi-layered[17] depending on its interaction with alternative partners[18,19], on activated pathways[19,20 21], and on interacting molecules such as heme[21]. In erythrocytes, GATA1 enhances the expression of enzymes involved in heme synthesis such as ALAS2[11]. In turn, labile heme enhances GATA1 function[11]. The molecular mechanisms underlying such regulation are yet unknown. It is hypothesized that such mechanism can be BACH1-dependent or that heme could directly bind to heme regulated motifs (HERM) DNA sequences, thereby altering transcription [22].

EIF2AK1

EIF2AK1, also known as Heme Regulated Inhibitor (HRI)[23], is a protein kinase serving as regulator of the integrated stress response (ISR) together with PERK, GCN2 and PKR[24]. These kinases sense and respond to various stress-inducing stimuli such as: heme deficiency (EIF2AK1, HRI), endoplasmic reticulum stress (PERK), amino acid starvation (GCN2) or viral double stranded RNA (PKR)[24]. In normal or high intracellular heme conditions (Figure 3B), heme binds to EIF2AK1's HBM and inhibits its catalytic activity[13] (Figure 3B). In conditions of heme deficiency, EIF2AK1 remains active and phosphorylates eIF2α, thereby halting general protein translation and enhancing the selective translation of the transcription factor ATF4[13] (Figure 3A). In turn, ATF4 induces the expression of GADD34 (also known as PPP1R15A), which, together with PP1, can de-phosphorylate eIF2α[25], thereby breaking the feedback loop (Figure 3A).

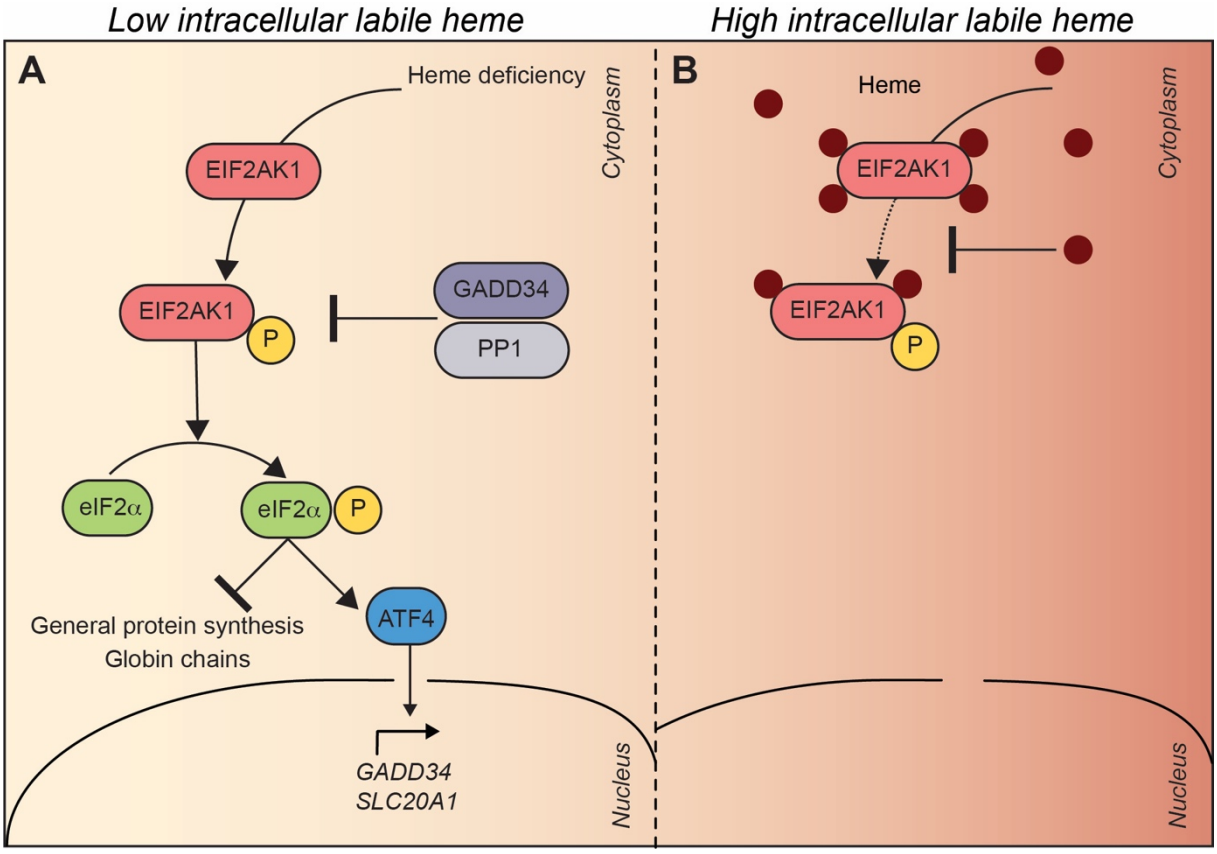

Figure 3 - Heme-associated regulation of EIF2AK1 activity.
(A) When intracellular labile heme concentration is low, EIF2AK1's HBMs are not bound by heme, allowing the kinase to auto-phosphorylate and phosphorylate eIF2α, thereby inhibiting general protein synthesis while sustaining selective translation of the transcription factor ATF4. In turn, ATF4 sustains the expression of genes such as *GADD34* and *SLC20A1*. (B) When intracellular labile heme concentration is high, EIF2AK1's HBMs are completely bound by heme, which inhibits its auto-phosphorylation and activation.

1.1.2 The pathological roles of heme

While heme is an essential molecule for core physiological processes, it can also be very deleterious. It has been demonstrated that heme can catalyze the synthesis of ROS and free radicals by reacting with H_2O_2, with low reactive organic peroxides or by sustaining NADH oxidase activation[26]. As such, heme causes unfettered protein, lipid and DNA damages[5]. Furthermore, the interaction of labile heme with specific targets can result in the activation or inhibition of specific signaling pathways, possibly leading to cytotoxic (Figure 4) or non-cytotoxic consequences[5] (Figure 5).

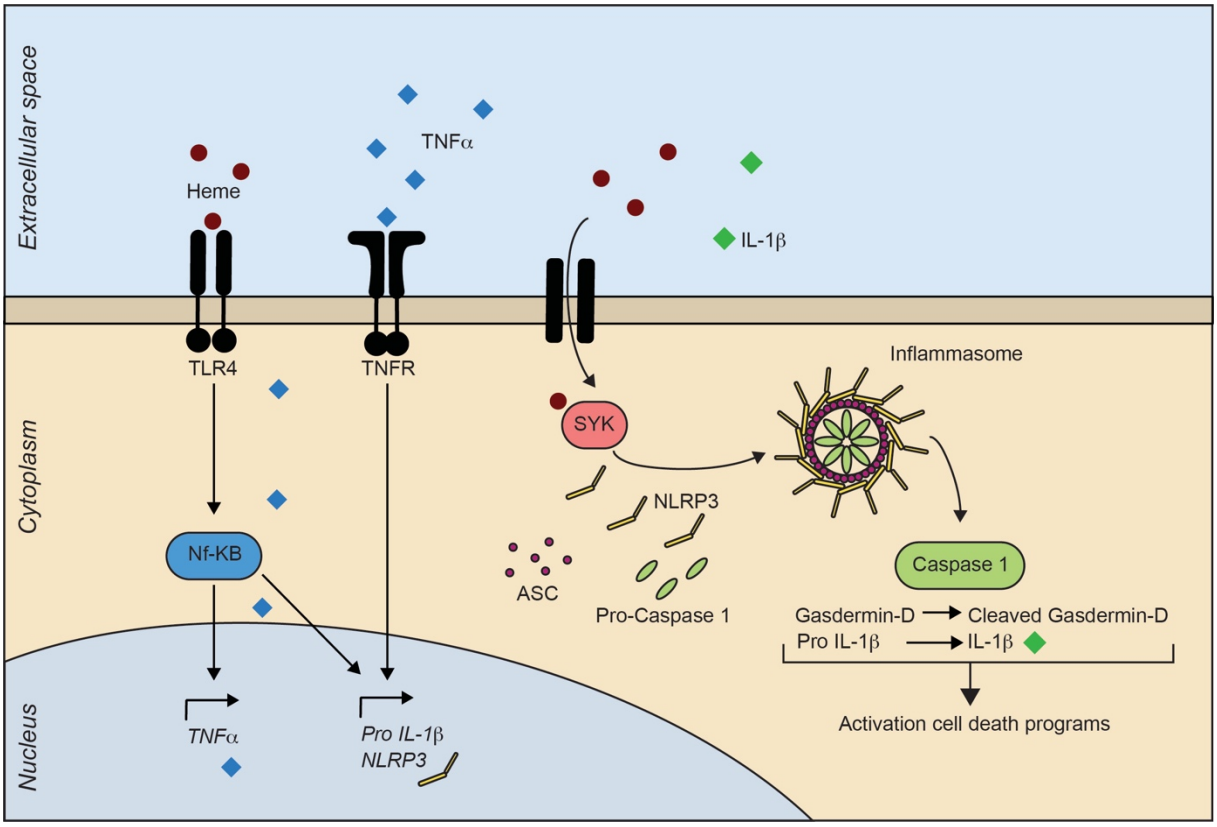

Figure 4 - Heme activates pro-inflammatory and programmed cell death pathways.
By binding to TLR4, heme induces the activation of the NF-kB pathway, thereby sustaining TNFα synthesis. Autocrine TNFα signaling and TLR4 activation induce the synthesis of key components of the inflammasome complex. Heme import causes the activation of the SYK kinase, thereby inducing inflammasome assembly, IL-1β secretion and activation of cell death programs.

Targeted, cytotoxic consequences of heme

Heme triggers pro-inflammatory responses via direct interaction with immune receptors and kinases (Figure 4). By binding to the pattern recognition receptor Toll-like receptor 4 (TLR4), heme activates the NF-kB signaling pathway and ultimately induces TNFα synthesis[27], NLRP3 and proIL-1β. Moreover, heme-mediated activation of the tyrosine-kinase Syk induces the assembly of the inflammasome and the activation of caspase1, leading to IL-1β maturation[28] and/or gasdermin-D cleavage (Figure 4). Finally, gasdermin-D cleavage causes the activation of the inflammatory programmed cell death program called pyroptosis[29] (Figure 4).

Targeted, non-cytotoxic consequences of heme

Not all heme-induced damages arise from its cytotoxic potential. In a previous investigation, our lab identified that the guanine nucleotide exchange factor DOCK8

can be bound by heme[30] (Figure 5). Upon heme binding, DOCK8 activates its target, the GTP-binding Rho family protein Cdc42 causing an alteration of actin cytoskeleton polymerization and remodeling[30] (Figure 5). Such dysregulation of actin cytoskeleton dynamics strongly impairs the capability of a broad range of innate immune cells to phagocytose and migrate[30] (Figure 5). Hence, in a model of Gram-negative sepsis, mice experiencing an increase of free serum heme have an impaired bacterial clearance and reduced survival[30].

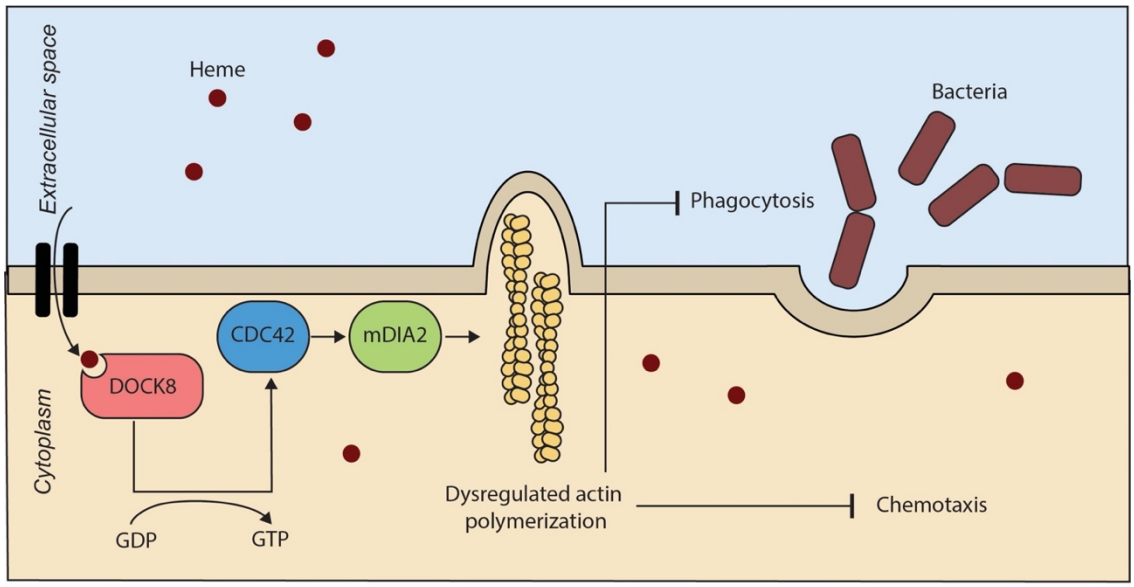

Figure 5 - Heme impairs leukocyte phagocytosis and chemotaxis.

Heme binding to DOCK8 causes the hyper-activation of the GEF. Next, DOCK8 activates CDC42, resulting in constant activation of mDIA2, and ultimately inhibits phagocytosis and chemotaxis (adapted from Martins et al., 2018)[1].

1.2 Regulation of heme metabolism

Organisms developed refined systems to exploit heme while minimizing its detrimental effects by controlling heme synthesis (as described in paragraph *"1.2.1 Heme synthesis"*), trafficking and compartmentalization (as described in paragraph *"1.2.2 Heme trafficking"*) and degradation (as described in paragraph*"1.2.3 Heme scavenging and degradation"*) (Figure 6).

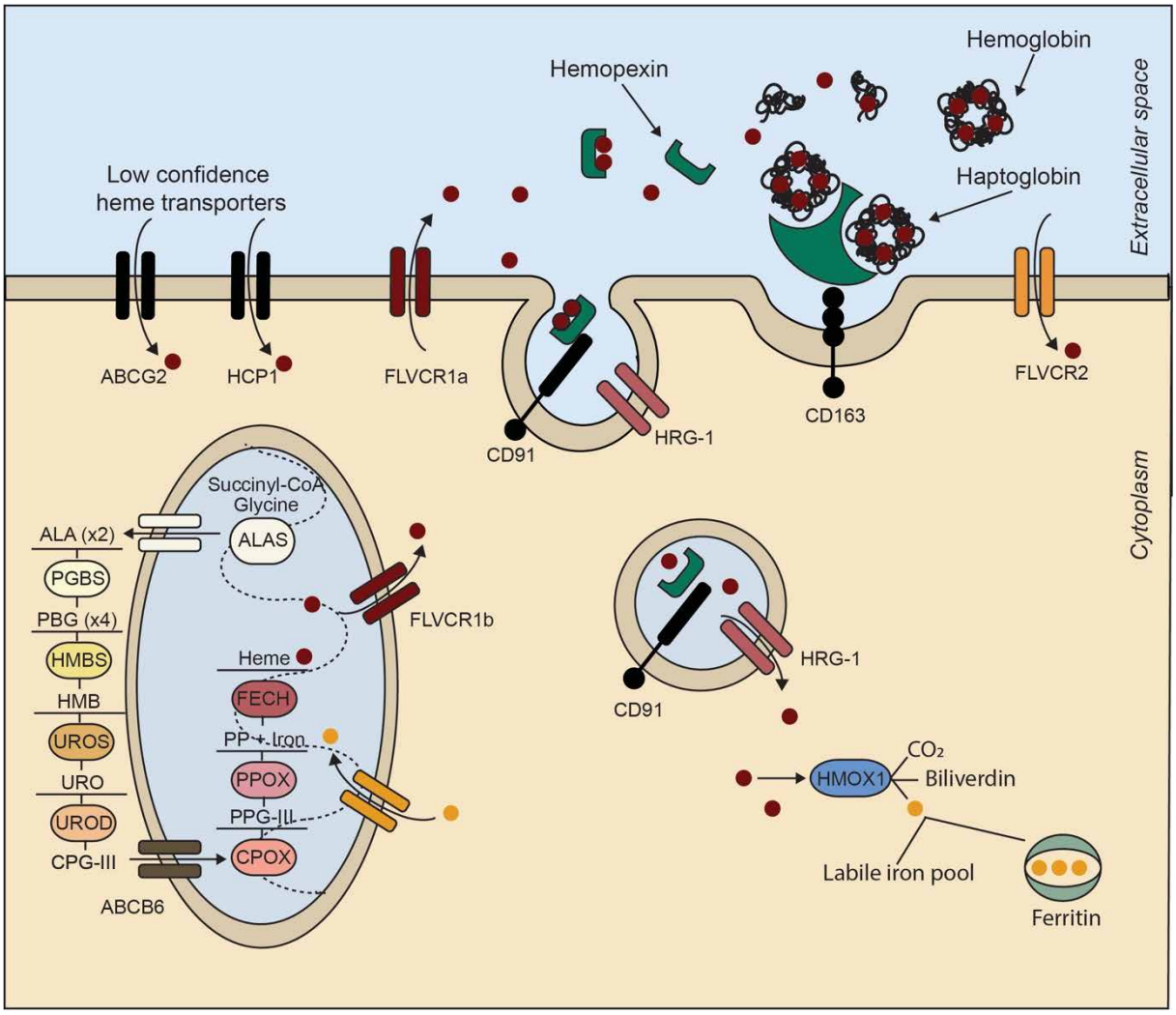

Figure 6 – Heme metabolism overview.
Heme is synthetized through a series of enzymatic reactions transforming the building blocks glycine and succinyl-CoA in protoporphyrin (PP). Addition of an iron ion to the PP ring finally generates heme, which is then exported to the cytosol through FLVCR1b. Heme import across the cytosolic membrane is initiated with the endocytosis of hemoglobin-loaded haptoglobin or heme-loaded hemopexin, respectively, and the membrane receptors CD91 and CD163. Upon acidification of the endocytic vesicle, heme is released and is directly imported by HRG1 and FLVCR2 into the cytosol. The low-confidence heme transporters ABCG2 and HCP1 might also participate in the heme import across the plasma membrane. Unbound intracellular heme forms the intracellular labile heme pool, which is further degraded via HMOX1.

1.2.1 Heme synthesis

In eukaryotes, heme synthesis occurs through multiple reaction steps occurring in mitochondria and the cytoplasm, which requires a controlled flux and compartmentalization of reaction intermediates (Figure 6). The first reaction step occurs in the mitochondrial matrix, where glycine and succinyl-CoA, a Krebs cycle reaction intermediate, are condensed into 5-aminolevulinic acid (ALA) in the presence of pyridoxal phosphate[31]. The reaction is catalyzed by ALA synthase (ALAS), an enzyme encoded in mammals by two genes with alternative expression: ALAS1 is ubiquitously expressed, while ALAS2 is uniquely expressed by erythroid cells. Next, ALA is exported to the cytosol and here two ALA molecules are converted into porphobilinogen (PBG) by PBG synthase (PBGS). Then, four PBG molecules are transformed into hydroxymethylbilane (HMB) by HMB synthase (HMBS). HBM is then inverted and cyclized into uroporphobilinogen (URO) by URO synthase (UROS) and, finally, decarboxylated by URO decarboxylase (UROD) into coproporphyrinogen (CPG-III). CPG-III is then transported by the putative transporter ABCB6 into the inner mitochondrial space, where it is converted by the coproporphyrinogen oxidase (CPOX) into protophorphyrogen III (PPG-III), and then in protoporphyrin (PP) by PP oxidase (PPOX). In the last step, the enzyme ferrochelatase (FECH) inserts an ion of iron into the PP ring and generates heme. The newly synthesized heme can then be exported from the mitochondria into the cytosol by FLVCR1b[32] (Figure 6).

1.2.2 Heme trafficking

The transporters of heme and its metabolic intermediates are not entirely known. Given the amphiphilic nature of heme, it has been speculated for a long time that heme might passively diffuse through cell membranes[33]. However, given the pro-oxidant and cytotoxic potential of heme, it would be surprising if organisms would have not evolved mechanisms to transport heme via controlled mechanisms to prevent potential oxidation-mediated membrane damages. Though we cannot exclude that heme might passively diffuse through membranes, novel evidence highlighted the involvement of Solute Carrier Protein (SLC) and the ATP-binding cassette (ABC) transporters in heme import[34]. Among those, HRG1 (SLC48A1)[35] and FLVCR2[36] are involved in the import of heme from the extracellular compartment into the cytosol through endocytic vesicles[34] (Figure 6). The interaction of heme-loaded scavenger complexes with receptors, as CD91 or CD163, induces the formation of endocytic vesicles[6] (Figure 6).

Upon acidification of such vesicles, the heme-complexes are disassembled, and heme is released and can be imported into the cytoplasm via HRG1[35] and FLVCR2[36]. In addition to these transporters, ABCG2[37] and HCP1 (SLC46A1)[38,39] have also been attributed the role of heme importers, however the findings supporting such hypotheses are controversial. Finally, FLVCR1a (SLC49A1a)[32] and FLVCR1b (SLC49A1b)[32] export heme, respectively, from the cytosol and mitochondria(Figure 6). The expression of heme transporters varies across tissues, cell-types and activation states, highlighting a specific functional role for each one of the transporters.

HRG1

Heme Regulated Gene 1, HRG1, localizes in the plasma membranes and in endocytic vesicles. HRG-1 was originally identified as a putative heme importer by screening of heme-regulated genes in the heme auxotroph organism *C.elegans*[40]. *In-vivo* HRG1 is expressed by those cell types handling high concentrations of heme as RPMs[35] and erythroblasts[40]. Mice lacking *Hrg1 (Hrg1$^{-/-}$)* have a reduced and functionally impaired pool of RPMs. *Hrg1$^{-/-}$* RPMs cannot uptake heme from endocytic vesicles, therefore the heme accumulates and precipitates forming hemozoin. Moreover, *Hrg1* deletion impairs erythropoiesis on a yet undefined basis[16,40].

FLVCR2

Feline leukemia virus C receptor 2 (FLVCR2, i.e. SLC49A2) is a putative heme importer[36]. Since it is a paralogue of the known heme exporter FLVCR1, it was hypothesized that it could also be involved in heme transport. However, differently from FLVCR1, its expression is specific to the endothelium and pericytes of the central nervous system[41]. Deletion of FLVCR2 causes perinatal lethality as a consequence of dysregulated cerebral angiogenesis [41].

FLVCR1

The Feline leukemia virus C receptor 1 (*FLVCR1*, aka *SLC49A1*) gene encodes for two functionally distinct exporter isoforms, FLVCR1a and FLVCR1b, which differ in their sub-cellular localization. FLVCR1a is localized in the plasma membrane and mediates the export of heme from the cytosol to the extracellular space. FLVCR1b is localized in the mitochondrial outer membrane and exports heme from the

mitochondrial matrix to the cytosol[42]. The gene is expressed in many different cell types and tissues, therefore, it is believed to have housekeeping functions. The first indication for a role in heme transport came from the observation that it is highly expressed by cell lines having large intracellular heme pools[43]. *In-vivo*, mice lacking both exporter isoforms (*Flvcr1*$^{-/-}$) die during embryonic development around E12.5[43]. The lethality is a result of severe anemia, caused by a block during terminal erythroid differentiation at the pro-erythroblast stage. Furthermore, fetuses are characterized by skeletal and limb malformations. When only *Flvcr1a* is specifically deleted (*Flvcr1a*$^{-/-}$), mice succumb between E14.5 and birth as a consequence of severe vascularization defects[32]. Compared to *Flvcr1*$^{-/-}$, *Flvcr1a*$^{-/-}$ mice show skeletal malformations but do not have erythropoietic alterations[42].

ABCG2

ABCG2 is a multi-drug resistance gene which allows the transport of multiple substrates across the plasma membrane, including heme[37]. The link of the transporter to heme metabolism is clear in mice lacking the transporter. *In-vivo Abcg2* deficiency results in protoporphyria characterized by elevated phototoxicity and accumulation of unconjugated bilirubin (an intermediate of heme degradation)[37].

HCP1

Heme carrier protein 1 (HCP1) was identified as putative heme transporter by differential gene expression analysis of intestinal mucosa specialized in heme import (duodenal) and intestinal mucosa not transporting heme (ileal)[38]. However, further studies demonstrated that the transporter has a 10-fold higher affinity to folate and that patients lacking HCP1 suffer from folate malabsorption[38].Therefore, while it might be possible that the transporter can transport heme, its main cargo is folate.

1.2.3 Heme scavenging and degradation

To limit the cytotoxic potential of heme, organisms evolved numerous mechanisms aiming at scavenging heme. Such mechanisms range from molecule binding, to its compartmentalization and degradation and can be broadly classified in extracellular and intracellular (Figure 6).

Extracellular scavenging

The majority of heme present in our body runs in the peripheral blood, packed in red blood cells (RBCs) which contain up to 0.15 mM heme each[44]. During hemolysis hemoglobin is released in the bloodstream and, upon its oxidation, heme is released. In the plasma numerous heme- and hemoglobin- binding proteins are present, such as hemopexin, haptoglobin, albumin, low density lipoprotein (LDL) and high density lipoprotein (HDL)[6].

Hemopexin

Hemopexin is the plasma protein with the highest binding affinity to heme[31]. Hemopexin is an acute-phase protein synthetized in the liver upon inflammation and regulated by several cytokines as IL-6, IL-1β and TNF-α [31]. Upon heme binding, the complex binds to the CD91 (i.e. LRP1) receptor and is endocytosed.

Haptoglobin

Haptoglobin is a plasma glycoprotein, capable of binding to hemoglobin. Haptoglobin-hemoglobin complexes bind to the myeloid-cell expressed CD163 receptor and get endocytosed. The clearance of haptoglobin-hemoglobin complexes is rapid: in murine models its half life is less then 50 minutes[45].

Albumin, LDL and HDL

Other plasma proteins, such as albumin and lipoproteins, including the low-density lipoprotein (LDL), or high density lipoprotein (HDL) can bind to heme. Though their affinity to hemoglobin or heme is lower than haptoglobin or hemopexin, given their steady and high abundance in the plasma, they are believed assist in heme scavenging during hemolytic crises, once the hemopexin capacity is exhausted[46].

Intracellular scavenging

When the intracellular labile heme levels are in a tolerable range for the cell, the molecule can be employed into hemeproteins or it can serve regulatory functions[47]. However, when the intracellular labile heme pool increases and becomes dangerous, the cell can remove it or degrade it to dampen its cytotoxic potential(Figure 6). Heme export is mediated by FLVCR1a as described in the previous paragraph. Heme

degradation (i.e. heme catabolism) is a multi-step process consisting of two complementary pathways, one dedicated to the degradation of the porphyrin and one to recycle iron[6]. The first reaction step is catalyzed by the heme oxygenase, which cleaves the α-methene bridge of the protoporphyrin causing the release of the iron atom and the production of biliverdin and carbon monoxide (CO). Biliverdin is then converted into bilirubin by biliverdin reductase (BVR). In mammals, bilirubin is finally secreted in the bloodstream and delivered to hepatocytes where it is converted in bile pigments and secreted in the small intestine. The iron ion, liberated during the first reaction step of heme degradation, can either become part of the labile iron pool or it can be stored in ferritin.

1.3 Erythropoiesis

Erythropoiesis is a multi-step process that allows a population of committed self-renewing stem cells to provide continuous replenishment of mature red blood cells (RBCs) (Figure 7). The process happens in different specific tissues, which vary in different developmental stages (as described in "*1.3.1 Erythropoiesis across development"*). Erythropoiesis can be divided into two main parts: an initial phase, when stem cells proliferate and commit to the erythroid lineage giving rise to erythroblasts (as described in "*1.3.2 Stem cell expansion and commitment to the erythroid lineage*"), and a second phase, named "terminal erythroid differentiation" (as described in "*1.3.3 Terminal erythroid differentiation*"), when the erythroid progenitors complete the differentiation into mature RBCs by producing hemoglobin (i.e. hemoglobinization, as described in "*1.3.4 Regulation of hemoglobinization*"). Terminal erythroid differentiation happens in a highly specialized niche, named the erythroblastic island (as described in "1.*3.5 The erythroblastic island*") (Figure 7).

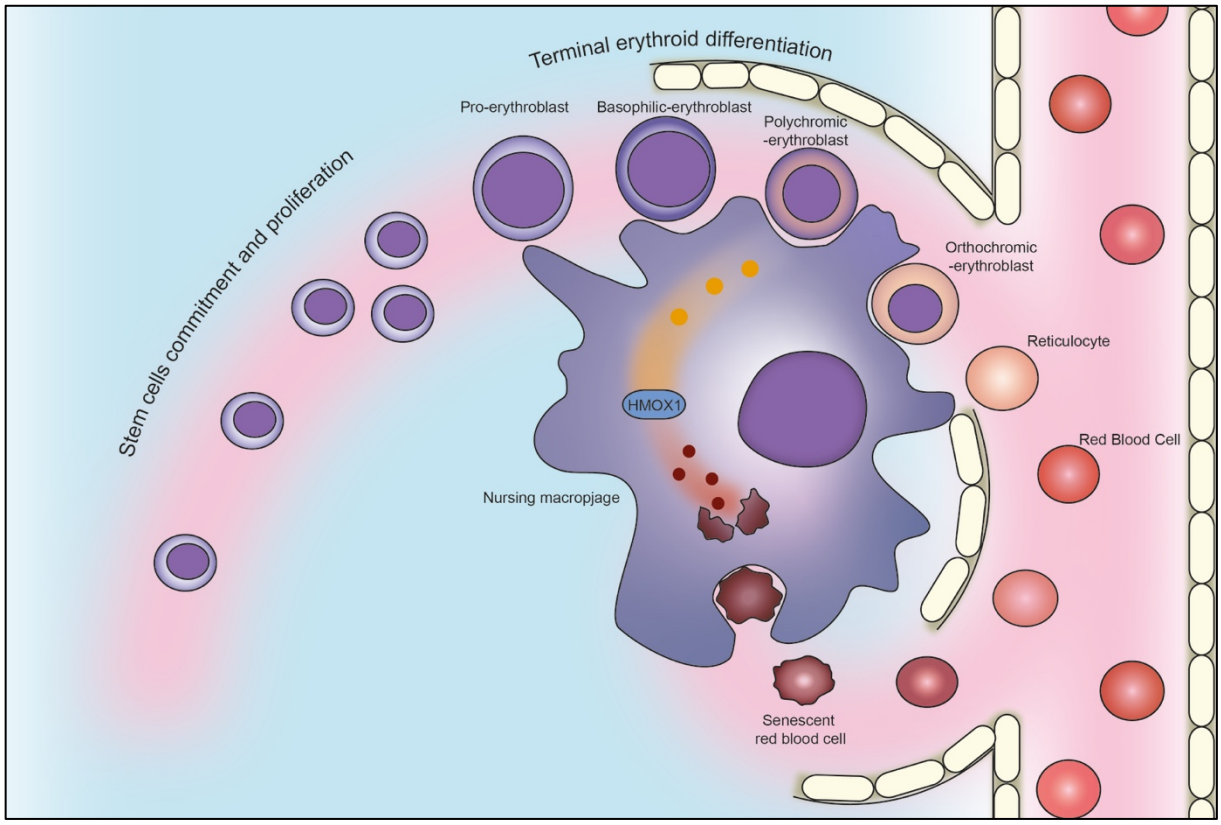

Figure 7 - Erythropoiesis overview.
Erythropoiesis can be divided into two phases, an initial phase when stem cells commit to the erythroid lineage and a second phase, the terminal erythroid differentiation. This second phase happens in the erythroblastic island, where a central nursing macrophage supports the differentiation of erythroid precursors. Upon completion of differentiation, reticulocytes mature into RBCs. Senescent RBCs can return to the splenic erythroblastic islands where they are engulfed by red pulp macrophages, which recycles heme and provide iron necessary to sustain the developing erythroblasts.

1.3.1 Erythropoiesis across development

In mammals, the organs where erythropoiesis takes place (i.e. erythropoietic organs) vary across development[2] (Figure 8). During intrauterine life, the first wave of erythropoiesis, known as primitive erythropoiesis, originates in the yolk sac (murine embryonic day E7.5, human embryonic day d17) and it is followed by the fetal definitive erythropoiesis[48-50]. Definitive erythroid progenitors emerge in the yolk sac or in the aortic gonad mesonephros (AGM, murine E10.5, human d27) and seed in the fetal liver (murine E11.5, human d30)[2,48]. Lastly, the erythroid progenitors transition and seed to their definitive location, the bone marrow (murine E16.5, human week 10)[2,48]. After birth, in humans, steady-state erythropoiesis occurs exclusively in the bone marrow, whereas during pathological states requiring an increase of erythrocyte production (i.e. stress erythropoiesis), erythropoiesis might occur additionally in the spleen. Differently from humans, in mice steady-state erythropoiesis happens in the bone marrow and, marginally, in the spleen[2,48,50]. Upon stress erythropoiesis, the spatial constraints of the bone marrow cumber the expansion of the erythroid progenitors, which, thereby, migrate and differentiate in secondary extramedullary organs such as the spleen and liver [51].

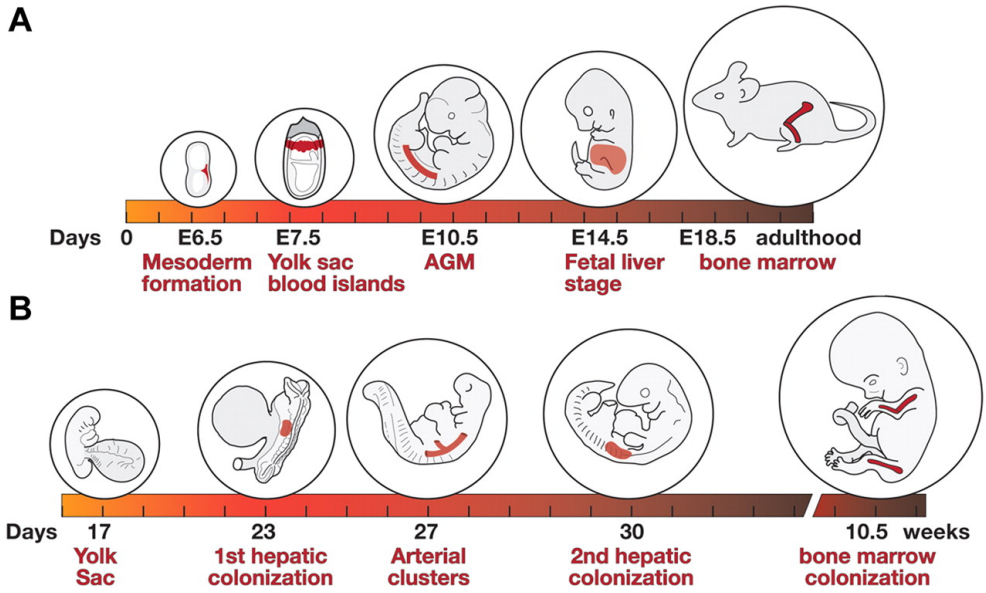

Figure 8 - Erythropoiesis across development

Figure 8 – Erythropoiesis across development.
The erythropoietic organs change throughout murine (A) and human (B) embryogenesis, fetal development and adulthood (from Baron et al., 2012)[2].

1.3.2 Stem cell expansion and commitment to the erythroid lineage

In the initial phase of erythropoiesis, hematopoietic stem cells (HSC) proliferate and get progressively committed towards the erythroid lineage. In this paragraph, the path and modalities of stem cell commitment towards the erythroid lineage will be described.

The path from stem cell to committed progenitors

Differentiation trees summarize the commitment trajectory and differentiation pseudo-time of hematopoietic cells. An accurate definition of the differentiation tree is still a matter of debate[52]. According to the classical model, a cell would proceed step-wise in its differentiation, choosing at each step of the way between two alternative fates[53] (Figure 9A). The more choices the cell makes, the more it would commit to a certain lineage and the less it would be capable to transdifferentiate into a different lineage. According to this model, the erythroid progenitors arise from the megakaryocyte-erythroid progenitor (MEP), which is downstream the common myeloid progenitor (CMP), the short-term HSC (ST-HSC) and the long-term HSC (LT-HSC)[50]. Novel findings coming from single cell RNA sequencing (scRNAseq) challenge this model. It is now understood that cell differentiation does not follow defined stages, but it rather differentiates as a continuum of stages. Such continuum is observable only using high-throughput analysis such as scRNAseq and, until today, no new antigenic markers have been identified to discriminate every stage. Furthermore, the differentiation roadmaps have also been challenged. The two most prominent models argue in favor of a flat-hierarchy (Dick model)[54] or in favor of a conventional hierarchy (Socolovsksy model)[55]. According to the Dick model[54], during fetal development the MEP originate directly from the ST-HSC or from the oligopotent intermediate CMP. Whereas, during adulthood, the oligopotent intermediates (CMP) are absent and, thus, terminal differentiation arises uniquely from unipotent cells. According to the Socolovsky model[55], a multipotent progenitor diverges between the myeloid/lymphoid fate or the erythroid/megakaryocyte/basophil/mast-cell fate[55]. Approaching terminal erythroid differentiation, the unipotent erythroid progenitors proliferate, giving rise to the earliest erythroid colonies (i.e. burst-forming units, BFU-E) and then to late-stage erythroid colonies (CFU-E) and finally to erythroblasts, which will undergo terminal erythroid differentiation[55].

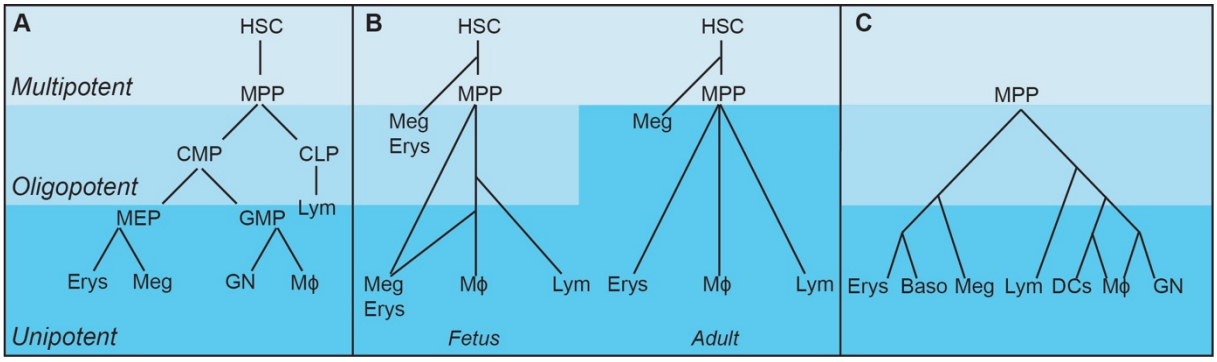

Figure 9 - Stem cells differentiation trees
Differentiation trajectories according to the classical (A), the Dick (B) and the Socolovsky (C) models. List of abbreviations used: HSC: hematopoietic stem cell, MPP: multipotent progenitor, CMP: common myeloid progenitor, CLP: common lymphoid progenitor, MEP: megakaryocyte-erythroid progenitor, GMP: granulocyte-myeloid progenitor, Erys: erythroid lineage, Meg: megakaryocyte lineage, GN: granulocyte-neutrophil lineage, MΦ: myeloid lineage, Lym: lymphoid lineage, Baso: basophil lineage, DCs: dendritic cell lineage.

Transcriptional regulation of erythroid commitment

Progressive cell specification depends on the balance between transcription factors, which promote alternative differentiation programs. GATA1 and KLF1 are the core transcription factors regulating erythropoiesis[17 56,57]. Mice lacking any of these genes die during embryonic development because of severe anemia[58,59]. The springboard to erythroid specification is the GATA-switching phenomenon, whereby GATA2 is downregulated and GATA1 is upregulated. GATA2 is an important transcription factor for stem-ness[17]. GATA1 enhances the expression of genes required for the erythroid specification, while repressing the expression of those genes driving alternative differentiations as PU.1, a key transcriptional factor of myeloid program[17]. As previously described, GATA1 enhances heme synthesis, which, in turn, positively regulates GATA1[11]. Similarly, KLF1 regulates genes required for hemoglobinization, however, it carries out its function at a later pseudotime-point than GATA1[60].

1.3.3 Terminal erythroid differentiation

Terminal erythroid differentiation consists of all those processes leading the committed erythroid progenitors to complete their differentiation into enucleated mature erythrocytes[61]. During this process, erythroblasts proliferate and progressively produce large quantities of hemoglobin[62] in response to a local milieu of hormones (as erythropoietin, Epo), cytokines (as TNF-α, INF-γ and TGF-β), and nutrients (as iron). At each cell division, the erythroblasts reduce their size, condense and, finally, expel

their nucleus[63]. Furthermore, hemoglobin accumulation changes the histological coloring of erythroblasts cytoplasm, transitioning from a more basophilic coloring of the immature forms to a more acidophilic color of the mature ones. Therefore, the terminally differentiating erythroblasts can be morphologically distinguished into six subsets: (1) pro-erythroblasts, (2) basophilic erythroblasts, (3) polychromatic erythroblasts, (4) orthochromic erythroblasts, (5) reticulocytes and (6) mature erythrocytes. Similarly, differential expression of membrane epitopes allows distinction of the stages [63,64]. The transition between stem-cell expansion phase and the terminal erythroid differentiation is characterized by the loss of expression of c-Kit and the induction of the erythropoietin receptor (EpoR) and Ter-119 (mouse) or GypA (humans) expression [64]. Only upon the acquisition of EpoR do the cells become sensitive to Epo. Meanwhile, terminally differentiating erythroblasts progressively lose the membrane expression of the transferrin receptor CD71 and CD44[63,64].

1.3.4 Hemoglobinization

Hemoglobin production is the core event driving terminal erythroid differentiation. For this purpose, the erythroblasts expand their protein synthesis capability by expanding the ribosome compartment[65], as well as their intracellular labile iron pool by its extracellular uptake. In this paragraph a brief description of the protein complex and the regulation of its synthesis will be provided.

Hemoglobin

Hemoglobin is the main functional protein complex of the erythrocyte, consisting of two sets of α-globin chains, two β-globin chains and four heme molecules. The type of α and β chains produced vary across organism development thus generating different forms of hemoglobin. During intrauterine development, the first hemoglobin types to be synthetized are the embryonic (HbE), followed by the fetal (HbF)[66] type. These hemoglobin types are characterized by higher oxygen affinity, allowing the binding of oxygen even in tissues characterized by low relative O_2 pressure (pO_2) as the placenta[67]. Right before birth, the organism starts producing the adult hemoglobin (Hb), characterized by an oxygen affinity tailored for the binding of O_2 in tissues characterized by higher pO_2 as the lungs [67]. The exchange between the different globin

genes expressed throughout development (i.e. globin switching) is regulated at the epigenetic level[66].

Regulation of hemoglobin synthesis

To assemble a functional hemoglobin, the cell has to produce stochiometric quantities of globin chains and heme[68], as the unbalanced production of either of the two is cytotoxic[69]. As we described previously, an increase of intracellular free heme can cause oxidative damage or disrupt cellular pathways[69]. Whereas excessive globin chain synthesis results in the precipitation of unbound globins, thereby causing cytotoxicity[70]. For this reason, hemoglobinization must be tightly regulated. The cell senses the labile heme as a quality-control parameter of hemoglobinization: its expansion or reduction can indicate that heme and globin chain synthesis is unmatched[23]. Upon expansion of the labile heme pool, BACH1 is degraded and, consequently, its targets are induced, between those HMOX1[14]. HMOX1 degrades free heme and, thereby, it reduces the labile heme pool. Furthermore, increased intracellular heme upregulates ribosomal genes expression via non-clarified means[65]. Conversely, the reduction of labile heme pool de-represses HRI, which phosphorylates eiF2a ultimately inhibiting globin chain synthesis[23], as previously described.

1.3.5 The erythroblastic island

The erythroblastic islands (EBI) are the anatomical functional units of definitive, homeostatic and stress terminal erythroid differentiation[71]. The EBIs locate in both medullary and extramedullary erythropoietic organs[71]. According to current understanding, EBIs are formed by a central nursing macrophage surrounded by differentiating erythroblasts. The central macrophages are characterized by high phagocytic activity and absence of respiratory burst[72]. Morphologically these macrophages are very large (with a diameter > 15 μm) and elaborately branched, probably to cradle erythroblasts. Adhesion molecules guarantee the reciprocal binding of the EBI components. The $\alpha 4\beta 1$ integrin (i.e. Very Late Antigen 4, VLA-4), the erythroid macrophage protein (Emp) and the intracellular adhesion molecule 4 (ICAM4) on the erythroblast side, respectively, interact with the vascular adhesion molecule 1 (VCAM-1), Emp and αV integrin on the central macrophage side[73]. Moreover, indirect interactions are established within the EBI by secretion of cytokines and soluble factors [74]. Overall, the interactions within the EBI aim at regulating terminal

erythroid differentiation mostly by providing signals promoting or restricting terminal differentiation, by phagocytosing and digesting the expelled nuclei and by regulating heme and iron recycling[72].

Central macrophages sustain erythroblast proliferation and survival

In-vitro reconstruction of EBIs highlighted that macrophages enhance erythroblast proliferation[75], survival[76] and expansion[77]. The direct interaction of the macrophages induces a shortening of the G0/G1 phase of the cell cycle[75], which is required to switch from CFU-E self-renewal to terminal erythroid differentiation[55,75]. Moreover, the central macrophages produce the insulin-like growth factor 1 (IGF1) and bone morphogenic factor 4 (BMP4), further sustaining the expansion of committed erythroid progenitors[78,79].

Central macrophages induce erythroblasts apoptosis

In response to environmental stimuli, central macrophages can synthetize and release cytokines as TNF-α, INF-γ and TGF-β. Such cytokines inhibit erythroblast proliferation and differentiation, while sustaining the induction of pro-apoptotic pathways[73]. TNF-α induces the cleavage of the master erythroid transcription factor GATA1, resulting in decreased proliferation and activation of pro-apoptotic pathways[80]. Likewise, INF-γ stimulation induces TRAIL synthesis in both erythroblasts and central macrophages thereby leading to an inhibition of differentiation[81]. TGF-β, instead, has a double feature of promoting terminal erythroid differentiation while inhibiting cell proliferation[82].

Central macrophages supply iron to developing erythroblasts

In addition to paracrine signaling, central macrophages serve as an iron source for the developing erythroblast[62]. It was initially believed that the majority of iron employed by the erythroblasts to synthetize heme would come from plasma di-ferric transferrin[83]. However, transferrin cannot be the sole iron source given that patients and mice lacking transferrin can still produce mature RBCs, though microcytic and hypochromic[84]. Therefore, this evidence indicated that iron could be supplied through yet undiscovered pathways[83]. Given that the central macrophage is equipped with iron and heme-handling proteins[85-87], it was speculated that macrophages might directly deliver iron to the developing erythroblasts. *In-vitro* models showed that the central

macrophages can synthetize and export iron-loaded ferritin to the erythroblasts, thereby equipping them with the means to sustain hemoglobinization[88]. Furthermore, given the expression of heme transporters on the membrane of both components of the EBI, there is the possibility that also heme could be delivered from the central macrophage to the developing erythroblast[83]. This would be particularly evident in the red pulp macrophages of the spleen, which serve both as erythrophagocytes and as central nurse cell during stress erythropoiesis[12,89].

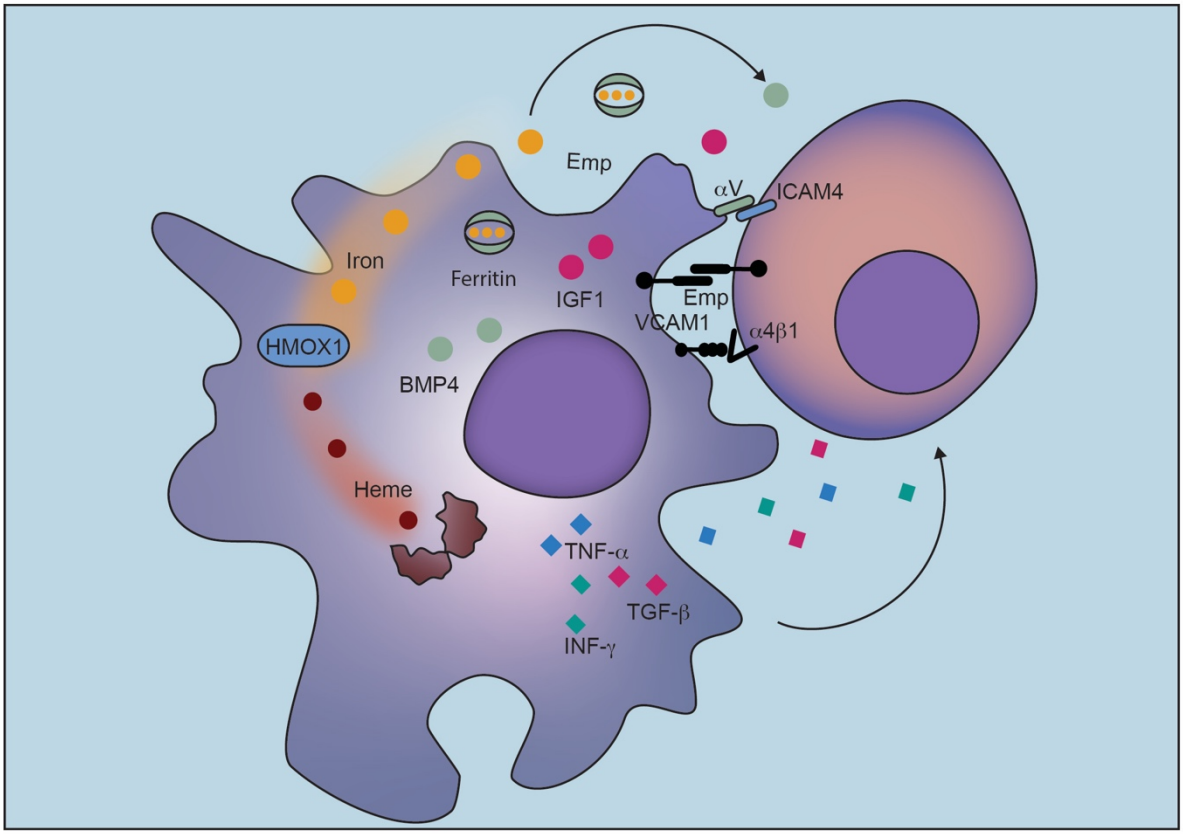

Figure 10 - Interactions in the erythroblastic island.
The adhesion is mediated via the expression of the macrophage adhesion molecules αV, Emp, VCAM1 and the erythroid adhesion molecules ICAM4, Emp and α4β1. The macrophage promotes erythroid proliferation by producing IGF1 and BMP4, and erythroid differentiation by delivering iron or iron loaded ferritin derived from heme recycling. The macrophage can also block erythroid differentiation by promoting erythroid apoptosis via TNF-α, INF-γ and TGF-β signaling.

1.4 Stress erythropoiesis

The term “stress erythropoiesis” defines all those processes allowing for an increased production of mature RBCs in response to diverse (patho)physiological states, such as development or anemia. The cellular and molecular mechanisms underlying stress erythropoiesis are different from steady state erythropoiesis[90]. While in homeostasis RBCs are constantly produced as a flux, during stress erythropoiesis, RBCs are produced as a bolus[51]. For this purpose 1) the erythropoietic pool (as described in “*1.4.2 Terminal stress erythropoiesis*”) and 2) the central nursing macrophage pool (as described in “*1.4.2 Expansion of the central nursing macrophages*”) expand to multiply the available erythroblastic islands, thereby guaranteeing increased RBCs production.

1.4.1 Expansion of the erythropoietic pool

Anemias have several different etiologies spanning from acute blood loss, intravascular hemolysis to inflammation. The reduction of peripheral blood oxygenation activates and stabilizes the Hypoxia Inducible Transcription factors, which in turn, activate a compensatory response to increase RBCs production. The set of all the activated process to increase RBCs production is defined stress erythropoiesis. During stress erythropoiesis, the erythroblasts proliferate and differentiate under the stimulation of differentiation signals, which are not employed for steady-state erythropoiesis. Upon initiation of stress erythropoiesis response, HSC produce BMP4, which acts on immature progenitor cells and drive their differentiation into Epo-responsive stress erythroid progenitors (10.1182/blood-2004-02-0703). Moreover, nursing-macrophage derived signaling factors, such as GDF15[91], and prostaglandins sustain the extra-medullary proliferation of Epo-responsive stress erythroid progenitors[92]. Upon anemia, the hypoxic stimulus drives an increase of Epo synthesis which, in turn, induces the Epo-responsive stress erythroid progenitor to initiate hemoglobin synthesis. To meet the massive hemoglobinization demand, the iron pool available for hemoglobinization has to be expanded. For this purpose, stress erythroblasts synthetize the hormone erythroferrone (ERFE), to induce hepatocytes, the main iron reservoirs in mammals, to release iron[93]. This regulation is achieved by ERFE-mediated suppression of hepcidin (HAMP)[62]. HAMP is a hormone which, by inhibiting the activity of the iron exporter SLC40A1 (ferroportin)[94], impedes iron export. As such, ERFE sustains the mobilization of iron from the reservoirs and renders it available to the developing erythroblasts[93].

1.4.2 Expansion of the central macrophages

The erythroblastic island are crucial to support terminal erythroid differentiation during stress erythropoiesis[89,95]. The expansion of erythroid progenitors needs to be matched with the expansion of the myeloid counterpart for efficient terminal erythroid differentiation[12,96] . Mice lacking central nursing macrophages, or those incapable to generate novel EBIs, cannot efficiently recover from anemia[89,95]. The expansion of EBI macrophages depends on monocyte recruitment to extramedullary erythropoietic organs, such as the spleen[12,96]. In anemic mice, monocytes are recruited via a CCL2 gradient into the spleen. Here, monocytes start to engulf senescent red blood cells[96]. The erythrophagocytosis-dependent increase of the intracellular heme pool causes the degradation of BACH1 and subsequent de-repression of Spi-C, the master transcriptional factor regulating RPM development[12]. Spi-C induces the expression of genes necessary to handle iron (transferrin receptor, CD71 and ferritin-H, FTH) and to bind to the developing erythroblasts (VCAM1, CD11b)[12]. This transition is marked, at first, by the downregulation of Ly-6C (pre-RPMs) and, finally, by the induction of F4-80 and the downregulation of CD11b (RPMs)[12], [96]. As previously mentioned, if Spi-C is not expressed, either because of genetic deletion or altered heme import, RPMs cannot differentiate[12,16].

1.5 SLC20A1

SLC20A1 is a membrane transporter of the Solute Carrier Class (SLC) [97]. Together with its paralogue SLC20A2, it forms the SLC20 family[97]. In both human and mice, SLC20A1 is expressed in a broad range of tissues and cell-types. The gene was originally discovered together with FLVCR1[98] as the entry receptor for the Feline Leukemia Virus-B (FeLV-B)[99,100], a virus causing multilineage hematopoietic failure and erythroblastopenia[101] and for the Gibbon Ape Leukemia Virus (GaLV)[102]. Later studies led to the classification of SLC20A1 as a sodium-phosphate cotransporter[103,104]. The first evidence suggesting the involvement of SLC20A1 in phosphate transport came from the observation of 25% amino acid similarity with the phosphate permease of neurospora crassa[105]. Later, confirmatory *in-vitro* studies highlighted a possible involvement of SLC20A1 in phosphate transport[106]. Unexpectedly, when mice lacking *Slc20a1* (*Slc20a1*$^{-/-}$) were generated, it was observed that such mice shared no phenotype trait with any other murine strains lacking known phosphate transporters[107-109]. *Slc20a1*$^{-/-}$ had no alteration in plasma phosphate, bone mineralization, trabeculae formation or calcifications[110-112]. Instead, *Slc20a1* deletion caused liver failure and severe anemia leading to in-utero lethality at embryonic day E12.5[110,112]. The anemia was characterized by a terminal erythroid differentiation blockage at the pro-erythroblast stage[112,113], and it phenocopied mice lacking *Flvcr1, Gata1* and *Klf1*.

The discovery of the *Slc20a1*$^{-/-}$ phenotype called for a reevaluation of SLC20A1 functionality[114] and the search for novel interactors of SLC20A1 to clarify the biological function of this transporter[115-117]

1.6 Thesis aims

In this introductory chapter it described how heme regulates cellular metabolism and specification by interacting with different partners. Despite its central role in cellular biology of almost every existing organism, surprisingly few heme interactors are known. In particular, the mechanisms of heme transport across the cell remain to be better explained. Identification of heme partners would grant 1) a better understanding of basic heme biology and of the grounds of heme-related pathologies, and 2) the opening of novel diagnostic and therapeutic avenues. Up to date, the identification of interaction partners has been achieved by reverse genetics approaches. In reverse genetics, the description of the phenotype of a cell or organism bearing a known genetic mutation is used to infer the functionality of such gene. A major drawback of such approach is the requirement of prior knowledge, which often biases conclusions[118]. In recent years the availability of sequence-specific programmable nucleases, as the CRISPR/Cas9 system, has permitted to identify novel interaction partners by forward genetics approach[119]. The forward genetics approach aims at identifying the underlying, phenotype causative, unknown genetic mutation given a certain phenotype. Such approach allows to correlate unbiased the phenotype to certain mutations and overcomes the bias limitation of the reverse genetics approach[120]. In my doctoral investigation, we aimed at identifying novel genes involved in heme transport and understanding the *in-vivo* biological relevance. We accomplished this by a combination of *in-vitro* forward-genetics based, loss of function phenotypic genetic screens as well as cell-biologic approaches, and *in-vivo* studies in conditional knockout mice.

2. Results

SLC20A1 facilitates heme transport and drives red pulp macrophage and erythroblast differentiation

Federica Quattrone[1,2], Rui Martins[1,2,#‡], Anna-Dorothea Gorki[1,2,#‡], Anastasiya Hladik[1], Karin Lakovits[1], Manuele Rebsamen[2‡], Enrico Girardi[2‡], Andrea Alvarez-Hernandez[3], Florian Mayrhofer[1], Asma Farhat[1,2], Martin L. Watzenboeck[1,2], Emile van den Akker[4,5], Marieke von Lindern[4,5], Giulio Superti-Furga[2,6], Ingrid Simonitsch-Klupp[3], Riem Gawish[1,2*] and Sylvia Knapp[1,2*].

[1]Department of Medicine I, Laboratory of Infection Biology, Medical University Vienna, Vienna, Austria; [2]CeMM, Research Center for Molecular Medicine of the Austrian Academy of Sciences, Vienna, Austria; [3]Clinical Institute of Pathology, Medical University Vienna, Vienna, Austria; [4]Department of Hematopoiesis, Sanquin Research, Amsterdam, The Netherlands; [5]Landsteiner Laboratory, Academic Medical Center, University of Amsterdam, Amsterdam, The Netherlands; [6]Center for Physiology and Pharmacology, Medical University Vienna, Vienna, Austria

[#] contributed equally; [*] contributed equally

Short title: SLC20A1 is a novel heme transporter

Text word count: 4214

Abstract word count: 233

Figures/Tables count: 5

Number of references: 52

Corresponding Author:
Sylvia Knapp, MD, PhD,
Laboratory of Infection Biology, Dept. of Medicine 1, Medical University Vienna
Waehringer Guertel 18-20, 1090 Vienna, Austria
Phone: +43-1-40400-51390, Fax: +43-1-40400-51670
E-mail: sylvia.knapp@meduniwien.ac.at

Key points

- SLC20A1 sustains erythropoiesis by regulating RPM and erythroblast differentiation.
- SLC20A1 affects heme import.

Abstract

Heme is an essential molecule that, when associated with hemoglobin, enables to carry oxygen. However, labile heme is a potent pro-oxidant molecule and exerts cytotoxic effects. For this reason, intracellular concentrations and trafficking of heme need to be tightly regulated. To identify proteins involved in heme trafficking, we performed a CRISPR-based loss-of-function screen focused on the solute carrier (SLC) class of transporters using heme as a selective pressure agent. Deletion of *SLC20A1* conferred a pronounced protection from heme-induced cytotoxicity. *In-vivo,* erythroid-specific *Slc20a1* deletion resulted in embryonic lethality around E12.5 due to severe anemia based on a block of erythroid differentiation at the pro-erythroblast stage. Transcriptional profiling of pro-erythroblasts indicated signs of heme deficiency. Conditional deletion of *Slc20a1* led to the rapid development of anemia, splenomegaly and the initiation of stress erythropoiesis. We found that inducible *Slc20a1* deletion led to impaired expansion of red pulp macrophages (RPM). This is in agreement with previous data showing that RPM act as nursing macrophages in stress erythropoiesis and that heme is central for Spi-C induction and RPM differentiation. Furthermore, using myeloid-specific *Slc20a1* deletion, we verified *in-vivo* that *Slc20a1* is required for the differentiation of RPMs. Functionally, we show that the absence of SLC20A1 impairs heme uptake, as well as the induction of the heme-detoxifying enzyme HMOX1. Our results reveal that SLC20A1 contributes to heme import and demonstrate its key role in the differentiation of erythroblasts and RPMs.

Introduction

To sustain the body's demand for oxygen, mammals rely on red blood cells (RBCs) to transport oxygen from the lungs to peripheral tissues[1]. While erythropoiesis takes place in the fetal liver during embryonic development, the bone marrow (BM) is the major erythropoietic organ in adult mammals[1]. The continuous differentiation of RBC progenitors maintains homeostatic levels of RBCs and is called steady-state erythropoiesis[2,3]. In mice, whenever the capacity of steady-state erythropoiesis is overwhelmed due to an increased demand like upon infection, hemorrhage or hemolysis, compensatory extramedullary erythropoiesis is initiated in organs such as the spleen and liver[4]. Extramedullary stress erythropoiesis supplies a bolus of RBC progenitors, which differentiate to reestablish homeostasis[2]. RBCs convey oxygen to peripheral tissues via its binding to hemoglobin (Hb), a protein complex composed of α- and β- globin chains and heme, which is stored in large quantities within RBCs. Hb production occurs during the terminal stages of erythroid differentiation within a specialized niche named erythroblastic island (EBI)[5]. At steady state, the EBI is composed of a central "nursing" macrophage, or, under stress erythropoiesis in the spleen of red pulp macrophages (RPMs), surrounded by developing erythroblasts[3]. Both, nursing macrophages and RPMs, support erythroid differentiation as well as heme and globin chain synthesis in erythroblasts by providing iron, nutrients and specific differentiation signals[5]. To sustain the massive expansion and differentiation of RBCs during stress erythropoiesis, novel EBIs are generated in the spleen via the recruitment of erythroid progenitors and the expansion of the RPM compartment. RPM differentiation from recruited peripheral blood monocytes requires the heme-dependent expression of *Spic*, the master regulator of RPM cell identity[6,7]. Monocytes can increase their intracellular heme concentration by engulfing and metabolizing senescent erythrocytes via erythrophagocytosis[8]. In addition, the solute carrier transporters HRG-1 (SLC48A1) and FLVCR1 (SLC49A1) have been identified as heme transporters in macrophages and erythroid progenitors[9-11]. However, it remains poorly understood if and how different transporters of heme itself, or components involved in intracellular heme metabolism, impact cellular differentiation within the erythropoietic niche. In our study, using forward-genetics, we identified SLC20A1 to contribute to heme transport. Using cell-type-specific gene deletion strategies in mice, we discovered that *Slc20a1* expression in erythroid-cells is essential for fetal, as well as steady-state erythropoiesis. Furthermore, we found that *Slc20a1* expression in

myeloid cells is required for the heme-induced *Spic* expression and subsequent differentiation of RPMs under conditions leading to stress erythropoiesis.

Material and Methods

Cell culture

HAP1 cells and BMM were grown in IMDM supplemented with 10% fetal bovine serum (FBS) and 1% penicillin-streptomycin (PS). HAP1 SLC20A1$^{-/-}$ clones were obtained from Haplogen Genomics. For BMM differentiation cells were supplemented with 20 ng/ml GM-CSF[6] and deletion of Slc20a1 was induced by adding 1 μM 4-OH tamoxifen. After 6 days cells were stimulated with 30 μM heme (Hemin, in DMSO, Sigma-Aldrich) or its vehicle for 48h[6]. Viability of HAP1 cells upon increasing heme concentrations (16h) in serum-free IMDM+1%PS was measured using CellTiter-Glo.

CRISPR Screen

A loss-of-function screen focused on the SLC-class of transporters in HAP1 cells was done by delivering the lentiviral CRISPR-Cas9 library targeting 388 SLC-class members and pseudogenes[13] at 0.3 multiplicity of infection. A pool of KO cells at 1000x coverage was obtained 7d after puromycin selection, and a sample was collected for initial sgRNA representation. To identify sensitivity to heme, cells were treated for 16h with 40 μM heme or vehicle, and repeated after 5d. Genomic DNA of surviving cells was isolated using the DNAeasy kit, the sgRNA-containing cassette was amplified using Q5 polymerase, and PCR products were sequenced and analyzed using MAGeCK[12].

Mouse strains and treatments

Sex- and age-matched 8–10-week-old mice were used and kept in SPF conditions, 12h light/dark cycle and access to food and water ad-libitum. All *in-vivo* experiments were approved by the Austrian Ministry of Science according to Austrian legislation (66.009/0362-WF/V/3b/2017). Tamoxifen-inducible *Slc20a1* knockout mice (*Slc20a1^{iKo}*) were obtained by crossing *Slc20a1$^{fl/fl}$* [13] with *Rosa26$^{ERT2Cre/eYFP\text{-}StopFlox}$* mice[14,15], erythroid-targeted deletion (*Slc20a1$^{\Delta EpoR}$*) by crossing *Slc20a1$^{fl/fl}$* with *EpoR$^{GFP\text{-}Cre/+}$* mice[16], and macrophage/myeloid-cell-targeted deletion by crossing *Slc20a1$^{fl/fl}$* with *CD169$^{Cre/+}$Rosa26$^{eYFP\text{-}StopFlox/+}$*[17,18] (*Slc20a1$^{\Delta CD169}$*) or *LysM$^{Cre/+}$ Rosa26$^{eYFP\text{-}StopFlox/+}$*mice[19] (*Slc20a1$^{\Delta LysM}$*), respectively. Genotyping primers are

provided in supplemental Table 1. To induce deletion of *Slc20a1, Slc20a1*^{iKo} and *Slc20a1*$^{fl/fl}$ mice were intraperitoneally (i.p.) injected with tamoxifen (75 mg/kg) or vehicle (oil) daily over 4 days. To induce hemolytic anemia, *Slc20a1*$^{\Delta LysM}$ mice and *Slc20a1*$^{fl/fl}$ littermates were treated i.p. with phenylhydrazine (PHZ, 40 mg/kg) for two consecutive days. The health status of mice was checked daily and weekly blood sampling (30 μl) via retro-orbital phlebotomy after anesthesia was done. EDTA blood analyses were performed on the VetABC. Mice appearing sick or experiencing a decline of the hematocrit to 20% were euthanized for ethical reasons.

Tissue preparation for flow cytometry

Femurs, spleens and fetal livers were mechanically disrupted and strained (70 μm filter). Analysis of non-erythroid cells was performed after RBC lysis and subsequent passage through a 40 μm cell strainer. Staining was performed in the presence of anti-mouse Fc-receptor blocking antibody (CD16/32) and a viability dye. Used antibodies are listed in supplemental Table 2. Samples were analyzed with a LSR-Fortessa (BD), sorting of cells was performed with a FACSAria (BD).

Histology, immunoblot and qPCR

Details are provided in the Supplemental data file.

RNA sequencing and data analysis

Details on RNASeq are provided in the Supplemental data file. Differential expression analysis was performed using DESeq2[20].Volcano plots were generated using ggplot2[21]. Gene lists of interest were retrieved from Molecular Signature Database[22,23] (Stable ID: M5923, M10214, access: 2021.02.21), Reactome[24] (Stable ID: R-HSA-9648895, access: 2021.02.21), Gene Ontology[25,26] (GO:0006783, access: 2021.02.21) and from published dataset[27] (SRX2682727).

Heme uptake assay

HAP1 cells were stimulated with heme for 30min in serum-free IMDM+1% PS, washed twice with ice-cold PBS, lysed in oxalic acid and boiled at 120° for 1h, and fluorescence was immediately read (excitation 420nm, emission 660nm)[28]. HAP1 cells were stimulated with ZnMP (Santa-Cruz Biotechnology) for 30min at 37°C or 4°C in heme uptake buffer (50 mM HEPES, 130 mM NaCl, 10 mM KCl, 1 mM $CaCl_2$, 1 mM $MgSO_4$,

pH 7.4)[29]. Next, cells were washed with heme uptake buffer + 5% BSA(Sigma-Aldrich) and acquired at LSR-Fortessa. The uptake index was calculated as (MFI × % positive cells at 37 °C) minus (MFI × % positive cells at 4 °C).

Data sharing statement

DNA and RNA sequencing data will be deposited at GEO.

Results

A CRISPR-screen identifies SLC20A1 as a novel driver of heme-cytotoxicity

While heme is an essential component of various hemoproteins, labile heme exerts cytotoxic effects due to its oxidative properties that promote the formation of oxygen radicals. A cell's sensitivity to heme-induced cell death depends on its capacity to regulate intracellular heme concentrations by balancing heme uptake and biosynthesis with degradation[30]. Thus, sensitivity to the cytotoxic effects of heme can be used as a readout to identify genes involved in cellular heme metabolism and trafficking. To identify factors involved in heme trafficking, we performed a CRISPR-Cas9 based loss-of-function genetic screen focused on the solute carrier (SLC)-class of transporters in the haploid human fibroblast cell line HAP1[31]. After titrating heme cytotoxicity (supplemental Figure 1A), we used 40 μM heme to apply selective pressure to cells transduced with the CRISPR-Cas9-SLC library[31], followed by sequencing of the surviving cell clones to monitor the relative abundance of sgRNAs (Figure 1A). Enriched sgRNAs indicated genes that promoted heme toxicity (Figure 1B), while depleted sgRNAs were indicative of gene products that prevented heme-induced cell death (supplemental Figure 1B). We found that cells lacking transporters of glutathione-precursors such as *SLC7A11/SLC3A2* and *SLC7A5/SLC3A2* (cystine/glutamate transport)[32] and transporters of iron-scavenging substrates like *SLC25A1* (citrate transport)[33] were more sensitive to heme-induced cell death (supplemental Figure 1B), supporting their importance in maintaining intracellular redox balance. Conversely, a reduction of intracellular heme levels might explain increased heme-resistance of cells lacking transporters of precursors or intermediates of heme biosynthesis such as *SLC25A28* (iron import)[34], *SLC25A11* (2-oxoglutarate transport)[35] and *SLC52A2* (riboflavin transport)[36] (Figure 1B). Strikingly, the strongest protection against heme-induced cell death was conferred by deletion of *SLC20A1* (Figure 1B), a gene which has not been associated with intracellular heme metabolism

so far. To verify the results from the screen, we treated *SLC20A1* deficient (*SLC20A1*$^{-/-}$) HAP1 cells with increasing heme doses and confirmed enhanced resistance to heme-induced cell death, when compared to WT control cells (Figure 1C). SLC20A1 has been classified earlier as a sodium-phosphate cotransporter[37]. However, and in line with previous studies[13,38], *SLC20A1*$^{-/-}$ HAP1 cells did not show alterations of intracellular phosphate concentrations at steady state or upon phosphate substitution, and phosphate supplementation did not impact on heme-induced cytotoxicity (supplemental Figures 1C-1E). Thus, we identified SLC20A1 as a novel and fundamental driver of heme-associated cytotoxicity and suggest that SLC20A1 promoted heme-induced cell death independently of its reported role in phosphate transport.

SLC20A1 sustains steady-state erythropoiesis

To investigate the biological function of SLC20A1, we first assessed its role at steady state. Since *Slc20a1*$^{-/-}$ mice were reported to die on day E12.5 during embryonic development due to defective liver development and severe anemia[13,38,39], we generated tamoxifen-inducible *Slc20a1* knockout mice with an eYFP reporter system (*Rosa26*$^{ERCre/Stop\text{-}eYFP}$ *Slc20a1*$^{fl/fl}$, further referred to as *Slc20a1*^{iKo}). In this model, tamoxifen induces the nuclear translocation of a Cre-estrogen receptor fusion protein[14] and subsequent deletion of *Slc20a1* with the simultaneous induction of eYFP expression[15], allowing the detection of successfully *Slc20a1* deleted cells (eYFP^{+}). Tamoxifen administration in adult *Slc20a1*^{iKo} mice (Figure 2A) resulted in a partial chimerism, with approximately 15-20% of viable BM and spleen cells, respectively, showing successful deletion of *Slc20a1* (eYFP^{+}) 28 days post tamoxifen treatment (Figure 2B). *Slc20a1*^{iKo} mice displayed severe anemia, with a substantial and progressive decline of RBC counts, Hb levels and hematocrit over the observation period of 28 days, while *Slc20a1*$^{fl/fl}$ littermate controls did not react to tamoxifen treatment (Figure 2C, D, supplemental Figure 2A). We did not observe signs of anisocytosis and white blood cell (WBC) counts did not change upon tamoxifen (supplemental Figure 2B-C). Similarly, when we treated *Slc20a1*^{iKo} mice with tamoxifen or vehicle to control for potential leakiness in Cre activity, we only observed a drop of RBC and Hb in tamoxifen-treated animals (supplemental Figure 2D-E). Considering that embryonic lethality of *Slc20a1*$^{-/-}$ mice had been attributed to defective liver development and hepatocyte apoptosis[13], we evaluated plasma liver transaminase

levels and the cell death marker LDH (supplemental Figure 2F-H), but did not observe any alterations, indicating that mice did not experience hepatocyte damage. Within 14 days from induction of *Slc20a1* deletion, we discovered signs of extramedullary stress-erythropoiesis and progressive splenomegaly (Figure 2E). Histological evaluation of spleens highlighted a drastic change of the splenic micro-architecture, including an enlargement of the red-pulp area and a complete loss of the white pulp area in *Slc20a1*^{iKo} mice (Figure 2F). Enlarged spleens of *Slc20a1*^{iKo} mice showed a substantial increase in the abundance of erythroblasts (Figure 2G-H), megakaryocyte-erythrocyte progenitors (MEP) (Figure 2I, supplemental Figure 2I) and RPMs (Figure 2J-K, supplemental Figure 2J). RPMs were further characterized by CD169 and VCAM1 expression (supplemental Figure 2K). Taken together, our data show that SLC20A1 is essential to sustain steady-state erythropoiesis and that even the partial deletion of *Slc20a1* caused severe anemia and compensatory extramedullary stress hematopoiesis.

Erythroid SLC20A1 is essential for terminal erythrocyte differentiation

We next asked in which cell compartment during erythropoiesis SLC20A1 needs to function to maintain erythrocyte homeostasis. Upon tamoxifen administration, *Slc20a1*^{iKo} mice displayed an accumulation of differentiating erythroblasts in the spleen and BM (Figure 3A-B). Analyzing the stages of erythroblast differentiation, we identified a shift toward the pro-erythroblast stage (stage I), with a reduced abundance of orthochromatic-erythroblasts (stage IV) in both the spleen (Figure 3B-C) and BM (Figure 3D) of *Slc20a1*^{iKo} mice. To test the cell-intrinsic impact of *Slc20a1* deletion on erythroblast differentiation in the chimeric, tamoxifen-treated *Slc20a1*^{iKo} mice, we separately analyzed *Slc20a1* deleted eYFP^{+} (*Slc20a1*$^{iKo/eYFP+}$) and undeleted eYFP^{-} (*Slc20a1*$^{iKo/eYFP-}$) cells (Supplemental Figure 3A). Doing so, we noticed a less severe, yet still visible shift in erythroblast differentiation in spleen (Figure 3E) and BM (Figure 3F). To assess in which cell compartment functional *Slc20a1* was essential for terminal erythroid cell differentiation, we generated erythroid-specific *Slc20a1*-deficient mice by crossing erythropoietin receptor Cre animals[16] with *Slc20a*$^{fl/fl}$ mice (*EpoR*$^{GFP\text{-}Cre/+}$ *Slc20a*$^{fl/fl}$ further referred to as *Slc20a1*$^{\Delta EpoR}$). By setting up a breeding scheme that should lead to 25% *Slc20a1*$^{\Delta EpoR}$ offspring, we noticed that those mice were not viable (no *Slc20a1*$^{\Delta EpoR}$ mice born out of 53 pups), while E11.5 embryos showed the expected Mendelian ratio (Figure 3G). *Slc20a1*$^{\Delta EpoR}$ fetuses phenocopied the full-body *Slc20a1*

deletion[13,38] and died in-utero after E11.5, while displaying a pale, bloodless appearance (Figure 3H). Analysis of E11.5 fetal livers confirmed the absence of Ter119$^+$ cells in *Slc20a1*$^{\Delta EpoR}$ mice (supplemental Figure 3B). By analyzing the differentiation stages of fetal liver erythroblasts, we discovered that erythroid-specific *Slc20a1* deletion resulted in a complete block at the pro-erythroblast stage (stage I) (Figure 3I). Transcriptome analysis of FACS-sorted pro-erythroblasts from fetal (E11.5) tissues of *Slc20a1*$^{\Delta EpoR}$ and littermate control *Slc20a1*$^{fl/fl}$ mice revealed that pro-erythroblasts clustered separately, depending on the genotype, in a principal component analysis (supplemental Figure 3C). A total of 1134 genes were found up-, and 2116 genes down-regulated. *Slc20a1* deletion was associated with the expression of genes involved in TGF-β and PI3K-Akt signaling pathways, heme deficiency signaling (*Eif2ak1*) and the related integrated-stress response pathway (*Atf4*, *Ppp1r15a*, *Cebpg*) (supplemental Figure 3D). Conversely, *Slc20a1* deletion strongly downregulated the expression of genes involved in ribosome biogenesis (supplemental Figure 3D). Collectively, our data support the importance of *Slc20a1* in the erythroid compartment and show that erythroid-specific deletion of *Slc20a1* stalled terminal RBC differentiation. However, considering the modest deletion efficiency in tamoxifen treated, chimeric *Slc20a1*^{iKo} mice (15-20%, Figure 2B), the severity of the resulting anemia (Figure 2C-D) seemed unexpected in these mice. This finding led us to question why tamoxifen-treated *Slc20a1*^{iKo} mice could not compensate for the modest defect in differentiation, and we hypothesized that other cellular players involved in erythropoiesis, in addition to RBC precursors, might be affected by the deletion of *Slc20a1*.

SLC20A1 is essential for RPM differentiation in stress erythropoiesis

Stress-erythropoiesis is induced upon anemia and entails the *de novo* formation of erythropoietic niches, which occurs in extramedullary sites such as the spleen in mice[7]. Thereby, erythropoietic progenitors expand and differentiate in the presence of, and supported by, nursing macrophages within EBIs[7,40]. In these situations, nursing macrophages are derived from peripheral blood monocytes that migrate to the spleen, where they differentiate into preRPMs and mature RPMs[6,7]. In keeping with this notion, we first asked whether *Slc20a1* deletion might affect the abundance of RPMs in stress erythropoiesis. To this end, we analyzed the spleens of *Slc20a1*^{iKo} mice and separately studied *Slc20a1* deleted eYFP$^+$ (*Slc20a1*$^{iKo/eYFP+}$) and undeleted eYFP$^-$ (*Sl20a1*$^{iKo/eYFP-}$

) spleen cells (supplemental Figure 4A). We discovered a substantial reduction in mature RPMs among the *Slc20a1*-deleted eYFP^{+} cells (Figure 4A, C), suggesting that the development and maturation of monocyte-derived RPMs requires *Slc20a1.* To assess whether *Slc20a1* is also required for the maintenance of RPMs at steady state, i.e. in the absence of stress erythropoiesis, we evaluated RPM numbers in *CD169$^{Cre/+}$Rosa26$^{Stop\text{-}eYFP/+}$Slc20a1$^{fl/fl}$* mice[17] (further referred to as *Slc20a1$^{\Delta CD169}$*). *Slc20a1$^{\Delta CD169}$* mice were born at a Mendelian ratio (data not shown) and did not show altered Hb, RBC or WBC counts (supplemental Figure 4B-D). Analysis of the cellular composition of the spleen at steady-state revealed that both *Slc20a1$^{\Delta CD169}$* and control littermates had similar percentages of RPMs (supplemental Figure 4E), indicating no contribution of *Slc20a1* to RPM abundance at steady state. Given the prominent role of monocytes in sustaining the stress erythropoiesis-associated RPM expansion[7], we hypothesized that impaired monocyte differentiation might account for the reduced pool of mature RPMs in tamoxifen-treated *Slc20a1^{iKo}* mice. Taking advantage of the chimerism of these mice, we tracked differentiating monocytes in spleens and observed no obvious difference in the distribution of RPM precursors (Figure 4B). To test if *Slc20a1* deletion altered the capability of preRPMs to modulate gene expression required for RPM development, we performed transcriptome analyses of sorted *Slc20a1^{iKo}*/eYFP^{-} preRPMs and RPMs as well as *Slc20a1^{iKo}*/eYFP^{+} preRPMs (but no *Slc20a1^{iKo}*/eYFP^{+} RPMs due to low cell numbers). Principal component analysis of transcriptome profiles revealed differential clustering of *Slc20a1^{iKo}*/eYFP^{-} preRPMs and RPMs (Figure 4D), whereas preRPM of *Slc20a1^{iKo}*/eYFP^{+} and *Slc20a1^{iKo}*/eYFP^{-} showed high similarity of sorted populations (Figure 4E). Comparison of induced transcripts from *Slc20a1^{iKo}*/eYFP^{-} preRPM and RPM displayed expression of monocyte-signature genes (*Itgam*, *Stat3*) in preRPM and an induction of genes regulating RPM-differentiation such as the RPM master transcription factor *Spic* among RPMs (Figure 4F)[6]. *Spic* expression is driven by the, often erythrophagocytosis-mediated, increase of intracellular labile heme[6]. To analyze if SLC20A1 is involved in heme-induced *Spic* expression, we made use of tamoxifen-treated *Slc20a1^{iKo}* and *Slc20a1$^{fl/fl}$* BMDMs. We detected that heme strongly induced the expression of *Spic* in *Slc20a1$^{fl/fl}$* cells, whereas the induction was markedly reduced in *Slc20a1^{iKo}* cells (Figure 4G), suggesting that *Slc20a1* is indeed required for the heme mediated induction of *Spic*. Taken together, our findings suggest that SLC20A1 is not required for monocyte-to-

preRPM development, but importantly contributes to the final differentiation steps to mature RPMs, presumably by promoting heme-dependent *Spic* expression.

SLC20A1 sustains anemia-induced RPM differentiation by contributing to heme import

Given that *SLC20A1* deletion conferred pronounced resistance to heme-induced cell death in HAP1 cells (Figure 1B, C) and that *Slc20a1* deficient preRPMs failed to differentiate into mature RPMs during stress erythropoiesis *in-vivo* (Figure 4C), likely because of failed heme-mediated *Spic* induction (Figure 4G), we hypothesized that SLC20A1 might facilitate heme import into cells. To test this hypothesis, we performed heme uptake assays by incubating HAP1 cells lacking *SLC20A1* with heme or its fluorescent analog zinc mesoporphyrin (ZnMP). We observed a reduced uptake of both heme (Figure 5A) and ZnMP (Figure 5B-C) in *SLC20A1*$^{-/-}$ HAP1 cells, as compared to WT control cells. Furthermore, while WT cells robustly induced the expression of heme oxygenase-1 (HMOX1) in response to heme incubation, *SLC20A1*$^{-/-}$ cells exhibited reduced HMOX1 induction at transcript (Figure 5D) and protein level (Figure 5E), further supporting the notion that the absence of SLC20A1 prevented heme from entering the cell. Given that *Slc20a1*$^{\Delta CD169}$ mice showed normal RPM ratios and considering that heme must be sensed in monocytes/preRPMs to induce *Spic* and subsequent RPM differentiation, we hypothesized that SLC20A1 might be instrumental at the monocyte stage (instead of the mature, CD169^{+} RPM stage) to impact RPM development. To test this idea, we generated mice in which *Slc20a1* is deleted at the monocyte stage, using lysozyme-driven Cre *CD169*$^{Cre/+}$*Rosa26*$^{Stop\text{-}eYFP/+}$*Slc20a1*$^{fl/f}$, referred to as *Slc20a1*$^{\Delta LysM}$)[19]. Mice were born at Mendelian ratios, and exhibited normal RBC counts at steady state (supplemental Figure 5A-B). To evaluate the impact of *Slc20a1* on stress erythropoiesis-induced RPM expansion, we induced hemolysis in *Slc20a1*$^{\Delta LysM}$ mice and littermate controls with phenylhydrazine (PHZ) (Figure 5F). PHZ treatment induced hemolytic anemia in mice, indicated by declining RBC counts in both *Slc20a1*$^{\Delta LysM}$ and littermate controls (Figure 5G), paralleled by the induction of extramedullary stress erythropoiesis, as indicated by the expansion of the splenic erythroblast pool (supplemental Figure 5C). Analysis of spleens from *Slc20a1*$^{\Delta LysM}$ mice on d5 revealed that, while monocytes and preRPMs were invading and initiating their differentiation in the spleen (supplemental Figure 5D), RPMs were significantly

reduced (Figure 5H), thus supporting our hypothesis that SLC20A1 in the myeloid compartment is required to sustain RPM differentiation. Strikingly, analysis of terminal erythroid differentiation in the spleen highlighted that *Slc20a1*$^{\Delta LysM}$ mice displayed a shift toward the pro-erythroblast stage (stage I) and a concomitant reduction of orthochromatic-erythroblasts (stage IV) in the spleen (Figure 5I), similarly to what we observed in *Slc20a1*^{iKo} animals upon tamoxifen treatment (Figure 3C). The overall recovery from anemia was modestly delayed in *Slc20a1*$^{\Delta LysM}$ mice (supplemental Figure 5E). Taken together, our data demonstrate that myeloid-cell expressed *Slc20a1* regulates terminal erythroblast differentiation during stress erythropoiesis, as *Slc20a1* was required for stress erythropoiesis associated RPM expansion and differentiation. Collectively, our data indicate that we have identified a novel player facilitating heme import, and that *Slc20a1* is essential in driving hemolysis-induced RPM differentiation.

Discussion

Hemoglobinization occurs during terminal erythroid differentiation within the EBI and is the critical step during steady state and stress erythropoiesis. Heme has emerged as critical signaling molecule within the splenic EBI[6,41,42], however due to its cytotoxic and inflammatory properties, heme metabolism and transport have to be tightly regulated[30]. In this study, we identified the solute carrier SLC20A1 as a novel contributor to heme transport and examined its role in the differentiation of erythroblasts and RPMs. We discovered that SLC20A1 is an essential factor required for the differentiation and maturation of erythroblasts at steady state, as well as the expansion and maturation of RPMs during stress erythropoiesis. It has been reported earlier that mice lacking *Slc20a1* (*Slc20a1*$^{-/-}$) were not viable, due to severe anemia resulting from a block of erythroid differentiation at the pro-erythroblast stage I[13,38,39]. We could replicate embryonic lethality in mice lacking *Slc20a1* specifically in the EpoR expressing cell compartment[16], showing that erythroid-expressed *Slc20a1* is essential during fetal erythropoiesis. Though EpoR was found expressed on a fraction of fetal liver nursing macrophages[43], the regular development of both *Slc20a1*$^{\Delta LysM}$ and *Slc20a1*$^{\Delta CD169}$ strains supports the significance of erythroid cell-intrinsic *Slc20a1*. Beside its vital role in embryogenesis, we found that tamoxifen-induced *Slc20a1* deletion in adult mice resulted in severe anemia. Surprisingly though, i) the anemia occurred in spite of a rather low chimerism rate, with 15-20% of tested cells lacking *Slc20a1*, and ii) mice failed to recover even four weeks post tamoxifen administration. Interestingly, it was

reported earlier that post-natal deletion of *Slc20a1* using type-I IFN-induced Cre (i.e. *Mx Cre*) resulted in a 30% reduction of RBC counts at three months of age, supporting our finding that even an incomplete deletion of *Slc20a1* impaired steady state and stress RBC development[38,39]. Taking advantage of an eYFP reporter system[15] we found that *Slc20a1*-deficient cells exhibited an early block at stage I/II of terminal erythroblast differentiation, resulting in the accumulation of undifferentiated erythroid precursors and the disruption of the erythropoietic niche. It appears that *Slc20a1* was most important in the early stages of erythroblast differentiation, i.e. the phase when hemoglobinization is initiated[3]. At this delicate stage, developing RBCs need to tightly balance heme abundance and globin chain synthesis via the intricate interplay of selected transcriptional and translational factors, which, in turn are regulated by the integration of intra- and extracellular stimuli[42,44]. Considering the notably protective effect of *SLC20A1* deficiency from heme-mediated cytotoxicity we observed in the CRISPR screen, we hypothesized that the putative phosphate transporter SLC20A1[45] might participate in the transport of heme, thus fine-tuning intracellular heme levels. In support of this idea, the phenotype of *Slc20a1* deficient mice is not shared with any other murine strains lacking known phosphate transporters[46-48]. In contrast, whole body and erythroid specific *Slc20a1* deficiency[13,38] phenocopies mice lacking both isoforms of the known heme transporter *Flvcr1*[10,11]. Just like *Slc20a1* deficiency, *Flvcr1* deletion results in embryonic lethality because of an early block in terminal erythroid differentiation[10,11].

The cytosolic heme pool is emerging as a key regulator of transcription and translation factors driving terminal erythrocyte differentiation[41,49]. In erythroblasts, heme mediates the degradation of the transcriptional repressor BACH1, thereby inducing globin chain synthesis[50] and GATA1 expression, a key driver of erythroblast differentiation[41]. Conversely, heme deficiency activates EIF2AK1 (HRI) to phosphorylate eiF2α, ultimately resulting in inhibition of globin chain synthesis while sustaining the integrated stress response via ATF4[49]. Given that *Slc20a1*$^{\Delta EpoR}$ pro-erythroblasts showed an increased expression of *Eif2ak1*, *Atf4* and its main target *Ppp1r15a*, it is tempting to speculate that *Slc20a1* might regulate the intracellular heme pool by mediating its uptake, ultimately regulating erythroid differentiation. The regulatory heme pool not only exerts essential functions in differentiating erythroblasts, but is equally important in the development of RPMs, the nursing macrophages of EBIs in the spleen. During the stress-induced *de novo* formation of EBIs in the spleen, the

differentiation of recruited peripheral blood monocytes to RPMs depends on the induction of *Spic*, the master transcriptional regulator of RPM identity[7,51]. *Spic* expression is suppressed by BACH1 in monocytes and thus requires an increase of the intracellular heme concentration in the preRPM state to allow for RPM differentiation[6]. We found reduced numbers of *Slc20a1*-deleted (eYFP$^+$) RPMs in anemic *Slc20a1^{iKo}* chimeras, but unaltered proportions of eYFP$^+$ monocyte/preRPMs, indicating that these precursors failed to differentiate to mature RPMs due to impaired heme-import. *In-vitro* experiments using *Slc20a1 ^{iKo}* BMDMs enabled us to prove that *Slc20a1* supported heme-induced *Spic* expression. Finally, deletion of *Slc20a1*in LysM expressing cells[19], which include monocytes and macrophages, caused impaired RPM development and splenic monocyte/preRPM accumulation during stress erythropoiesis induced by hemolysis. Interestingly, *Slc20a1$^{\Delta LysM}$* animals did not exhibit anemia at steady state, and only showed deregulated terminal RBC differentiation upon hemolytic stress. Similarly, *Spic*-deficient mice show a selective loss of mature RPMs at baseline and are not anemic at steady state[6]. However, their recovery from hemolytic anemia is delayed[6,40], showing that spleen RPMs are more important upon hematopoietic stress, while in steady state, the BM is the major site of erythropoiesis[2]. As the heme importer HRG-1 is expressed in the myeloid lineage[9], its activity might compensate to a certain extent for *Slc20a1*-deficiency, thereby allowing for residual *Spic* expression. Considering the biological importance of sustained stress-erythropoiesis and the role of heme therein, it is reasonable to expect organisms to express multiple heme importers to meet this demand. Our data support the hypothesis that the myeloid compartment is instrumental in the response to, and recovery from anemia upon stress[40]. Collectively, we have identified SLC20A1 as a transporter, which exerts critical functions in the erythroid compartment to enable proper terminal RBC differentiation under homeostatic conditions. At the same time, we discovered SLC20A1 to be essential for RPM differentiation, by regulating intracellular heme levels in differentiating monocytes upon hemolytic stress.

Acknowledgements

We thank Gerald Friedlander (Université Paris Descartes, Paris, France) for generously providing us with *Slc20a1*$^{fl/fl}$ mice, Vanja Nagy (Ludwig Boltzmann Institute for Rare and Undiagnosed Diseases, Medical University of Vienna, Vienna, Austria) for *Rosa26* $^{ERT2\ Cre}$ and *Rosa26* $^{eYFP\text{-}StopFlox}$ animals, Ursula Klingmüller (German Cancer Research Center, Heidelberg, Germany) for *EpoR*$^{GFP\text{-}Cre/+}$ mice, Miriam Merad (Icahn School of Medicine at Mount Sinai, New York, USA) for *CD169*$^{Cre/+}$ mice, which were provided by the RIKEN BRC through the National Bio-Resource Project of the MEXT, Japan. We thank the staff from the flow cytometry core facility of the Medical University of Vienna (MUW), the staff of the Biomedical Sequencing facility (BSF, CeMM/MUW) and the staff from the animal facilities at IMBA, CeMM and MUW for their assistance. FQ is supported by a DOC-fellowship from the Austrian Academy of Sciences. R.G. is supported by the Austrian Science Fund (FWF) via the Young Independent Researcher Group (ZK-57). S.K. is supported by the Austrian Science Fund (FWF), via the Special Research Programs Immunothrombosis (F5410) and Chromatin Landscapes (L-Mac: F6104).

Author Contributions

F.Q., R.M., A-D.G., A.H, K.L., A.F., F. M., R.G. performed experiments and analyzed data; F.Q., A-D.G, M.W. analyzed the bioinformatic data; F. Q., M.R., E.G. and G.S.F. performed CRISPR screen and analyzed the data; A.A-H., I.S-K. performed pathological evaluation; E.vdA. and M.vL. provided valuable reagents and technical advice; F.Q., R.G., S.K. conceptualized the study; F.Q., R.G., S.K. wrote the manuscript with input from co-authors.

Conflict-of-interest disclosure:

A-D.G. is currently employed and holds shares at G.ST Antivirals GmbH

E.G. is currently employed at Boehringer Ingelheim GmbH

G.S.F. is founder and shareholder of Solgate GmbH

4. References

1. Palis J. Primitive and definitive erythropoiesis in mammals. *Front Physiol*. 2014;5:3.

2. Paulson RF, Hariharan S, Little JA. Stress erythropoiesis: definitions and models for its study. *Exp Hematol*. 2020;89:43-54 e42.

3. Dzierzak E, Philipsen S. Erythropoiesis: development and differentiation. *Cold Spring Harb Perspect Med*. 2013;3(4):a011601.

4. Paulson RF, Ruan B, Hao S, Chen Y. Stress Erythropoiesis is a Key Inflammatory Response. *Cells*. 2020;9(3).

5. Klei TR, Meinderts SM, van den Berg TK, van Bruggen R. From the Cradle to the Grave: The Role of Macrophages in Erythropoiesis and Erythrophagocytosis. *Front Immunol*. 2017;8:73.

6. Haldar M, Kohyama M, So AY, et al. Heme-mediated SPI-C induction promotes monocyte differentiation into iron-recycling macrophages. *Cell*. 2014;156(6):1223-1234.

7. Liao C, Prabhu KS, Paulson RF. Monocyte-derived macrophages expand the murine stress erythropoietic niche during the recovery from anemia. *Blood*. 2018;132(24):2580-2593.

8. Klei TRL, Dalimot J, Nota B, et al. Hemolysis in the spleen drives erythrocyte turnover. *Blood*. 2020;136(14):1579-1589.

9. White C, Yuan X, Schmidt PJ, et al. HRG1 is essential for heme transport from the phagolysosome of macrophages during erythrophagocytosis. *Cell Metab*. 2013;17(2):261-270.

10. Keel SB, Doty RT, Yang Z, et al. A heme export protein is required for red blood cell differentiation and iron homeostasis. *Science*. 2008;319(5864):825-828.

11. Mercurio S, Petrillo S, Chiabrando D, et al. The heme exporter Flvcr1 regulates expansion and differentiation of committed erythroid progenitors by controlling intracellular heme accumulation. *Haematologica*. 2015;100(6):720-729.

12. Li W, Xu H, Xiao T, et al. MAGeCK enables robust identification of essential genes from genome-scale CRISPR/Cas9 knockout screens. *Genome Biol*. 2014;15(12):554.

13. Beck L, Leroy C, Beck-Cormier S, et al. The phosphate transporter PiT1 (Slc20a1) revealed as a new essential gene for mouse liver development. *PLoS One*. 2010;5(2):e9148.

14. Seibler J, Zevnik B, Kuter-Luks B, et al. Rapid generation of inducible mouse mutants. *Nucleic Acids Res*. 2003;31(4):e12.
15. Srinivas S, Watanabe T, Lin CS, et al. Cre reporter strains produced by targeted insertion of EYFP and ECFP into the ROSA26 locus. *BMC Dev Biol*. 2001;1:4.
16. Heinrich AC, Pelanda R, Klingmuller U. A mouse model for visualization and conditional mutations in the erythroid lineage. *Blood*. 2004;104(3):659-666.
17. Asano K, Takahashi N, Ushiki M, et al. Intestinal CD169(+) macrophages initiate mucosal inflammation by secreting CCL8 that recruits inflammatory monocytes. *Nat Commun*. 2015;6:7802.
18. Karasawa K, Asano K, Moriyama S, et al. Vascular-resident CD169-positive monocytes and macrophages control neutrophil accumulation in the kidney with ischemia-reperfusion injury. *J Am Soc Nephrol*. 2015;26(4):896-906.
19. Clausen BE, Burkhardt C, Reith W, Renkawitz R, Forster I. Conditional gene targeting in macrophages and granulocytes using LysMcre mice. *Transgenic Res*. 1999;8(4):265-277.
20. Love MI, Huber W, Anders S. Moderated estimation of fold change and dispersion for RNA-seq data with DESeq2. *Genome Biol*. 2014;15(12):550.
21. Wickham H. ggplot2 : Elegant Graphics for Data Analysis. Use R!,. Cham: Springer International Publishing : Imprint: Springer,; 2016:1 online resource (XVI, 260 pages 232 illustrations, 140 illustrations in color.
22. Liberzon A, Birger C, Thorvaldsdottir H, Ghandi M, Mesirov JP, Tamayo P. The Molecular Signatures Database (MSigDB) hallmark gene set collection. *Cell Syst*. 2015;1(6):417-425.
23. Subramanian A, Tamayo P, Mootha VK, et al. Gene set enrichment analysis: a knowledge-based approach for interpreting genome-wide expression profiles. *Proc Natl Acad Sci U S A*. 2005;102(43):15545-15550.
24. Jassal B, Matthews L, Viteri G, et al. The reactome pathway knowledgebase. *Nucleic Acids Res*. 2020;48(D1):D498-D503.
25. Ashburner M, Ball CA, Blake JA, et al. Gene ontology: tool for the unification of biology. The Gene Ontology Consortium. *Nat Genet*. 2000;25(1):25-29.
26. Gene Ontology C. The Gene Ontology resource: enriching a GOld mine. *Nucleic Acids Res*. 2021;49(D1):D325-D334.

27. Paolini NA, Moore KS, di Summa FM, Fokkema I, t Hoen PAC, von Lindern M. Ribosome profiling uncovers selective mRNA translation associated with eIF2 phosphorylation in erythroid progenitors. *PLoS One*. 2018;13(4):e0193790.
28. Sinclair PR, Gorman N, Jacobs JM. Measurement of heme concentration. *Curr Protoc Toxicol*. 2001;Chapter 8:Unit 8 3.
29. Worthington MT, Cohn SM, Miller SK, Luo RQ, Berg CL. Characterization of a human plasma membrane heme transporter in intestinal and hepatocyte cell lines. *Am J Physiol Gastrointest Liver Physiol*. 2001;280(6):G1172-1177.
30. Tolosano E, Fagoonee S, Morello N, Vinchi F, Fiorito V. Heme scavenging and the other facets of hemopexin. *Antioxid Redox Signal*. 2010;12(2):305-320.
31. Girardi E, Cesar-Razquin A, Lindinger S, et al. A widespread role for SLC transmembrane transporters in resistance to cytotoxic drugs. *Nat Chem Biol*. 2020;16(4):469-478.
32. Dixon SJ, Lemberg KM, Lamprecht MR, et al. Ferroptosis: an iron-dependent form of nonapoptotic cell death. *Cell*. 2012;149(5):1060-1072.
33. Silva AM, Kong X, Parkin MC, Cammack R, Hider RC. Iron(III) citrate speciation in aqueous solution. *Dalton Trans*. 2009(40):8616-8625.
34. Paradkar PN, Zumbrennen KB, Paw BH, Ward DM, Kaplan J. Regulation of mitochondrial iron import through differential turnover of mitoferrin 1 and mitoferrin 2. *Mol Cell Biol*. 2009;29(4):1007-1016.
35. Kabe Y, Ohmori M, Shinouchi K, et al. Porphyrin accumulation in mitochondria is mediated by 2-oxoglutarate carrier. *J Biol Chem*. 2006;281(42):31729-31735.
36. Yao Y, Yonezawa A, Yoshimatsu H, Masuda S, Katsura T, Inui K. Identification and comparative functional characterization of a new human riboflavin transporter hRFT3 expressed in the brain. *J Nutr*. 2010;140(7):1220-1226.
37. Kavanaugh MP, Miller DG, Zhang W, et al. Cell-surface receptors for gibbon ape leukemia virus and amphotropic murine retrovirus are inducible sodium-dependent phosphate symporters. *Proc Natl Acad Sci U S A*. 1994;91(15):7071-7075.
38. Liu L, Sanchez-Bonilla M, Crouthamel M, Giachelli C, Keel S. Mice lacking the sodium-dependent phosphate import protein, PiT1 (SLC20A1), have a severe defect in terminal erythroid differentiation and early B cell development. *Exp Hematol*. 2013;41(5):432-443 e437.

39. Forand A, Beck L, Leroy C, et al. EKLF-driven PIT1 expression is critical for mouse erythroid maturation in vivo and in vitro. *Blood*. 2013;121(4):666-678.
40. Chow A, Huggins M, Ahmed J, et al. CD169(+) macrophages provide a niche promoting erythropoiesis under homeostasis and stress. *Nat Med*. 2013;19(4):429-436.
41. Tanimura N, Miller E, Igarashi K, et al. Mechanism governing heme synthesis reveals a GATA factor/heme circuit that controls differentiation. *EMBO Rep*. 2016;17(2):249-265.
42. Chen JJ, Zhang S. Heme-regulated eIF2alpha kinase in erythropoiesis and hemoglobinopathies. *Blood*. 2019;134(20):1697-1707.
43. Li W, Wang Y, Zhao H, et al. Identification and transcriptome analysis of erythroblastic island macrophages. *Blood*. 2019;134(5):480-491.
44. Moore KS, von Lindern M. RNA Binding Proteins and Regulation of mRNA Translation in Erythropoiesis. *Front Physiol*. 2018;9:910.
45. Forster IC, Hernando N, Biber J, Murer H. Phosphate transporters of the SLC20 and SLC34 families. *Mol Aspects Med*. 2013;34(2-3):386-395.
46. Beck L, Karaplis AC, Amizuka N, Hewson AS, Ozawa H, Tenenhouse HS. Targeted inactivation of Npt2 in mice leads to severe renal phosphate wasting, hypercalciuria, and skeletal abnormalities. *Proc Natl Acad Sci U S A*. 1998;95(9):5372-5377.
47. Segawa H, Onitsuka A, Furutani J, et al. Npt2a and Npt2c in mice play distinct and synergistic roles in inorganic phosphate metabolism and skeletal development. *Am J Physiol Renal Physiol*. 2009;297(3):F671-678.
48. Yamada S, Wallingford MC, Borgeia S, Cox TC, Giachelli CM. Loss of PiT-2 results in abnormal bone development and decreased bone mineral density and length in mice. *Biochem Biophys Res Commun*. 2018;495(1):553-559.
49. Zhang S, Macias-Garcia A, Ulirsch JC, et al. HRI coordinates translation necessary for protein homeostasis and mitochondrial function in erythropoiesis. *Elife*. 2019;8.
50. Zenke-Kawasaki Y, Dohi Y, Katoh Y, et al. Heme induces ubiquitination and degradation of the transcription factor Bach1. *Mol Cell Biol*. 2007;27(19):6962-6971.
51. Kohyama M, Ise W, Edelson BT, et al. Role for Spi-C in the development of red pulp macrophages and splenic iron homeostasis. *Nature*. 2009;457(7227):318-321.

52. Lu Y, Basatemur G, Scott IC, et al. Interleukin-33 Signaling Controls the Development of Iron-Recycling Macrophages. *Immunity*. 2020;52(5):782-793 e785.

Figure 1 - *CRISPR-screen identifies SLC20A1 as a gene mediating heme-cytotoxicity*

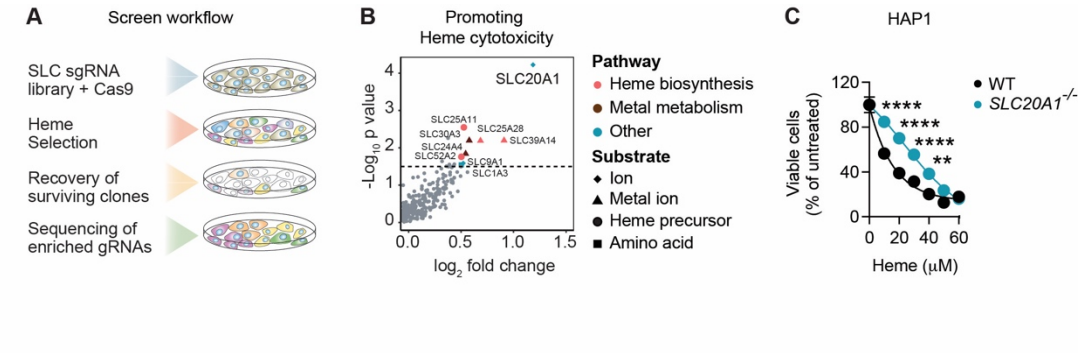

Figure 1: CRISPR-screen identifies SLC20A1 as a gene mediating heme-cytotoxicity

(A) An SLC-focused CRISPR screen was performed in HAP1 cells to identify genes involved in heme-mediated cytotoxicity by transducing cells with an SLC-focused sgRNA library, selecting cells via heme treatment and sequencing the surviving cell clones. (B) Using the MAGECK-VISPR algorithm, sgRNA nrichment of heme treated samples was calculated to identify genes which promote heme cytotoxicity. Scatter-plot of $\log_2$ fold change and $-\log_{10}$ p-value is depicted, the dotted line marks the cutoff of significance. Color coding annotates pathways, and shapes of symbols the classes of transported substrates. (C) The viability of *SLC20A1*$^{-/-}$ and WT HAP1 cells was assessed upon stimulation with indicated doses of heme for 16h in serum-free medium (n= 3; 2-way ANOVA, Bonferroni correction). Genetic-screening was performed as a single experiment. Data in (C) are representative of at least two independent experiments and expressed as mean ± S.E.M. ** $p < 0.01$ and **** $p < 0.0001$.

Figure 2 - *Slc20a1 sustains steady state erythropoiesis*

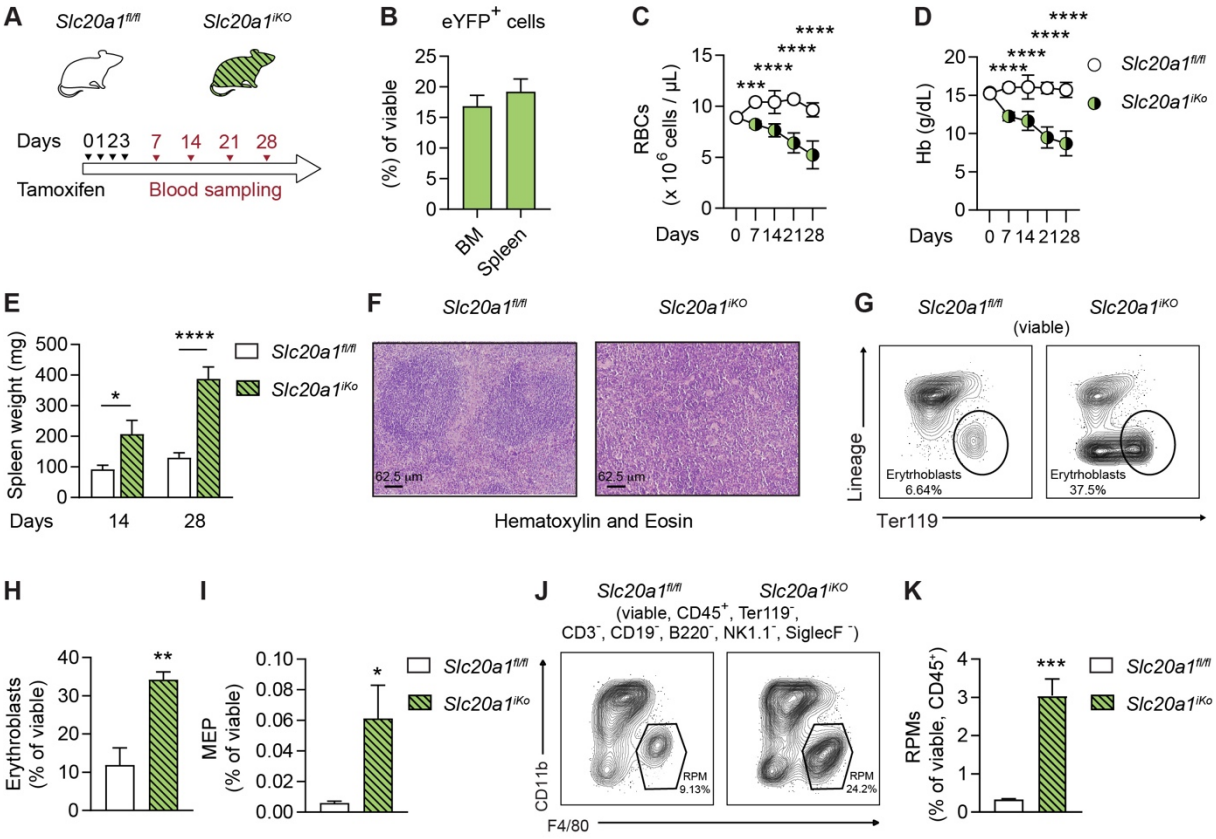

Figure 2: Slc20a1 sustains steady state erythropoiesis

(A) *Rosa26*$^{ERCre/Stop\text{-}eYFP}$ *Slc20a1*$^{fl/fl}$ (*Slc20a1*^{iKO}) and littermate control *Rosa26*$^{Stop\text{-}eYFP}$ *Slc20a1*$^{fl/fl}$ (*Slc20a1*$^{fl/fl}$) mice were treated i.p. with tamoxifen for 4 days. Blood drawings were performed before and after tamoxifen injections up to day 28. (B) The proportion of viable *Slc20a1*-deleted eYFP^{+} cells was identified in spleen and BM via flow cytometry. (C) RBC counts and (D) Hb levels were assessed in peripheral blood at indicated times (*Slc20a1*$^{fl/fl}$ n=4-6, *Slc20a1*^{iKo} n=3-6; 2-way ANOVA, Bonferroni correction). (E) Spleen weight was evaluated 14 and 28 days post-tamoxifen administration (*Slc20a1*$^{fl/fl}$ n=8-9, *Slc20a1*^{iKo} n=7-12; unpaired Student's t-test). (F) Spleen sections (1 µM) were stained with hematoxylin and eosin (H&E) 28-days post tamoxifen treatment (10x magnification). (G-K) The cellular composition of spleens was analyzed via flow cytometry (*Slc20a1*$^{fl/fl}$ n=3-5, *Slc20a1*^{iKo} n=5-6; unpaired Student's t-test) 28 days after tamoxifen treatment. (G) Erythroblasts were identified as Lin^{-}(CD3^{-}, B220^{-}, CD11b^{-}, CD11c^{-}, Ly-6G^{-}, Ly-6C^{-}) Ter119^{+} and (H) relative percentages are presented. (I) MEPs were identified as Lin^{-} (as above), Ter119^{-}, Il-7Ra^{-}, Sca-1^{-}, c-Kit^{+}, CD34^{-}, CD16/32^{lo} and the relative percentages are presented. (J) RPMs were defined as CD45^{+}, CD3^{-}, NK1.1^{-}, CD19^{-}, B220^{-}, SiglecF^{-}, CD11b^{lo}, F4/80^{+} and (K) relative percentages are presented. Data are representative of at least two independent experiments and expressed as mean ± S.E.M. * $p < 0.05$, ** $p < 0.01$, *** $p < 0.001$ and **** $p < 0.0001$.

Figure 3 - *Erythroid Slc20a1 is essential for terminal erythrocyte differentiation*

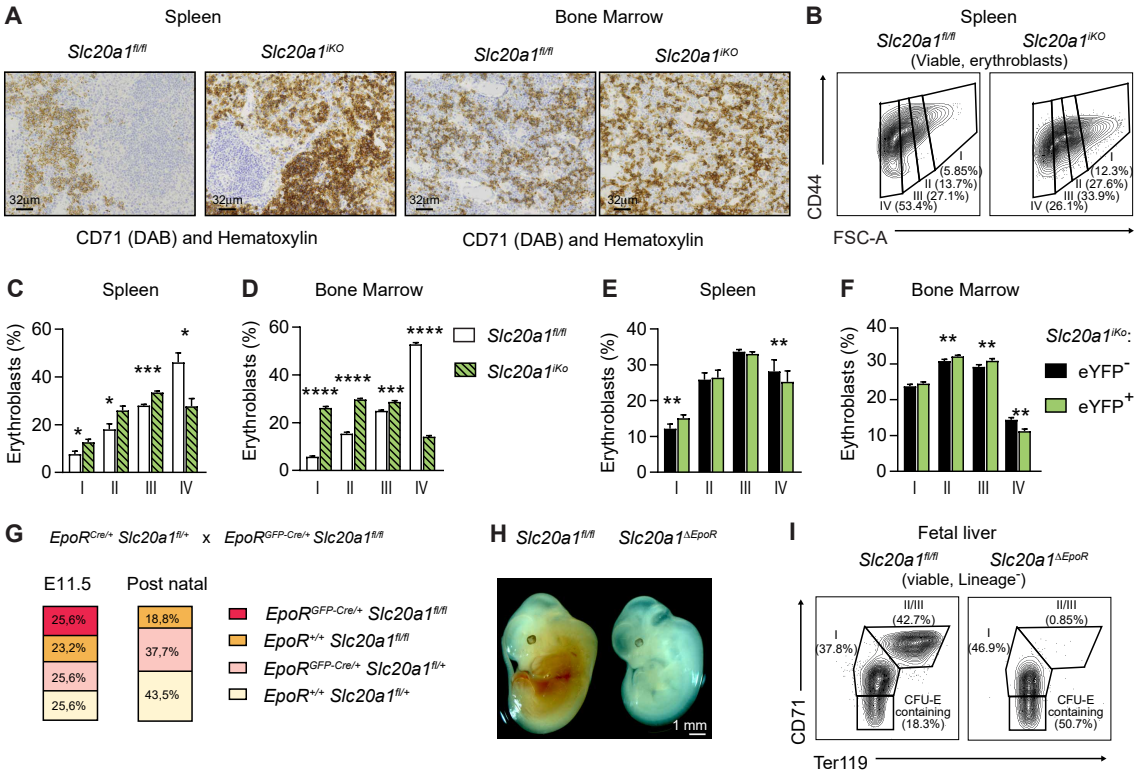

Figure 3: Erythroid Slc20a1 is essential for terminal erythrocyte differentiation

Slc20a1^{iKO} and *Slc20a1*$^{fl/fl}$ littermate control mice were treated with tamoxifen as described and 28 days later (A) spleen and BM sections were stained for the erythroid differentiation marker CD71 using immunohistochemistry (20x magnification). (B-F) Erythroblast (viable, lineage$^-$) differentiation in spleen and BM was analyzed by flow cytometry using CD44 and FSC-A (I: pro-, II: basophilic-III: polychromic-IV: orthochromatic- erythroblasts) 28 days after tamoxifen administration. (B) Representative FACS-plots showing the gating strategy for spleen erythroblasts. Relative percentages of erythroblast stages in (C) spleen and (D) BM (*Slc20a1*$^{fl/fl}$ n=3-5, *Slc20a1*^{iKo} n=5; unpaired Student's t-test). (E-F) In tamoxifen-treated *Slc20a*^{iKO} mice, cells were separated in *Slc20a1* deleted (*Slc20a*^{iKo} eYFP$^+$) and undeleted (*Slc20a1*^{iKO} eYFP$^-$), and splenic and BM erythroblast stages were analyzed as in (B). Relative proportion of spleen (E) and BM (F) erythroblast stages (*Slc20a1*^{iKo} n=5; paired Student's t-test). (G) Erythroid-specific *Slc20a1* KO (*Slc20a1*$^{\Delta EpoR}$) mice were generated by crossing *EpoR*$^{GFP\text{-}Cre/+}$ *Slc20a1*$^{fl/+}$ *x EpoR*$^{+/+}$ *Slc20a1*$^{fl/fl}$ animals, and Mendelian inheritance was evaluated in E11.5 fetuses and after birth. Relative percentages are plotted (E11.5 n=39, post-natal P0.5 n=53). (H) Appearance of *Slc20a1* $^{\Delta EpoR}$ fetus and littermate control at E11.5 (SteREO Lumar.V12). (I) Erythroblast stages of fetal (E11.5) livers from *Slc20a1*$^{\Delta EpoR}$ and *Slc20a1*$^{fl/fl}$ mice were analyzed using CD71 and Ter119 (CFU-E containing gate, I: pro-erythroblasts, II-III: terminally differentiating erythroblasts). Data are representative of at least two independent experiments and expressed as mean ± S.E.M. * $p < 0.05$, ** $p < 0.01$, *** $p < 0.001$ and **** $p < 0.0001$.

Figure 4 - *Slc20a1 is essential for RPM differentiation in stress erythropoiesis*

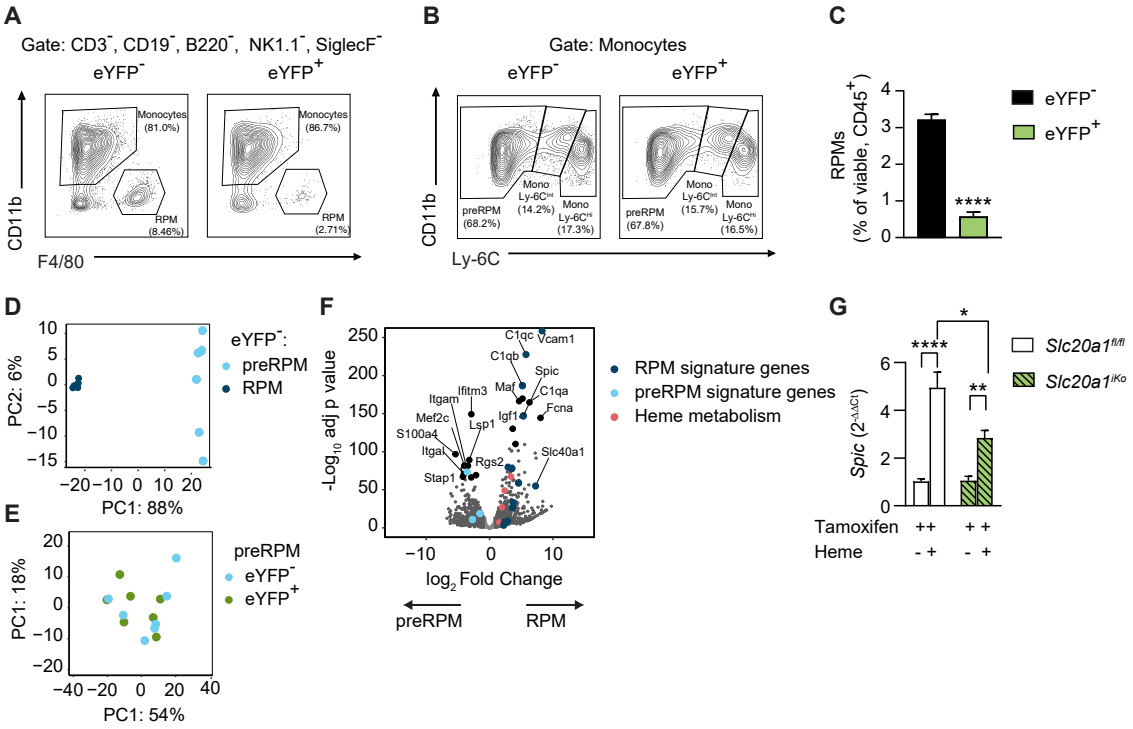

Figure 4: Slc20a1 is essential for RPM differentiation in stress erythropoiesis

(A-B) *Slc20a1* deleted (*Slc20a1*$^{iKo\ eYFP+}$) and undeleted (*Slc20a1*$^{iKO\ eYFP-}$) RPMs, pre-RPMs and monocytes were identified in the spleen of *Slc20a1*^{iKo} mice and (C) the relative percentage of RPMs are plotted (n=5, unpaired Student's t-test). (D-F) *Slc20a1*$^{iKo/eYFP+}$ preRPMs (n=6), *Slc20a1*$^{iKo/eYFP-}$ preRPMs (n=7) and RPMs (n=7) were sorted and the transcriptome sequenced. Principal component analyses (PCA) were performed on transcriptomes from (D) *Slc20a1*$^{iKo\ /eYFP-}$ preRPMs and RPMs, and (E) *Slc20a1*$^{iKo/eYFP+}$ and *Slc20a1*$^{iKo/eYFP-}$ preRPMs. (F) Volcano plot presenting differentially expressed genes in *Slc20a1*$^{iKo\ /eYFP-}$ RPMs (log_2 fold change > 1) and preRPMs (log_2 fold change < -1) ($-Log_{10}$ adj pval > 1). Color coding annotates known signature RPM or preRPM genes[6,52] (G) *Slc20a1*^{iKo} and *Slc20a1*$^{fl/fl}$ BM-derived macrophages were differentiated in a medium containing tamoxifen to induce *Slc20a1* deletion upon Cre activation. The induction of *Spic* expression was evaluated via qPCR and expressed as relative fold increase ($2^{-\Delta\Delta Ct}$). Data in (A-C, G) are representative of at least two independent experiments and expressed as mean ± S.E.M. * $p < 0.05$, ** $p < 0.01$ and **** $p < 0.0001$.

Figure 5 - *SLC20A1 sustains stress erythropoiesis-induced RPM differentiation by importing heme*

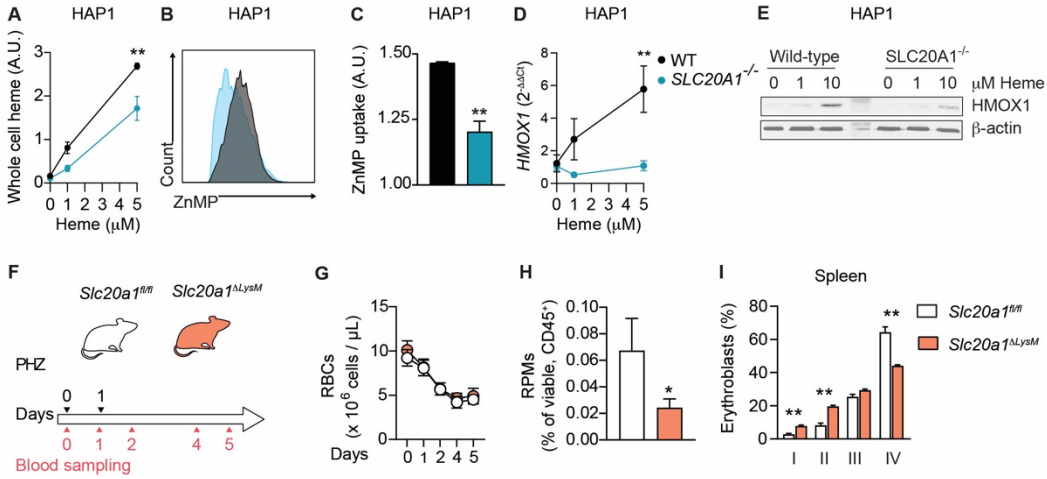

Figure 5: SLC20A1 sustains stress erythropoiesis-induced RPM differentiation by importing heme

(A) WT and *SLC20A1*$^{-/-}$ HAP1 cells were incubated with indicated heme concentrations and uptake was evaluated using the oxalic acid assay. (B-C) Uptake of the fluorescent heme analog ZnMP by WT and *SLC20A1*$^{-/-}$ HAP1 cells was quantified by flow-cytometry. (D) The induction of the heme-induced detoxification enzyme *HMOX1* was evaluated 1h post-stimulation with indicated doses of heme via qPCR and (E) 16h post-stimulation via immunoblot. (F) *Slc20a1*$^{\Delta LysM}$ mice and littermate controls were treated with PHZ at days 0 and 1 to induce hemolysis and stress erythropoiesis. (G) RBC counts were evaluated before, and up to 5 days after PHZ. (H-I) On d5 post-PHZ treatment, the cellular composition of the spleen was evaluated by flow-cytometry. Relative percentages of (H) RPMs and (I) erythroblasts are shown (*Slc20a1*$^{\Delta LysM}$ n = 3, *Slc20a1*$^{fl/fl}$ n = 3, unpaired Student's t-test). Data are representative of at least two independent experiments and expressed as mean ± S.E.M. * $p < 0.05$ and ** $p < 0.01$

Supplemental File

SLC20A1 facilitates heme transport and drives red pulp macrophage and erythroblast differentiation

Federica Quattrone[1,2], Rui Martins[1,2,#‡], Anna-Dorothea Gorki[1,2,#‡], Anastasiya Hladik[1], Karin Lakovits[1], Manuele Rebsamen[2‡], Enrico Girardi[2], Andrea Alvarez-Hernandez[3], Florian Mayrhofer[1], Asma Farhat[1,2], Martin L. Watzenboeck[1,2], Emile van den Akker[4,5], Marieke von Lindern[4,5], Giulio Superti-Furga[2,6], Ingrid Simonitsch-Klupp[3], Riem Gawish[1,2*] and Sylvia Knapp[1,2*].

Supplemental Materials and Methods

Phosphate transport

Cells were washed twice with phosphate uptake buffer (100 mM NaCl, 2 mM KCl, 1 mM $CaCl_2$, 1 mM $MgCl_2$, and 10 mM HEPES-KOH, pH 7.5) before stimulation with KH_2PO_4 or heme for 1h[1]. Next, cells were washed twice with the same buffer and lysed with RIPA (NaCl 150 mM, Tris pH 7.5 50 mM, SDS 0.1%, Triton-X-100 1%, DOC 0.5%, benzonase 25 U/mL). Intracellular inorganic phosphate concentration was evaluated using the Phosphate Colorimetric Kit (Abcam).

Timed pregnancies

We performed timed-pregnancies by breeding *EpoR*$^{GFP\text{-}Cre/+}$ *Slc20a1* $^{fl/+}$ with *Slc20a* $^{fl/fl}$ mice. Breeding pairs were set-up and successful mating evaluated 12h later by presence of vaginal plugs (E0.5). At E11.5 pregnant dams were euthanized, fetuses retrieved, and fetal liver harvested for analysis, other tissues for genotyping. Imaging of E11.5 embryos was performed using SteREO Lumar.V12.

Histology

Histological staining was performed on 1μm sections of formalin-fixed tissues. After heat-mediated epitope retrieval, slides were incubated with anti-mouse CD71 antibody (1:3000, Abcam) diluted with BOND antibody diluent and BOND Polymer Refine Kit DS9800 (Leica Biosystems) and counterstained with hematoxylin. Images were acquired using the FSX100 microscope (Olympus).

qPCR

Total mRNA was extracted with NucleoSpin RNA Kit and retrotranscribed with iScript. qPCR was performed using the SYBR Green Master Mix, supplemented with the primers of interest and run with StepOnePlus™ Real-TimePCR. Primers are listed in supplemental Table 1. Gene expression was calculated as relative fold induction and normalized to indicated housekeeper genes.

Quant-Seq

Total cellular mRNA was extracted via the RNAeasy Micro Kit (Qiagen) from FACS-sorted myeloid cells and Quant-seq libraries were prepared with 150 ng total RNA input

according to the manufacturer's instructions using the QuantSeq3' mRNA-Seq library Prep Kit (FWD) for Illumina and the UMI Second Strand Synthesis Module for Quantseq FWD (Lexogen). Sample quality was evaluated using the Bioanalyzer 2100 (Agilent Technologies) and pooled libraries were 65 bp single-end sequenced on a HiSeq4000 (Illumina) at the BSF facility (CeMM, MUW). Demultiplexing, mapping (to mouse genome GRCm38 mm10) and removal of PCR duplicates with identical mapping and UMI sequences was performed using the Bluebee® software (version Quantseq 2.3.6 FWD UMI).

Smart Seq

Erythroid progenitors were FACS-sorted in plates containing lysis buffer (0.2%(v/v) Triton X-100 (Sigma-Aldrich), 0.5 μl RNAse inhibitor (Clonetech), spun down and frozen at-80°C. Cellular mRNA was retrotranscribed using SuperScript II (Invitrogen), PCR-amplified using with KAPA HiFi HotStart Ready Mix (Kapa Biosystems), purified with two rounds of SPRI (Beckman Coulter) and quantified with a Qubit fluorometer (Life Technologies). 1 ng of cDNA were used for library preparation using the Nextera XT DNA Sample Preparation Kit (Illumina), then purified using followed by SPRI (Beckman Coulter) size selection. Obtained libraries were sequenced on Illumina HiSeq 2000/2500 at BSF.

RNA sequencing data analysis

Differential expression analysis between cell types and genotypes was performed using the Bioconductor DESeq2 package[2]. Differentially expressed genes (DEG) were defined as log2 fold change >1.5 and adjusted p value < 0.05. Volcano plots were generated using the Bioconductor ggplot2[3]. Gene lists of interest were retrieved from Molecular Signature Database[4,5] (Stable ID: M5923, M10214, access: 2021.02.21), Reactome[6] (Stable ID: R-HSA-9648895, access: 2021.02.21), Gene Ontology[7,8] (GO:0006783, access: 2021.02.21) and from published dataset[9] (SRX2682727).

Immunoblot

Cells were lysed in RIPA buffer, boiled 5min at 95°C, resolved on 10% polyacrylamide gels and blotted onto PVDF membranes. Membranes were blocked (TBS 0.1% Tween20, 5% milk) before being incubated overnight at 4°C with anti-Rabbit HMOX1 antibody (1:500, Abcam) and anti-mouse β-actin (1:1000, Sigma-Aldrich) followed by

incubation with anti-Rabbit-680w and anti-mouse-800w (both 1:10000, Licor) and read on an Odyssey instrument.

Supplemental References:

1. Bottger P, Hede SE, Grunnet M, Hoyer B, Klaerke DA, Pedersen L. Characterization of transport mechanisms and determinants critical for Na+-dependent Pi symport of the PiT family paralogs human PiT1 and PiT2. *Am J Physiol Cell Physiol*. 2006;291(6):C1377-1387.
2. Love MI, Huber W, Anders S. Moderated estimation of fold change and dispersion for RNA-seq data with DESeq2. *Genome Biol*. 2014;15(12):550.
3. Wickham H. ggplot2 : Elegant Graphics for Data Analysis. Use R!,. Cham: Springer International Publishing : Imprint: Springer,; 2016:1 online resource (XVI, 260 pages 232 illustrations, 140 illustrations in color.
4. Liberzon A, Birger C, Thorvaldsdottir H, Ghandi M, Mesirov JP, Tamayo P. The Molecular Signatures Database (MSigDB) hallmark gene set collection. *Cell Syst*. 2015;1(6):417-425.
5. Subramanian A, Tamayo P, Mootha VK, et al. Gene set enrichment analysis: a knowledge-based approach for interpreting genome-wide expression profiles. *Proc Natl Acad Sci U S A*. 2005;102(43):15545-15550.
6. Jassal B, Matthews L, Viteri G, et al. The reactome pathway knowledgebase. *Nucleic Acids Res*. 2020;48(D1):D498-D503.
7. Ashburner M, Ball CA, Blake JA, et al. Gene ontology: tool for the unification of biology. The Gene Ontology Consortium. *Nat Genet*. 2000;25(1):25-29.
8. Gene Ontology C. The Gene Ontology resource: enriching a GOld mine. *Nucleic Acids Res*. 2021;49(D1):D325-D334.
9. Paolini NA, Moore KS, di Summa FM, Fokkema I, t Hoen PAC, von Lindern M. Ribosome profiling uncovers selective mRNA translation associated with eIF2 phosphorylation in erythroid progenitors. *PLoS One*. 2018;13(4):e0193790.

Supplemental Figure 1 - *CRISPR-screen identifies SLC20A1 as a gene mediating heme-cytotoxicity*

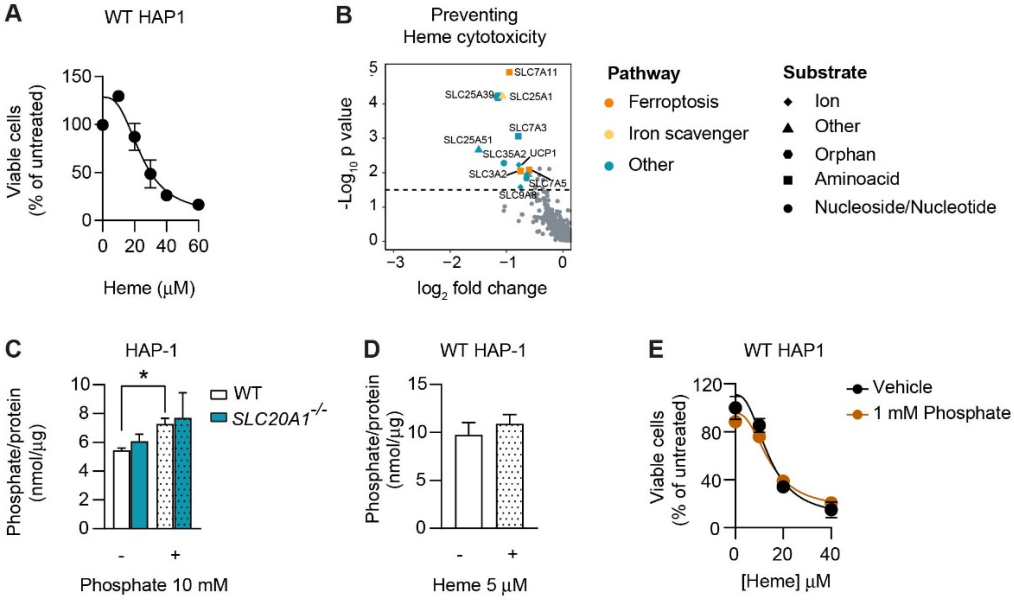

Supplemental Figure 1: CRISPR-screen identifies SLC20A1 as a gene mediating heme-cytotoxicity
(A) The cytotoxic potential of heme was evaluated by assessing the viability of WT HAP1 cells upon stimulation with increasing heme concentrations in serum-free medium for 16 hours. (B) Using the MAGECK-VISPR algorithm, sgRNA depletion of heme treated samples was calculated to identify genes whose presence exerted protective effects. Scatter-plot of log_2 fold change and $–log_{10}$ p-value is depicted, the dotted line marks the cutoff of significance. Color coding annotates pathways, symbols annotate substrate types. (C) Whole-cell phosphate concentration was evaluated in WT and *SLC20A1*$^{-/-}$ HAP1 cells at baseline and upon stimulation with 10 mM phosphate for 1h (n=3, unpaired Student's t-test). (D) Whole-cell phosphate concentration was evaluated in WT HAP1 cells upon stimulation for 1h with 5 μM heme or vehicle in phosphate-free medium (n=3, unpaired Student's t-test). (E) The viability to heme-induced cell death of WT HAP1 cells was assessed upon prior stimulation with 1mM phosphate or its vehicle for 3h (n= 4, 2-way ANOVA). The CRISPR screen was performed as a single experiment. The other depicted data are representative of at least two independent experiments and expressed as mean ± S.E.M. * $p \leq 0.05$.

Supplemental Figure 2 - *Slc20a1 sustains steady state erythropoiesis*

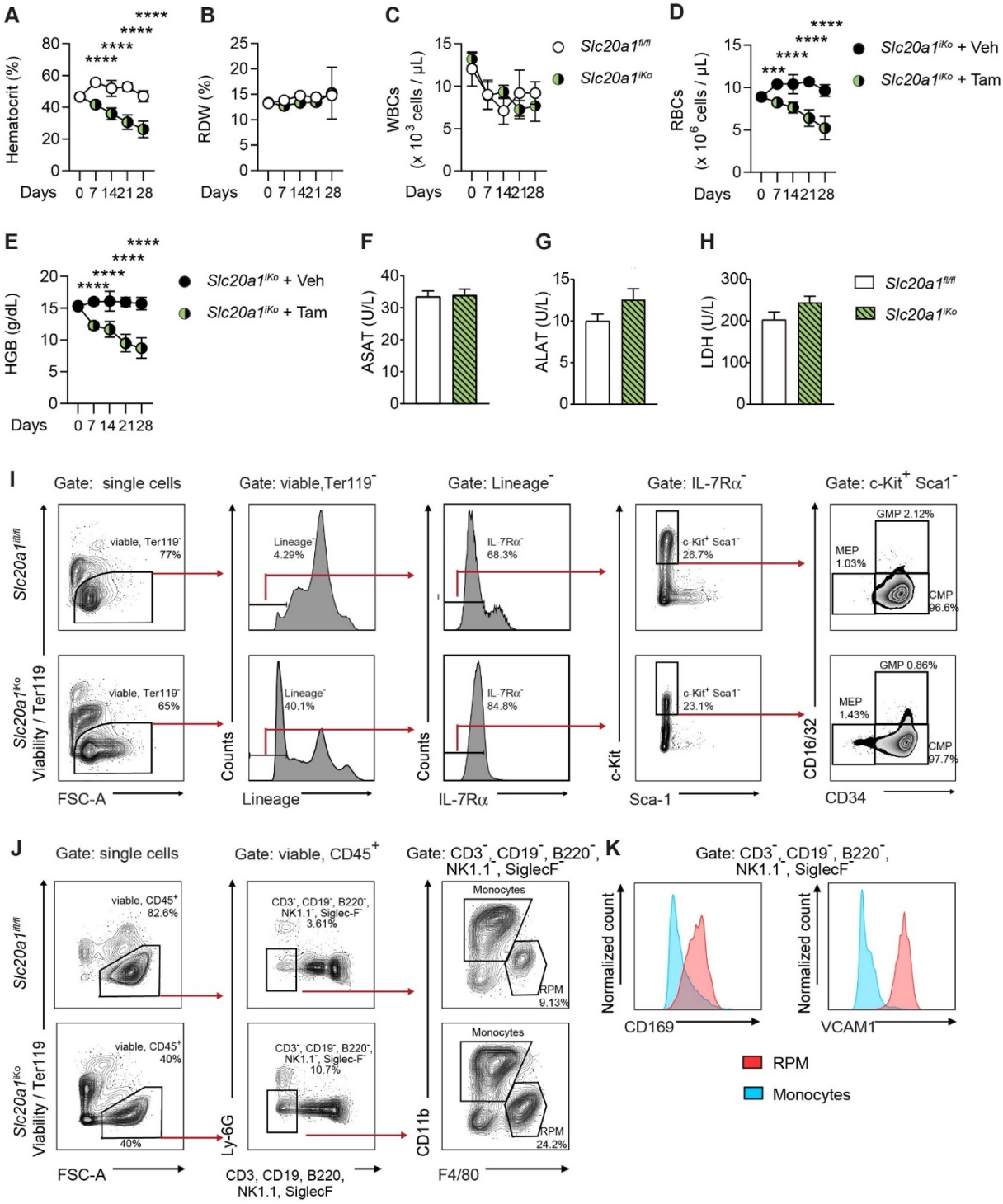

Supplemental Figure 2: Slc20a1 sustains steady state erythropoiesis

(A-C) *Slc20a1*^{iKO} and *Slc20a1*$^{fl/fl}$ littermate control mice were treated with tamoxifen and (A) HCT, (B) red cell distribution width (RDW) and (C) WBCs were evaluated in peripheral blood up to 28-days post-treatment (*Slc20a1*$^{fl/fl}$ n=4-6, *Slc20a1*^{iKo} n=3-6; 2-way ANOVA, Bonferroni Correction). (D-E) *Slc20a1*^{iKO} mice were treated i.p. with tamoxifen (Tam) or vehicle (Veh) for 4 days, before (D) RBCs and (E) Hb levels were evaluated in peripheral blood (vehicle n=2-6, tamoxifen n=5-6; 2-way ANOVA, Bonferroni Correction). (F-H) *Slc20a1*^{iKO} and *Slc20a1*$^{fl/fl}$ mice were treated as in (A-C), and ASAT, ALAT and LDH

plasma levels were evaluated 28 days after tamoxifen treatment (*Slc20a1*$^{fl/fl}$ n=4, *Slc20a1*^{iKo} n=7; unpaired Student's t-test). (I-J) Representative FACS-plots showing the gating strategy to identify (I) MEPs and (J) RPMs. (K) Characterization of CD169 and VCAM1 membrane expression in RPMs and monocytes. Data are representative of at least two independent experiments and expressed as mean ± S.E.M. *** $p \leq 0.001$ and **** $p \leq 0.0001$.

Supplemental Figure 3 - *Erythroid SLC20A1 is essential for terminal erythrocyte differentiation*

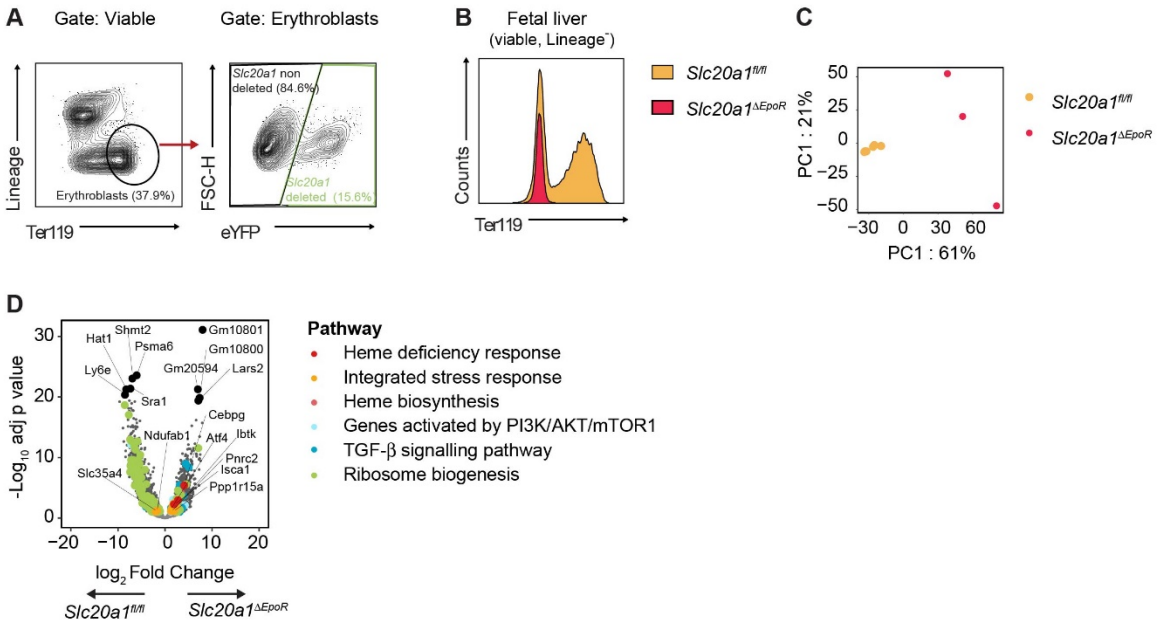

Supplemental Figure 3: Erythroid SLC20A1 is essential for terminal erythrocyte differentiation

(A) Representative FACS-plots showing the gating strategy for the identification of erythroblasts in adult spleens. (B) Fetal liver cells from E11.5 embryos of *Slc20a1*$^{\Delta\ EpoR}$ and *Slc20a1*$^{fl/fl}$ mice were analyzed by flow cytometry, and expression of Ter119 of viable, Lin$^-$ cells is shown (representative of *Slc20a1*$^{\Delta EpoR}$ n=2, *Slc20a1*$^{fl/fl}$, *Slc20a*$^{fl/+}$, *Slc20a*$^{fl/+}$ *EpoR*$^{GFP\text{-}Cre/+}$= 5).(C) The transcriptome of pro-erythroblasts (stage I) sorted from the fetal liver of *Slc20a1*$^{\Delta EpoR}$ and *Slc20a1*$^{fl/fl}$ was analyzed (*Slc20a1*$^{\Delta EpoR}$ n = 3, *Slc20a1*$^{fl/fl}$ n=6). Principal component analysis (PCA) was performed on differentially expressed transcripts from *Slc20a1*$^{\Delta EpoR}$ and *Slc20a1*$^{fl/fl}$ pro-erythroblasts. (D) Volcano plot presents differentially expressed genes (-Log$_{10}$ adj pval > 1) in *Slc20a1*$^{\Delta EpoR}$ (log$_2$ fold change > 1) and *Slc20a1*$^{fl/fl}$ pro-erythroblasts (log$_2$ fold change < -1). Color coding annotates pathways [4-6,9].

Supplemental Figure 4 - *Slc20a1 is essential for RPM differentiation*

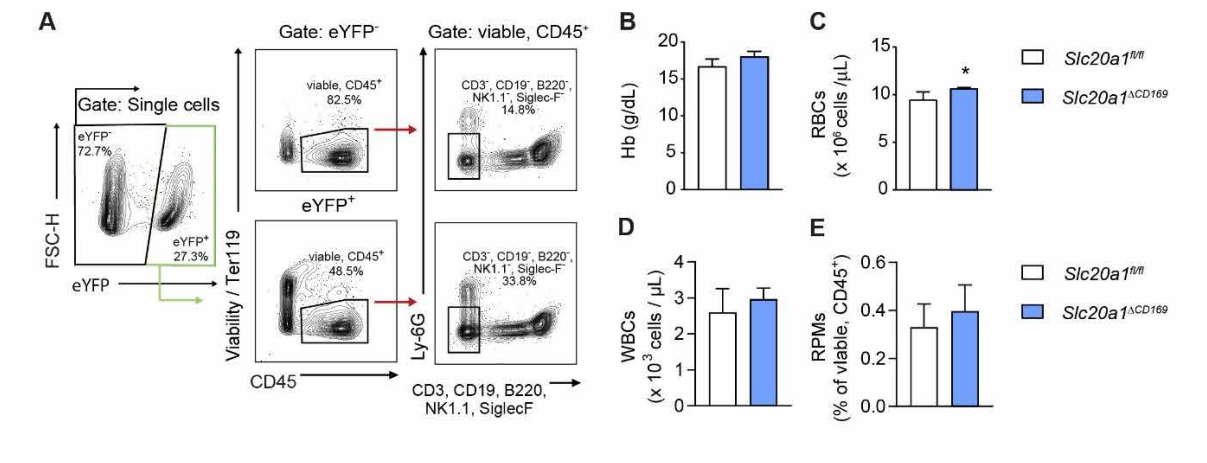

Supplemental Figure 4: Slc20a1 is essential for RPM differentiation

(A) Representative FACS-plots showing the gating strategy to analyze the myeloid compartment within the eYFP$^+$ and eYFP$^-$ populations of tamoxifen treated *Slc20a1^{iKO}* mice. (B-E) Mice lacking *Slc20a1* in CD169$^+$ tissue-resident macrophages (including RPMs) were generated (*Slc20a1$^{\Delta CD169}$*) and steady state hematopoiesis was evaluated in the peripheral blood: (B) Hb levels, (C) RBCs and (D) WBCs. (E) The relative percentage of RPMs in the spleen was assessed by flow cytometry. (*Slc20a1$^{fl/fl}$* n=3, *Slc20a1$^{\Delta CD169}$* n=6; unpaired Student's t-test). Data are representative of at least two independent experiments and expressed as mean ± S.E.M. * $p \leq 0.05$.

Supplemental Figure 5 -*SLC20A1 sustains anemia-induced RPM differentiation by importing heme*

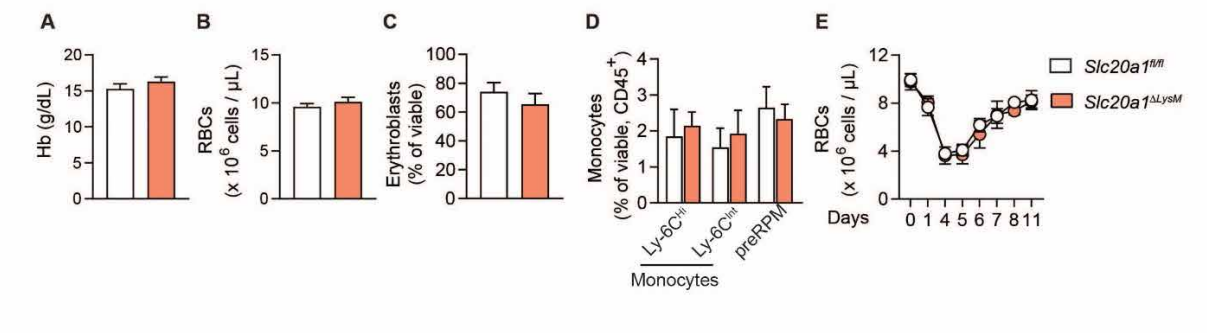

Supplemental Figure 5: SLC20A1 sustains anemia-induced RPM differentiation by importing heme

(A) Hb and (B) RBCs were analyzed in the peripheral blood of *Slc20a1*$^{\Delta LysM}$ and *Slc20a1*$^{fl/fl}$ at steady state (*Slc20a1*$^{fl/fl}$ n=5, *Slc20a1*$^{\Delta LysM}$ n=5; unpaired Student's t-test). Hemolytic anemia was induced in *Slc20a1*$^{\Delta LysM}$ and *Slc20a1*$^{fl/fl}$ mice by PHZ treatment. On d5 post-PHZ treatment, the relative percentages of expanding (C) erythroblasts and (D) differentiating splenic monocytes were evaluated by flow-cytometry (*Slc20a1*$^{fl/fl}$ n=3, *Slc20a1*$^{\Delta LysM}$ n=3; unpaired Student's t-test). (E) RBC counts in the peripheral blood of PHZ-treated mice were evaluated for 11 days (*Slc20a1*$^{fl/fl}$ n=4, *Slc20a1*$^{\Delta LysM}$ n=4; unpaired Student's t-test). (E) was performed as single experiment, the other depicted data are representative of at least two independent experiments and expressed as mean ± S.E.M.

Supplemental Tables

Supplemental Table 1 - *List of primers used for genotyping or qPCR purposes*

Application	Gene	Species	Sense	Sequence	Producer
Genotyping	*Slc20a1*	Mouse	Forward	CTCTGGCCTGTTTTTGTTTTTCC	Mycrosynth
Genotyping	*Slc20a1*	Mouse	Reverse	TGGTCCCATCCTGTGTTTCTT	Mycrosynth
Genotyping	*Slc20a1*	Mouse	Reverse	AATGCTTATTTCCTGATGTCCTG	Mycrosynth
Genotyping	*eYFPStopFlox*	Mouse	Forward	AAGACCGCGAAGAGTTTGTCC	Mycrosynth
Genotyping	*eYFPStopFlox*	Mouse	Reverse	TAAGCCTGCCCAGAAGACTCC	Mycrosynth
Genotyping	*eYFPStopFlox*	Mouse	Reverse	AAGGGAGCTGCAGTGGAGTA	Mycrosynth
Genotyping	*ERT2-Cre*	Mouse	Forward	GCG AAG AGT TTG TCC TCA ACC	Mycrosynth
Genotyping	*ERT2-Cre*	Mouse	Reverse	AAA GTC GCT CTG AGT TGT TAT	Mycrosynth
Genotyping	*ERT2-Cre*	Mouse	Reverse	GGA GCG GGA GAA ATG GAT ATG	Mycrosynth
Genotyping	*ER-GFPCre*	Mouse	Forward	GTGTGGCTGCCCCTTCTGCCA	Mycrosynth
Genotyping	*ER-GFPCre*	Mouse	Reverse	GGCAGCCTGGGCACCTTCAC	Mycrosynth
Genotyping	*ER-GFPCre*	Mouse	Reverse	CAGGAATTCAAGCTCAACCTCA	Mycrosynth
Genotyping	*LysM cre*	Mouse	Forward	CCCAGAAATGCCAGATTACG	Mycrosynth
Genotyping	*LysM cre*	Mouse	Reverse	CTTGGGCTGCCAGAATTTCT	Mycrosynth
Genotyping	*LysM cre*	Mouse	Reverse	TTACAGTCGGCCAGGCTGA	Mycrosynth
qPCR	*Spic*	Mouse	Forward	TCCGCAACCCAAGACTCTTCAA	Mycrosynth
qPCR	*Spic*	Mouse	Reverse	GGGTTCTCTGTGGGTGACATTCCAT	Mycrosynth
qPCR	*Hprt*	Mouse	Forward	GTTAAGCAGTACAGCCCCAAAATG	Mycrosynth
qPCR	*Hprt*	Mouse	Reverse	AAATCCAACAAAGTCTGGCCTGTA	Mycrosynth
qPCR	*HMOX1*	Human	Forward	TCCGATGGGTCCTTACACTC	Mycrosynth
qPCR	*HMOX1*	Human	Reverse	TAAGGAAGCCAGCCAAGAGA	Mycrosynth
qPCR	*GAPDH*	Human	Forward	GGTCGTATTGGGCGCCTGGTCACC	Mycrosynth
qPCR	*GAPDH*	Human	Reverse	CACACCCATGACGAACATGGGGGC	Mycrosynth

Supplemental Table 2 - *List of antibodies used for flow-cytometry, divided by panel*

Antigen	Color	Clone	Catalog	Producer	Panel
Ter-119	Pacific Blue	TER-119	116231	Biolegend	Erythroblast staging
CD71	PE	RI7217	113808	Biolegend	Erythroblast staging
CD44	APC	IM7	103012	Biolegend	Erythroblast staging
Ly-6C	PE-Cy7	HK1.4	128017	Biolegend	Erythroblast staging
Ly-6G	PE-Cy7	1A8	127617	Biolegend	Erythroblast staging
CD45R	PE-Cy7	RA3-6B2	103222	Biolegend	Erythroblast staging
CD3e	PE-Cy7	145-2C11	100319	Biolegend	Erythroblast staging
CD11b	PE-Cy7	M1/70	101215	Biolegend	Erythroblast staging
c-Kit	BV421	ACK2	135124	Biolegend	MEP
CD16/32	PE	93	101308	Biolegend	MEP
Sca1	BV605	D7	108133	Biolegend	MEP
CD127/IL-7Ra	PE/Dazzle 594	A7R34	135031	Biolegend	MEP
CD34	PerCP/Cy5	HM34	128607	Biolegend	MEP
Ly-6C	PE-Cy7	HK1.4	128017	Biolegend	MEP
Ly-6G	PE-Cy7	1A8	127617	Biolegend	MEP
CD45R	PE-Cy7	RA3-6B2	103222	Biolegend	MEP
CD3e	PE-Cy7	145-2C11	100319	Biolegend	MEP
CD11b	PE-Cy7	M1/70	101215	Biolegend	MEP
Ter-119	APC-Cy7	TER-119	116223	Biolegend	MEP
VCAM1	PE	MVCAM.A	105713	Biolegend	Macrophages
Ly-6c	BV510	HK1.4	128033	Biolegend	Macrophages
CD19	PE/ -TexasRed	6D5	115507	Biolegend	Macrophages
CD45R	PE	RA3-6B2	103208	Biolegend	Macrophages
CD3	PE/ -Texas Red	17A2	100205	Biolegend	Macrophages
NK1.1	PE	PK136	108708	Biolegend	Macrophages
Siglec F	PE	E50-2440	552126	Biolegend	Macrophages
Ly-6g	BV605	1A8	127639	Biolegend	Macrophages
F4/80	PerCP/Cy5	BM8	45-4801-82	eBioscience	Macrophages
CD169	APC	SER-4	50-5755-80	Invitrogen	Macrophages
CD45	AF700	30-F11	103128	Biolegend	Macrophages
CD11b	PE-Cy7	M1/70	101215	Biolegend	Macrophages
Ter-119	APC-Cy7	TER-119	116223	Biolegend	Macrophages

Supplemental Table 3 - *CRISPR-Screen Top 50 depleted sgRNA after heme treatment*

id	neg|score	neg|p-value	neg|fdr	neg|rank	id	neg|score	neg|p-value	neg|fdr	neg|rank
SLC7A11	3,62E-07	1,19E-05	0,00495	1	SLC25A32	0,010871	0,041501	0,654749	26
SLC25A1	1,46E-05	5,96E-05	0,008251	3	SLC35G6	0,011194	0,042598	0,654749	27
SLC25A39	6,37E-06	5,96E-05	0,008251	2	SLC45A4	0,012115	0,045867	0,678901	28
SLC7A3	0,0001503	0,00087081	0,090347	4	SLC35F3	0,012547	0,047441	0,678901	29
SLC25A51	0,00038661	0,002183	0,181188	5	SLC42A3	0,014941	0,055791	0,771782	30
SLC35A2	0,00092028	0,0052845	0,336184	6	SLC38A7	0,01577	0,058225	0,77819	31
UCP1	0,0010609	0,0059764	0,336184	7	SLC6A14	0,017223	0,062901	0,77819	32
SLC30A9	0,0014399	0,0076464	0,336184	8	SLC27A4	0,017331	0,063307	0,77819	33
SLC5A9	0,0014777	0,0078611	0,336184	9	SLC14A2	0,017627	0,064142	0,77819	34
SLC7A5	0,0016368	0,0084576	0,336184	10	SLC6A17	0,018416	0,066671	0,77819	35
SLC3A2	0,0017329	0,0089109	0,336184	11	SLC11A1	0,0187	0,067506	0,77819	36
SLC25A24	0,00236	0,011774	0,356082	12	SLC26A10	0,019276	0,069486	0,779368	37
SLC38A3	0,002375	0,011798	0,356082	13	SLC35G5	0,022657	0,080508	0,879234	38
SLC31A1	0,0024168	0,012012	0,356082	14	SLC2A9	0,024146	0,085041	0,902351	39
SLC35A1	0,0030159	0,014613	0,40099	15	SLC25A18	0,024802	0,086974	0,902351	40
SLC25A31	0,0032263	0,01552	0,40099	16	SLC35F2	0,02638	0,092055	0,93178	41
SLC1A7	0,0034645	0,016426	0,40099	17	U2AF2	0,027796	0,096302	0,951556	42
SLC30A1	0,0060216	0,025397	0,568364	18	SLC12A6	0,032372	0,10833	0,987197	43
SLC9A8	0,006259	0,026327	0,568364	19	SLCO5A1	0,033582	0,11102	0,987197	44
SLC26A2	0,0069259	0,028498	0,568364	20	SLC29A2	0,03659	0,11792	0,987197	45
SLC10A5	0,0069897	0,028761	0,568364	21	SLC6A7	0,037563	0,12018	0,987197	46
SLC38A2	0,0087144	0,033962	0,63703	22	SLC29A1	0,039542	0,12462	0,987197	47
SLC7A8	0,0090982	0,035441	0,63703	23	SLC7A5P1	0,041083	0,12741	0,987197	48
SLC25A53	0,0097106	0,03766	0,63703	24	MTCH2	0,041603	0,12853	0,987197	49
SLC37A1	0,0099632	0,038375	0,63703	25	SLC17A1	0,042035	0,12958	0,987197	50

Supplemental Table 4 - *CRISPR-Screen Top 50 enriched sgRNA after heme treatment*

id	pos|score	pos|p-value	pos|fdr	pos|rank	id	pos|score	pos|p-value	pos|fdr	pos|rank
SLC20A1	0,000013897	5,96E-05	2,48E-02	1	SLC16A8	0,013832	0,051616	0,792807	26
SLC25A11	0,00049877	2,83E-03	4,46E-01	2	SLC22A16	0,014233	0,052714	0,792807	27
SLC22A5	0,0010343	5,50E-03	4,46E-01	3	SLC17A5	0,015251	0,056197	0,792807	28
SLC39A14	0,001156	0,0063342	0,44637	4	SLC38A9	0,015556	0,057223	0,792807	29
SLC30A3	0,0011655	0,0063581	0,44637	5	SLC29A1	0,016625	0,060348	0,792807	30
SLC25A28	0,0011928	0,0064535	0,44637	6	SLC38A11	0,017223	0,06271	0,792807	31
SLC24A4	0,0031186	0,014398	0,773102	7	SLC16A13	0,017331	0,06314	0,792807	32
SLC52A2	0,0039383	0,017357	0,773102	8	SLC10A2	0,017439	0,063474	0,792807	33
SLC45A2	0,0054675	0,022939	0,773102	9	SLC22A13	0,017912	0,064953	0,792807	34
SLC9A1	0,0062983	0,025802	0,773102	10	SLC25A38	0,019147	0,068913	0,816419	35
SLC18A4	0,0068001	0,027472	0,773102	11	SLC20A2	0,019667	0,070822	0,816419	36
SLC26A1	0,0069259	0,027973	0,773102	12	SLC17A1	0,020529	0,0739	0,82572	37
SLC1A3	0,0070443	0,02857	0,773102	13	SLC25A36	0,021774	0,078361	0,82572	38
SLC6A11	0,007673	0,031027	0,773102	14	SLC22A17	0,021971	0,078886	0,82572	39
SLC26A3	0,0077231	0,031123	0,773102	15	SLC25A40	0,02239	0,080198	0,82572	40
SLC24A5	0,0080624	0,032029	0,773102	16	SLC2A6	0,02296	0,081749	0,82572	41
SLC42A2	0,0080683	0,032029	0,773102	17	SLC25A30	0,024042	0,084373	0,82572	42
SLC35F6	0,0085098	0,033532	0,773102	18	SLC8A2	0,024786	0,086139	0,82572	43
SLC10A7	0,0093465	0,036013	0,782797	19	SLC35D3	0,025468	0,087546	0,82572	44
SLC5A9	0,010364	0,039258	0,782797	20	SLC15A1	0,028324	0,094203	0,843337	45
SLC24A2	0,011753	0,044459	0,782797	21	SLC35D1	0,028567	0,094871	0,843337	46
SLCO4A1	0,011787	0,044507	0,782797	22	SLC35C1	0,02944	0,09697	0,843337	47
SLC4A7	0,011879	0,044841	0,782797	23	SLC35E3	0,029684	0,097543	0,843337	48
SLC1A6	0,011982	0,04527	0,782797	24	SLC39A6	0,030673	0,10026	0,849161	49
SLC39A1	0,012654	0,04799	0,792807	25	SLC25A23	0,033074	0,1062	0,881485	50

3. Discussion

Heme is a key molecule for the majority of living organisms: it regulates several cellular signaling pathways, cell differentiation and it sustains essential processes such as electron- and oxygen- usage and transport[6,46]. At the same time, heme can be harmful to organisms as it promotes ROS-synthesis, inflammation and it can activate cell death programs[1,5,26]. As such, the organisms balance heme synthesis, scavenging and degradation to exploit the molecule, while reducing its toxic effects[31]. The enzymes required for the synthesis of heme have been described, as well as the pathways in place to degrade heme. Conversely, the transporters regulating the trafficking of heme or the synthesis/degradation intermediates are still largely unknown. For many years it has been speculated that heme could passively diffuse through membranes given its amphiphilic structure. However, such claim does not take into account that heme intercalation in the membrane layer sustains lipid peroxidation, ultimately leading to membrane damage and cell death[6]. As such, it is likely unplausible that organisms did not evolve targeted transport mechanisms to ensure damage-free heme transport. Furthermore, in the extracellular compartment, heme is mostly bound to scavengers as hemopexin and, as such, it is not allowed to freely diffuse through the membrane[31,46]. Nonetheless, in pathological conditions as hemolytic crises, whereby the local unbound heme concentration overwhelms the scavenging systems, the leftover free-floating heme could intercalate and passively diffuse through membranes.

Although ~10% of the human genome encodes for membrane transporters[121], the study of those molecules has been difficult because of technical hardships[121,122]. However, recent technological advances prompted a renaissance for the study of transporters, by allowing easier gene manipulation and high-throughput phenotypic screenings[122]. Genetic screens are instrumental for the unbiased identification of genes contributing to a phenotype/pathway of interest: given a certain phenotype, genetic screen allow to identify discrete groups from a general pool of cells bearing unique gene deletions. Genetic screens proved to have a high discovery power as they could identify several unrecognized genes involved in the regulation even of well-known phenotypes[123]. Aiming at discovering genes involved in heme trafficking and/or toxicity, we performed a genetic screen. We hypothesized that cells lacking genes involved in heme transport would be more fit to survive heme cytotoxicity. Considering that all the described heme transporters are part of the SLC-family and given the

availability of a human cell line expressing most of the SLC-transporters[124], we focused our screen on the SLC-class of transporters. By limiting the screen to the SLC-class, we missed information from genes from other classes involved in heme trafficking, as endosome formation and acidification[125] or other transporters of the ABC-class. Such limitation could have been overridden by employing genome-wide libraries. However, screening for larger libraries comes at the cost of 1) lowering the coverage (i.e. how many cells a targeted by the same single guide RNA, sgRNA, are present), resulting in a poorer discrimination of enriched or depleted genes, 2) diluting the representation of gene classes of interest to the biological question. By using a focused library, we could achieve a high screen coverage (1000x) and we could interrogate a non-diluted subset of genes of interest thereby gaining statistical power, at the cost of not taking in consideration other interesting classes of transporters.

Genetic screens identify interacting genes giving rise to a certain phenotype but provide no information regarding their functionality. As such, direct evidence is needed to build hypothesis to discriminate between known genes giving rise to the screened phenotype and the novel ones. As an example of the first group, cells lacking transporters involved in the homeostatic redox balance (*SLC7A11/SLC3A2* and *SLC7A5/SLC3A2*) or iron scavenging (*SLC25A1)* were found to be more sensitive to heme cytotoxicity. Possibly, the loss of cellular redox buffering capability is the reason for their higher sensitivity to the cytotoxic effects of heme[126,127]. As an example of the latter group, cells lacking *SLC20A1* were found to be most resistant to heme cytotoxicity. To this end, SLC20A1 was considered a phosphate transporter[103-106]. While murine strains lacking known phosphate transporters are characterized by defective cartilage and bone calcification or kidney disease, we could not discern such a phenotype in animals lacking *Slc20a1*. Instead, *Slc20a1*-deletion leads to severe anemia caused by a block in terminal erythroid differentiation at the pro-erythroblast stage. This disease trait is shared with mice lacking both isoforms of the heme exporter *Flvcr1*[130]. Taking all evidence together, we hypothesized that SLC20A1 could have a role associated to heme transport. In line with this hypothesis, we demonstrated that *SLC20A1*$^{-/-}$ HAP1 cells have reduced heme import capability. Taking in consideration 1) the anemic phenotype of *Slc20a1*$^{-/-}$ mice and 2) the essentiality of heme transport in the erythroblastic island, we focused our in-vivo investigation on dissecting this disease trait.

To complete erythroid differentiation, erythroblasts produce stochiometric quantities of globin chains and heme to produce hemoglobin[68]. As such, erythroblasts require heme transporters to export heme from the mitochondria to the cytosol, where it can be complexed with globin chains into hemoglobin[42]. Cytosolic heme exporters can shunt heme to control the intracellular labile heme, and, thereby, cytotoxicity[69]. Recently, the identification of heme importers in the cytosolic membrane of erythroblasts has raised the hypothesis of a role for heme import in these cells[10]. Erythroid-specific *Slc20a1* deletion blocked the terminal erythroid differentiation of fetal liver cells at the proerythroblast stage. *Slc20a1*-deleted erythroblasts showed signs of heme deficiency as highlighted by the induction of EIF2AK1, the downstream targets ATF4 and GADD34. On the same line, heme-induced upregulation of the ribosome machinery[131] did not occur in *Slc20a1*-deleted pro-erythroblasts. Though indirect, evidence highlights that *Slc20a1*-deleted pro-erythroblasts are, possibly, heme deficient and, thereby, it indicates that *Slc20a1* might facilitate heme import in these cells. Currently, it is not known why erythroblasts would require to import exogenous heme in light of their massive endogenous production capacity[10]. The peak expression of heme importers is concomitant to the one of GATA1[132]. Given that GATA1 activity is enhanced by increased intracellular labile heme[11,22], it is plausible that pro-erythroblasts might import exogenous heme to boost GATA1 function. Notably, both GATA1 and ATF4 can bind to the promoter of *Slc20a1* and sustain its expression, further tying labile heme mediated gene regulation with *Slc20a1*.

Central nursing macrophages orchestrate terminal erythroid differentiation by providing signals and nutrients to the developing erythroblasts[71,74]. A particular subset of these nursing macrophages are the RPMs, which serve both as cradle and as grave for RBCs[72]. As such, RPMs recycle large quantities of heme from senescent RBCs to provide iron to the developing erythroblasts[72]. In these cells, heme serves also as a fundamental signaling molecule: it induces and sustains the expression of the master transcription factor Spi-C[12], which, in turn, equips the cell with instruments to handle large quantities of heme[15]. As such, mice lacking *Spic*[12] or the heme importer *Hrg1*[16] have a reduced RPM pool as a consequence of failed *Spic* expression. Mice lacking myeloid *Slc20a1* had a normal RPM compartment at steady state, however, they could not properly expand their RPM compartment in response to anemia because of failed

Slc20a1 induction. Given that RPMs express *Hrg1*[35], it is possible that the expression of the heme importer could partially compensate *Slc20a1* deletion.

Altogether, our findings demonstrate that SLC20A1 facilitates heme uptake and that such function is essential to regulate pro-erythroblast and RPM differentiation, and consequently their interaction. Throughout all the complex processes making up erythropoiesis, we are recently re-discovering[88] the importance of the interaction between the erythroid and myeloid lineage. The modulation of such interaction has the potential to become a disease modifier for those patients suffering from erythroid-related diseases as anemias or polycythemia vera, or heme-related diseases as porphyria. In particular, given its stark effects on both components of the erythroblastic islands, SLC20A1 has the potential to become an exploitable therapeutic target.

Bibliography

1. Martins R, Knapp S. Heme and hemolysis in innate immunity: adding insult to injury. *Curr Opin Immunol*. 2018;50:14-20.
2. Baron MH, Isern J, Fraser ST. The embryonic origins of erythropoiesis in mammals. *Blood*. 2012;119(21):4828-4837.
3. Marden MC, Griffon N, Poyart C. Oxygen delivery and autoxidation of hemoglobin. *Transfus Clin Biol*. 1995;2(6):473-480.
4. Shimizu T, Lengalova A, Martinek V, Martinkova M. Heme: emergent roles of heme in signal transduction, functional regulation and as catalytic centres. *Chem Soc Rev*. 2019;48(24):5624-5657.
5. Soares MP, Bozza MT. Red alert: labile heme is an alarmin. *Curr Opin Immunol*. 2016;38:94-100.
6. Chiabrando D, Vinchi F, Fiorito V, Mercurio S, Tolosano E. Heme in pathophysiology: a matter of scavenging, metabolism and trafficking across cell membranes. *Front Pharmacol*. 2014;5:61.
7. Wissbrock A, Paul George AA, Brewitz HH, Kuhl T, Imhof D. The molecular basis of transient heme-protein interactions: analysis, concept and implementation. *Biosci Rep*. 2019;39(1).
8. Zhang L, Guarente L. Heme binds to a short sequence that serves a regulatory function in diverse proteins. *EMBO J*. 1995;14(2):313-320.
9. Liu R, Hu J. HemeBIND: a novel method for heme binding residue prediction by combining structural and sequence information. *BMC Bioinformatics*. 2011;12:207.
10. Soares MP, Hamza I. Macrophages and Iron Metabolism. *Immunity*. 2016;44(3):492-504.
11. Tanimura N, Miller E, Igarashi K, et al. Mechanism governing heme synthesis reveals a GATA factor/heme circuit that controls differentiation. *EMBO Rep*. 2016;17(2):249-265.
12. Haldar M, Kohyama M, So AY, et al. Heme-mediated SPI-C induction promotes monocyte differentiation into iron-recycling macrophages. *Cell*. 2014;156(6):1223-1234.
13. Chen JJ, Zhang S. Heme-regulated eIF2alpha kinase in erythropoiesis and hemoglobinopathies. *Blood*. 2019;134(20):1697-1707.

14. Igarashi K, Sun J. The heme-Bach1 pathway in the regulation of oxidative stress response and erythroid differentiation. *Antioxid Redox Signal*. 2006;8(1-2):107-118.
15. Kohyama M, Ise W, Edelson BT, et al. Role for Spi-C in the development of red pulp macrophages and splenic iron homeostasis. *Nature*. 2009;457(7227):318-321.
16. Pek RH, Yuan X, Rietzschel N, et al. Hemozoin produced by mammals confers heme tolerance. *Elife*. 2019;8.
17. Katsumura KR, Bresnick EH, Group GFM. The GATA factor revolution in hematology. *Blood*. 2017;129(15):2092-2102.
18. Pal S, Cantor AB, Johnson KD, et al. Coregulator-dependent facilitation of chromatin occupancy by GATA-1. *Proc Natl Acad Sci U S A*. 2004;101(4):980-985.
19. Blobel GA, Nakajima T, Eckner R, Montminy M, Orkin SH. CREB-binding protein cooperates with transcription factor GATA-1 and is required for erythroid differentiation. *Proc Natl Acad Sci U S A*. 1998;95(5):2061-2066.
20. McIver SC, Katsumura KR, Davids E, et al. Exosome complex orchestrates developmental signaling to balance proliferation and differentiation during erythropoiesis. *Elife*. 2016;5.
21. Kadri Z, Maouche-Chretien L, Rooke HM, et al. Phosphatidylinositol 3-kinase/Akt induced by erythropoietin renders the erythroid differentiation factor GATA-1 competent for TIMP-1 gene transactivation. *Mol Cell Biol*. 2005;25(17):7412-7422.
22. Liao R, Zheng Y, Liu X, et al. Discovering How Heme Controls Genome Function Through Heme-omics. *Cell Rep*. 2020;31(13):107832.
23. Chen JJ. Translational control by heme-regulated eIF2alpha kinase during erythropoiesis. *Curr Opin Hematol*. 2014;21(3):172-178.
24. Dalton LE, Healey E, Irving J, Marciniak SJ. Phosphoproteins in stress-induced disease. *Prog Mol Biol Transl Sci*. 2012;106:189-221.
25. Harding HP, Zhang Y, Scheuner D, Chen JJ, Kaufman RJ, Ron D. Ppp1r15 gene knockout reveals an essential role for translation initiation factor 2 alpha (eIF2alpha) dephosphorylation in mammalian development. *Proc Natl Acad Sci U S A*. 2009;106(6):1832-1837.
26. Dutra FF, Bozza MT. Heme on innate immunity and inflammation. *Front Pharmacol*. 2014;5:115.

27. Belcher JD, Chen C, Nguyen J, et al. Heme triggers TLR4 signaling leading to endothelial cell activation and vaso-occlusion in murine sickle cell disease. *Blood*. 2014;123(3):377-390.
28. Dutra FF, Alves LS, Rodrigues D, et al. Hemolysis-induced lethality involves inflammasome activation by heme. *Proc Natl Acad Sci U S A*. 2014;111(39):E4110-4118.
29. Man SM, Kanneganti TD. Converging roles of caspases in inflammasome activation, cell death and innate immunity. *Nat Rev Immunol*. 2016;16(1):7-21.
30. Martins R, Maier J, Gorki AD, et al. Heme drives hemolysis-induced susceptibility to infection via disruption of phagocyte functions. *Nat Immunol*. 2016;17(12):1361-1372.
31. Tolosano E, Fagoonee S, Morello N, Vinchi F, Fiorito V. Heme scavenging and the other facets of hemopexin. *Antioxid Redox Signal*. 2010;12(2):305-320.
32. Mercurio S, Petrillo S, Chiabrando D, et al. The heme exporter Flvcr1 regulates expansion and differentiation of committed erythroid progenitors by controlling intracellular heme accumulation. *Haematologica*. 2015;100(6):720-729.
33. Hamdi A, Roshan TM, Kahawita TM, Mason AB, Sheftel AD, Ponka P. Erythroid cell mitochondria receive endosomal iron by a "kiss-and-run" mechanism. *Biochim Biophys Acta*. 2016;1863(12):2859-2867.
34. Khan AA, Quigley JG. Control of intracellular heme levels: heme transporters and heme oxygenases. *Biochim Biophys Acta*. 2011;1813(5):668-682.
35. White C, Yuan X, Schmidt PJ, et al. HRG1 is essential for heme transport from the phagolysosome of macrophages during erythrophagocytosis. *Cell Metab*. 2013;17(2):261-270.
36. Duffy SP, Shing J, Saraon P, et al. The Fowler syndrome-associated protein FLVCR2 is an importer of heme. *Mol Cell Biol*. 2010;30(22):5318-5324.
37. Desuzinges-Mandon E, Arnaud O, Martinez L, Huche F, Di Pietro A, Falson P. ABCG2 transports and transfers heme to albumin through its large extracellular loop. *J Biol Chem*. 2010;285(43):33123-33133.
38. Shayeghi M, Latunde-Dada GO, Oakhill JS, et al. Identification of an intestinal heme transporter. *Cell*. 2005;122(5):789-801.
39. Andrews NC. When is a heme transporter not a heme transporter? When it's a folate transporter. *Cell Metab*. 2007;5(1):5-6.

40. Rajagopal A, Rao AU, Amigo J, et al. Haem homeostasis is regulated by the conserved and concerted functions of HRG-1 proteins. *Nature*. 2008;453(7198):1127-1131.
41. Santander N, Lizama CO, Meky E, et al. Lack of Flvcr2 impairs brain angiogenesis without affecting the blood-brain barrier. *J Clin Invest*. 2020;130(8):4055-4068.
42. Chiabrando D, Marro S, Mercurio S, et al. The mitochondrial heme exporter FLVCR1b mediates erythroid differentiation. *J Clin Invest*. 2012;122(12):4569-4579.
43. Quigley JG, Yang Z, Worthington MT, et al. Identification of a human heme exporter that is essential for erythropoiesis. *Cell*. 2004;118(6):757-766.
44. Liu SC, Zhai S, Palek J. Detection of hemin release during hemoglobin S denaturation. *Blood*. 1988;71(6):1755-1758.
45. Levy AP, Asleh R, Blum S, et al. Haptoglobin: basic and clinical aspects. *Antioxid Redox Signal*. 2010;12(2):293-304.
46. Hamza I, Dailey HA. One ring to rule them all: trafficking of heme and heme synthesis intermediates in the metazoans. *Biochim Biophys Acta*. 2012;1823(9):1617-1632.
47. Yuan X, Rietzschel N, Kwon H, et al. Regulation of intracellular heme trafficking revealed by subcellular reporters. *Proc Natl Acad Sci U S A*. 2016;113(35):E5144-5152.
48. Palis J. Ontogeny of erythropoiesis. *Curr Opin Hematol*. 2008;15(3):155-161.
49. Palis J, Malik J, McGrath KE, Kingsley PD. Primitive erythropoiesis in the mammalian embryo. *Int J Dev Biol*. 2010;54(6-7):1011-1018.
50. Dzierzak E, Philipsen S. Erythropoiesis: development and differentiation. *Cold Spring Harb Perspect Med*. 2013;3(4):a011601.
51. Paulson RF, Ruan B, Hao S, Chen Y. Stress Erythropoiesis is a Key Inflammatory Response. *Cells*. 2020;9(3).
52. Nazaraliyev A, Richard E, Sawai CM. In-vivo differentiation of adult hematopoietic stem cells from a single-cell point of view. *Curr Opin Hematol*. 2020;27(4):241-247.
53. Orkin SH, Zon LI. Hematopoiesis: an evolving paradigm for stem cell biology. *Cell*. 2008;132(4):631-644.

54. Notta F, Zandi S, Takayama N, et al. Distinct routes of lineage development reshape the human blood hierarchy across ontogeny. *Science*. 2016;351(6269):aab2116.
55. Tusi BK, Wolock SL, Weinreb C, et al. Population snapshots predict early haematopoietic and erythroid hierarchies. *Nature*. 2018;555(7694):54-60.
56. Gnanapragasam MN, Bieker JJ. Orchestration of late events in erythropoiesis by KLF1/EKLF. *Curr Opin Hematol*. 2017;24(3):183-190.
57. Barbarani G, Fugazza C, Strouboulis J, Ronchi AE. The Pleiotropic Effects of GATA1 and KLF1 in Physiological Erythropoiesis and in Dyserythropoietic Disorders. *Front Physiol*. 2019;10:91.
58. Fujiwara Y, Browne CP, Cunniff K, Goff SC, Orkin SH. Arrested development of embryonic red cell precursors in mouse embryos lacking transcription factor GATA-1. *Proc Natl Acad Sci U S A*. 1996;93(22):12355-12358.
59. Nuez B, Michalovich D, Bygrave A, Ploemacher R, Grosveld F. Defective haematopoiesis in fetal liver resulting from inactivation of the EKLF gene. *Nature*. 1995;375(6529):316-318.
60. Drissen R, von Lindern M, Kolbus A, et al. The erythroid phenotype of EKLF-null mice: defects in hemoglobin metabolism and membrane stability. *Mol Cell Biol*. 2005;25(12):5205-5214.
61. Koulnis M, Porpiglia E, Hidalgo D, Socolovsky M. Erythropoiesis: from molecular pathways to system properties. *Adv Exp Med Biol*. 2014;844:37-58.
62. Camaschella C, Pagani A, Nai A, Silvestri L. The mutual control of iron and erythropoiesis. *Int J Lab Hematol*. 2016;38 Suppl 1:20-26.
63. Liu J, Zhang J, Ginzburg Y, et al. Quantitative analysis of murine terminal erythroid differentiation in vivo: novel method to study normal and disordered erythropoiesis. *Blood*. 2013;121(8):e43-49.
64. Valent P, Busche G, Theurl I, et al. Normal and pathological erythropoiesis in adults: from gene regulation to targeted treatment concepts. *Haematologica*. 2018;103(10):1593-1603.
65. Doty RT, Yan X, Meng C, Lausted C, Tian Q, Abkowitz JL. Single-cell analysis of erythropoiesis in Rpl11 haploinsufficient mice reveals insight into the pathogenesis of Diamond-Blackfan anemia. *Exp Hematol*. 2021;97:66-78 e66.
66. Sankaran VG, Orkin SH. The switch from fetal to adult hemoglobin. *Cold Spring Harb Perspect Med*. 2013;3(1):a011643.

67. McCarthy EF. The oxygen affinity of human maternal and foetal haemoglobin. *J Physiol*. 1943;102(1):55-61.
68. Chen JJ. Regulation of protein synthesis by the heme-regulated eIF2alpha kinase: relevance to anemias. *Blood*. 2007;109(7):2693-2699.
69. Doty RT, Phelps SR, Shadle C, Sanchez-Bonilla M, Keel SB, Abkowitz JL. Coordinate expression of heme and globin is essential for effective erythropoiesis. *J Clin Invest*. 2015;125(12):4681-4691.
70. Origa R. beta-Thalassemia. *Genet Med*. 2017;19(6):609-619.
71. Heideveld E, van den Akker E. Digesting the role of bone marrow macrophages on hematopoiesis. *Immunobiology*. 2017;222(6):814-822.
72. Klei TR, Meinderts SM, van den Berg TK, van Bruggen R. From the Cradle to the Grave: The Role of Macrophages in Erythropoiesis and Erythrophagocytosis. *Front Immunol*. 2017;8:73.
73. Chasis JA, Mohandas N. Erythroblastic islands: niches for erythropoiesis. *Blood*. 2008;112(3):470-478.
74. de Back DZ, Kostova EB, van Kraaij M, van den Berg TK, van Bruggen R. Of macrophages and red blood cells; a complex love story. *Front Physiol*. 2014;5:9.
75. Rhodes MM, Kopsombut P, Bondurant MC, Price JO, Koury MJ. Adherence to macrophages in erythroblastic islands enhances erythroblast proliferation and increases erythrocyte production by a different mechanism than erythropoietin. *Blood*. 2008;111(3):1700-1708.
76. Heideveld E, Masiello F, Marra M, et al. CD14+ cells from peripheral blood positively regulate hematopoietic stem and progenitor cell survival resulting in increased erythroid yield. *Haematologica*. 2015;100(11):1396-1406.
77. Spike BT, Dibling BC, Macleod KF. Hypoxic stress underlies defects in erythroblast islands in the Rb-null mouse. *Blood*. 2007;110(6):2173-2181.
78. Sawada K, Krantz SB, Dessypris EN, Koury ST, Sawyer ST. Human colony-forming units-erythroid do not require accessory cells, but do require direct interaction with insulin-like growth factor I and/or insulin for erythroid development. *J Clin Invest*. 1989;83(5):1701-1709.
79. Millot S, Andrieu V, Letteron P, et al. Erythropoietin stimulates spleen BMP4-dependent stress erythropoiesis and partially corrects anemia in a mouse model of generalized inflammation. *Blood*. 2010;116(26):6072-6081.

80. Bibikova E, Youn MY, Danilova N, et al. TNF-mediated inflammation represses GATA1 and activates p38 MAP kinase in RPS19-deficient hematopoietic progenitors. *Blood*. 2014;124(25):3791-3798.
81. Zamai L, Secchiero P, Pierpaoli S, et al. TNF-related apoptosis-inducing ligand (TRAIL) as a negative regulator of normal human erythropoiesis. *Blood*. 2000;95(12):3716-3724.
82. Zermati Y, Fichelson S, Valensi F, et al. Transforming growth factor inhibits erythropoiesis by blocking proliferation and accelerating differentiation of erythroid progenitors. *Exp Hematol*. 2000;28(8):885-894.
83. Korolnek T, Hamza I. Like iron in the blood of the people: the requirement for heme trafficking in iron metabolism. *Front Pharmacol*. 2014;5:126.
84. Levy JE, Jin O, Fujiwara Y, Kuo F, Andrews NC. Transferrin receptor is necessary for development of erythrocytes and the nervous system. *Nat Genet*. 1999;21(4):396-399.
85. Nairz M, Theurl I, Swirski FK, Weiss G. "Pumping iron"-how macrophages handle iron at the systemic, microenvironmental, and cellular levels. *Pflugers Arch*. 2017;469(3-4):397-418.
86. Sukhbaatar N, Weichhart T. Iron Regulation: Macrophages in Control. *Pharmaceuticals (Basel)*. 2018;11(4).
87. Kovtunovych G, Eckhaus MA, Ghosh MC, Ollivierre-Wilson H, Rouault TA. Dysfunction of the heme recycling system in heme oxygenase 1-deficient mice: effects on macrophage viability and tissue iron distribution. *Blood*. 2010;116(26):6054-6062.
88. Policard A, Bessis M. Micropinocytosis and rhopheocytosis. *Nature*. 1962;194:110-111.
89. Chow A, Huggins M, Ahmed J, et al. CD169(+) macrophages provide a niche promoting erythropoiesis under homeostasis and stress. *Nat Med*. 2013;19(4):429-436.
90. Paulson RF, Shi L, Wu DC. Stress erythropoiesis: new signals and new stress progenitor cells. *Curr Opin Hematol*. 2011;18(3):139-145.
91. Hao S, Xiang J, Wu DC, et al. Gdf15 regulates murine stress erythroid progenitor proliferation and the development of the stress erythropoiesis niche. *Blood Adv*. 2019;3(14):2205-2217.

92. Chen Y, Xiang J, Qian F, et al. Epo receptor signaling in macrophages alters the splenic niche to promote erythroid differentiation. *Blood*. 2020;136(2):235-246.
93. Kautz L, Jung G, Valore EV, Rivella S, Nemeth E, Ganz T. Identification of erythroferrone as an erythroid regulator of iron metabolism. *Nat Genet*. 2014;46(7):678-684.
94. Nemeth E, Tuttle MS, Powelson J, et al. Hepcidin regulates cellular iron efflux by binding to ferroportin and inducing its internalization. *Science*. 2004;306(5704):2090-2093.
95. Ramos P, Casu C, Gardenghi S, et al. Macrophages support pathological erythropoiesis in polycythemia vera and beta-thalassemia. *Nat Med*. 2013;19(4):437-445.
96. Liao C, Prabhu KS, Paulson RF. Monocyte-derived macrophages expand the murine stress erythropoietic niche during the recovery from anemia. *Blood*. 2018;132(24):2580-2593.
97. Forster IC, Hernando N, Biber J, Murer H. Phosphate transporters of the SLC20 and SLC34 families. *Mol Aspects Med*. 2013;34(2-3):386-395.
98. Stewart H, Adema KW, McMonagle EL, Hosie MJ, Willett BJ. Identification of novel subgroup A variants with enhanced receptor binding and replicative capacity in primary isolates of anaemogenic strains of feline leukaemia virus. *Retrovirology*. 2012;9:48.
99. Takeuchi Y, Vile RG, Simpson G, O'Hara B, Collins MK, Weiss RA. Feline leukemia virus subgroup B uses the same cell surface receptor as gibbon ape leukemia virus. *J Virol*. 1992;66(2):1219-1222.
100. Sugai J, Eiden M, Anderson MM, Van Hoeven N, Meiering CD, Overbaugh J. Identification of envelope determinants of feline leukemia virus subgroup B that permit infection and gene transfer to cells expressing human Pit1 or Pit2. *J Virol*. 2001;75(15):6841-6849.
101. Hardy WD, Jr. Immunopathology induced by the feline leukemia virus. *Springer Semin Immunopathol*. 1982;5(1):75-106.
102. O'Hara B, Johann SV, Klinger HP, et al. Characterization of a human gene conferring sensitivity to infection by gibbon ape leukemia virus. *Cell Growth Differ*. 1990;1(3):119-127.
103. Bottger P, Hede SE, Grunnet M, Hoyer B, Klaerke DA, Pedersen L. Characterization of transport mechanisms and determinants critical for Na+-

dependent Pi symport of the PiT family paralogs human PiT1 and PiT2. *Am J Physiol Cell Physiol*. 2006;291(6):C1377-1387.

104. Kavanaugh MP, Miller DG, Zhang W, et al. Cell-surface receptors for gibbon ape leukemia virus and amphotropic murine retrovirus are inducible sodium-dependent phosphate symporters. *Proc Natl Acad Sci U S A*. 1994;91(15):7071-7075.

105. Johann SV, Gibbons JJ, O'Hara B. GLVR1, a receptor for gibbon ape leukemia virus, is homologous to a phosphate permease of Neurospora crassa and is expressed at high levels in the brain and thymus. *J Virol*. 1992;66(3):1635-1640.

106. Ravera S, Murer H, Forster IC. An externally accessible linker region in the sodium-coupled phosphate transporter PiT-1 (SLC20A1) is important for transport function. *Cell Physiol Biochem*. 2013;32(1):187-199.

107. Beck L, Karaplis AC, Amizuka N, Hewson AS, Ozawa H, Tenenhouse HS. Targeted inactivation of Npt2 in mice leads to severe renal phosphate wasting, hypercalciuria, and skeletal abnormalities. *Proc Natl Acad Sci U S A*. 1998;95(9):5372-5377.

108. Segawa H, Onitsuka A, Furutani J, et al. Npt2a and Npt2c in mice play distinct and synergistic roles in inorganic phosphate metabolism and skeletal development. *Am J Physiol Renal Physiol*. 2009;297(3):F671-678.

109. Yamada S, Wallingford MC, Borgeia S, Cox TC, Giachelli CM. Loss of PiT-2 results in abnormal bone development and decreased bone mineral density and length in mice. *Biochem Biophys Res Commun*. 2018;495(1):553-559.

110. Beck L, Leroy C, Beck-Cormier S, et al. The phosphate transporter PiT1 (Slc20a1) revealed as a new essential gene for mouse liver development. *PLoS One*. 2010;5(2):e9148.

111. Bourgine A, Pilet P, Diouani S, et al. Mice with hypomorphic expression of the sodium-phosphate cotransporter PiT1/Slc20a1 have an unexpected normal bone mineralization. *PLoS One*. 2013;8(6):e65979.

112. Liu L, Sanchez-Bonilla M, Crouthamel M, Giachelli C, Keel S. Mice lacking the sodium-dependent phosphate import protein, PiT1 (SLC20A1), have a severe defect in terminal erythroid differentiation and early B cell development. *Exp Hematol*. 2013;41(5):432-443 e437.

113. Forand A, Beck L, Leroy C, et al. EKLF-driven PIT1 expression is critical for mouse erythroid maturation in vivo and in vitro. *Blood*. 2013;121(4):666-678.

114. Beck-Cormier S, Beck L. The Need of a Paradigm Shift to Better Understand PiT1 and PiT2 Biology: Response to "Why Is There No PiT1/SLC20A1 Pathogenic Variants Yet Linked to Primary Familial Brain Calcification?". *J Bone Miner Res*. 2020;35(4):825-826.
115. Beck L, Leroy C, Salaun C, Margall-Ducos G, Desdouets C, Friedlander G. Identification of a novel function of PiT1 critical for cell proliferation and independent of its phosphate transport activity. *J Biol Chem*. 2009;284(45):31363-31374.
116. Koumakis E, Millet-Botti J, Benna JE, et al. Novel function of PiT1/SLC20A1 in LPS-related inflammation and wound healing. *Sci Rep*. 2019;9(1):1808.
117. Salaun C, Leroy C, Rousseau A, Boitez V, Beck L, Friedlander G. Identification of a novel transport-independent function of PiT1/SLC20A1 in the regulation of TNF-induced apoptosis. *J Biol Chem*. 2010;285(45):34408-34418.
118. Beutler B, Du X, Xia Y. Precis on forward genetics in mice. *Nat Immunol*. 2007;8(7):659-664.
119. Jinek M, Chylinski K, Fonfara I, Hauer M, Doudna JA, Charpentier E. A programmable dual-RNA-guided DNA endonuclease in adaptive bacterial immunity. *Science*. 2012;337(6096):816-821.
120. Shalem O, Sanjana NE, Hartenian E, et al. Genome-scale CRISPR-Cas9 knockout screening in human cells. *Science*. 2014;343(6166):84-87.
121. Hediger MA, Clemencon B, Burrier RE, Bruford EA. The ABCs of membrane transporters in health and disease (SLC series): introduction. *Mol Aspects Med*. 2013;34(2-3):95-107.
122. Cesar-Razquin A, Snijder B, Frappier-Brinton T, et al. A Call for Systematic Research on Solute Carriers. *Cell*. 2015;162(3):478-487.
123. Parnas O, Jovanovic M, Eisenhaure TM, et al. A Genome-wide CRISPR Screen in Primary Immune Cells to Dissect Regulatory Networks. *Cell*. 2015;162(3):675-686.
124. Girardi E, Cesar-Razquin A, Lindinger S, et al. A widespread role for SLC transmembrane transporters in resistance to cytotoxic drugs. *Nat Chem Biol*. 2020;16(4):469-478.
125. Sobh A, Loguinov A, Zhou J, et al. Genetic screens reveal CCDC115 as a modulator of erythroid iron and heme trafficking. *Am J Hematol*. 2020;95(9):1085-1098.

126. Dixon SJ, Lemberg KM, Lamprecht MR, et al. Ferroptosis: an iron-dependent form of nonapoptotic cell death. *Cell*. 2012;149(5):1060-1072.
127. Badgley MA, Kremer DM, Maurer HC, et al. Cysteine depletion induces pancreatic tumor ferroptosis in mice. *Science*. 2020;368(6486):85-89.
128. Menche J, Sharma A, Kitsak M, et al. Disease networks. Uncovering disease-disease relationships through the incomplete interactome. *Science*. 2015;347(6224):1257601.
129. Zhou X, Menche J, Barabasi AL, Sharma A. Human symptoms-disease network. *Nat Commun*. 2014;5:4212.
130. Keel SB, Doty RT, Yang Z, et al. A heme export protein is required for red blood cell differentiation and iron homeostasis. *Science*. 2008;319(5864):825-828.
131. Doty RT, Yan X, Lausted C, et al. Single-cell analyses demonstrate that a heme-GATA1 feedback loop regulates red cell differentiation. *Blood*. 2019;133(5):457-469.
132. Kingsley PD, Greenfest-Allen E, Frame JM, et al. Ontogeny of erythroid gene expression. *Blood*. 2013;121(6):e5-e13.

Curriculum Vitae

Personal information

Name	Federica Quattrone
Nationality	Italian
Contact information	Federica.quattrone@meduniwien.ac.at

Research interests

Heme biology	Macrophages	Erythropoiesis	Differentiation trajectories

Education

Oct.2015 – Present, *Vienna*	**Doctoral program in Immunology** *Medical University of Vienna* Dissertation: "The role of SLC20A1 in physiological and pathological erythropoiesis." Supervisor: Univ.-Prof. Dr.med. Sylvia Knapp, PhD: Department of Internal Medicine I, Medical University of Vienna and CeMM Research Center for Molecular Medicine of the Austrian Academy of Sciences. Representative for the CeMM PhD students a.y. 2018-2019
Nov. 2014 – Jun. 2015 *Milan*	**Postgraduation program in Eurpean and Italian Patent law** *Università degli Studi di Milano*
Oct. 2012 – Nov.2014 *Milan*	**Master's degree in Molecular and Cellular Medical Biotechnology** *Università Vita-Salute San Raffaele, Milano.* Distinction at final examination (110/110). Dissertation: "How human endometrial stromal cells manage iron: insights into the pathogenesis of endometriosis"

Oct. 2009 – Oct.-2012 *Milan*	**Bachelor's degree in Medical Biotechnology** *Università degli studi di Milano* Dissertation: "Evaluation of mitochondrial DNA content of primary human trophoblast cell cultures from physological placentas subject to hypoxia"

Research experience

Jun. 2018 *Amsterdam*	**Visiting Scientist** *Sanquin Research* Dr. Marieke von Lindern lab.
Nov. 2014 – Jul.2015 *Milan*	**Research fellow** *San Raffaele Scientific Institute* Dr. Paola Panina-Bordignon lab Dr. Anna Mondino lab
Sept. 2013 – Nov. 2014 *Milan*	**Master's thesis internship** *San Raffaele Scientific Institute* Dr. Paola Panina-Bordignon lab
Sept. 2013 – Nov. 2014 *Milan*	**Bachelor's thesis internship** *Ospedale L. Sacco, Università degli Studi di Milano* Dr.Irene Cetin lab

Awards and Fellowships

Jun. 2018	**DOC Fellowship** Austrian Academy of Sciences, Vienna, Austria.
Jul. 2017	**ÖGAI Travel Grant** Austrian Society for Allergology and Immunology, to participate and present at Gordon Research Conference "Red Cells" 2017
Oct. 2006	**"Genius and Excellence" Merit Diploma** Council of Lombardy Region

Publications

* Contributed equally

QUATTRONE F, Martins R, Gorki A-D, Hladik A, Lakovits K, Rebsamen M, Girardi E, Alvarez-Hernandez A, Mayrhofer F, Farhat A, Watzenboeck M, van den Akker E, von lindern M, Superti-Furga G, Simonitsch-Klupp I, Gawish R and Knapp S. **SLC20A1 facilitates heme transport and drives red pulp macrophage and erythroblast differentiation** (Submitted)

Watzenboeck M*, Gorki A-D*, **QUATTRONE F*** , Gawish R*, Schwartz S, Lambers C, Jaksch P, Lakovits K, Zahalka s, Rahimi N, Starkl P, Symmank D, Artner T, Pattaroni C, Fortelny N, Klavins K, Marsland B-J, Hoetzenecker K, Knapp S and Widder S. **Multi-omics Profiling Unravels Dynamics of Pulmonary Adaptation after Lung Transplantation** *European Respiratory Journal* (Accepted)

Watzenboeck M, Drobits B, Zahalka S, Gorki A-D, Farhat A, **QUATTRONE F,** Hladik A, Lakovits K, Richard G-M, Lederer T, Strobl B, Versteeg G-A, Boon L, Starkl P, Knapp S **Lipocalin 2 modulates dendritic cell activity and shapes immunity to influenza in a microbiome dependent manner** *Plos Pathogens* (2021)

Sanchez AM, **QUATTRONE F**, Pannese M, Ulisse A, Candiani M, Diaz-Alonso J, Velasco G, Panina-Bordignon P. **The cannabinoid receptor CB1 contributes to the development of ectopic lesions in a mouse model of endometriosis** *Human Reproduction* (2017)

Martins R, Maier J, Gorki AD, Huber K, Sharif O, Starkl P, Saluzzo S, **QUATTRONE F,** Gawish R, Lakovits K, Aichinger M, Radic-Sarikas B , Lardeau CH , Hladik A , Korosec A , Brown M, Vaahtomer K , Duggan M , Kerjaschki D, Esterbauer H, Colinge J, Eisenbarth S, Decker T , Bennett K, Kubicek S , Sixt M , Superti-Furga G, Knapp S**.. Heme drives hemolysis-induced susceptibility to infection and sepsis via disruption of phagocyte cytoskeletal dynamics** *Nature Immunology* (2016)

QUATTRONE F*and Sanchez AM*, Pannese M, Hemmerle T, Viganò P, Candiani M, Petraglia F, Neri D, Panina-Bordignon P. **The targeted delivery of IL4 inhibits development of endometriotic lesions in a mouse model** *Reproductive Sciences* (2015)

Gregori S, Amodio G, **QUATTRONE F** and Panina-Bordignon P **HLA-G orchestrates the early interaction of human trophoblasts with the maternal niche** *Frontiers in Immunology* (2015)

Sanchez AM, Viganò P, **QUATTRONE F,** Pagliardini L, Papaleo E, Candiani M, Panina-Bordignon P. **The WNT/β-catenin signaling pathway and expression of survival promoting genes in luteinized granulosa cells: endometriosis as a paradigm for a dysregulated apoptosis pathway** *Fertility and Sterility* (2014)

Conference participation

- European School of Hematology Erythropoiesis Control and Ineffective Erythropoiesis from Bench to Bedside, Virtual (2021)
- American Society of Hematology 62nd Annual Meeting, Virtual, (2020)
- American Society of Hematology 61st Annual Meeting, Orlando, USA (2019), **oral presentation**
- SFB Scientific Advisory Board Meeting, Vienna, Austria (2018 and 2020), **oral presentation**
- Young Scientist's Association PhD symposium, Vienna, Austria (2018), **oral presentation**
- European School of Hematology - GR-EX 2nd International Symposium on Red Blood Cells: Genesis and Pathophysiology, Paris, France (2018)
- Gordon Research Conference "Red cells" Newport, Rhode Island, USA (2017), **poster presentation**
- Special Research Program (SFB) "Inthro" grant hearing (2017), **poster presentation**
- CeMM Scientific Advisory Board Meeting, Vienna, Austria (2017), **oral presentation**
- Young Scientist's Association PhD symposium, Vienna, Austria (2017)
- Young Scientist's Association PhD symposium, Vienna, Austria (2016), **poster presentation**
- 7th International PhD workshop: Joint Symposium IAI-CCHD-MCCA-ICA, Vienna, Austria (2016)
- Haploday, Vienna, Austria (2016)